

Air Force Institute of Technology

**AFIT Scholar**

---

Theses and Dissertations

Student Graduate Works

---

3-2023

## **Anisotropic Characterization of Additively Manufactured TI 6-4 via Tension, Compression, and Three Point Bend Experimentation**

James M. Gunderson

Follow this and additional works at: <https://scholar.afit.edu/etd>



Part of the [Materials Science and Engineering Commons](#)

---

### **Recommended Citation**

Gunderson, James M., "Anisotropic Characterization of Additively Manufactured TI 6-4 via Tension, Compression, and Three Point Bend Experimentation" (2023). *Theses and Dissertations*. 7020.  
<https://scholar.afit.edu/etd/7020>

This Thesis is brought to you for free and open access by the Student Graduate Works at AFIT Scholar. It has been accepted for inclusion in Theses and Dissertations by an authorized administrator of AFIT Scholar. For more information, please contact [AFIT.ENWL.Repository@us.af.mil](mailto:AFIT.ENWL.Repository@us.af.mil).



**ANISOTROPIC CHARACTERIZATION OF ADDITIVELY MANUFACTURED  
TI 6-4 VIA TENSION, COMPRESSION, AND THREE POINT BEND  
EXPERIMENTATION**

THESIS

James M. Gunderson, First Lieutenant, USAF

AFIT-ENY-MS-23-M-270

**DEPARTMENT OF THE AIR FORCE  
AIR UNIVERSITY**

**I. AIR FORCE INSTITUTE OF TECHNOLOGY**

Wright-Patterson Air Force Base, Ohio

**DISTRIBUTION STATEMENT A.**  
APPROVED FOR PUBLIC RELEASE; DISTRIBUTION UNLIMITED.

The views expressed in this thesis are those of the author and do not reflect the official policy or position of the United States Air Force, Department of Defense, or the United States Government. This material is declared a work of the U.S. Government and is not subject to copyright protection in the United States.

AFIT-ENY-MS-23-M-270

ANISOTROPIC CHARACTERIZATION OF ADDITIVELY MANUFACTURED TI 6-4 VIA TENSION, COMPRESSION, AND THREE POINT BEND EXPERIMENTATION

THESIS

Presented to the Faculty

Department of Aeronautics and Astronautics

Graduate School of Engineering and Management

Air Force Institute of Technology

Air University

Air Education and Training Command

In Partial Fulfillment of the Requirements for the  
Degree of Master of Science in Aeronautical Engineering

James M. Gunderson, BS

First Lieutenant, USAF

March 2023

**DISTRIBUTION STATEMENT A.**  
APPROVED FOR PUBLIC RELEASE; DISTRIBUTION UNLIMITED.

AFIT-ENY-MS-23-M-270

**ANISOTROPIC CHARACTERIZATION OF ADDITIVELY MANUFACTURED  
TI 6-4 VIA TENSION, COMPRESSION, AND THREE POINT BEND  
EXPERIMENTATION**

**THESIS**

James M. Gunderson, BS

First Lieutenant, USAF

Approved:

\_\_\_\_\_  
Major John S. Brewer Jr., Ph.D. (Chairman)

\_\_\_\_\_  
Date

\_\_\_\_\_  
Major Ryan A. Kemnitz, Ph.D. (Member)

\_\_\_\_\_  
Date

\_\_\_\_\_  
Dr. Carl R. Hartsfield (Member)

\_\_\_\_\_  
Date

**Abstract**

Titanium's ability to fill existing material gaps because of its higher strength and higher melting temperature compared to other common materials used in aircraft structures requires a need to understand the behavior of the material. Titanium's properties and the development of additive manufacturing also open an opportunity for it to be used in aerospace systems of the future in applications where traditionally manufactured titanium cannot meet the desired system requirements. Compressive, tensile, and three point bend experimental data collected from this research under varying temperatures, print orientations, print layer build heights, and surface finishes were analyzed to determine favorable material parameters for the Titanium alloy Ti-6Al-4V.

### **Acknowledgments**

I would like to take this time to thank my advisor, Major John Brewer, for his guidance, knowledge, and insight into the execution of this thesis. I would also like to thank those who supported me throughout my experimentation and post processing analysis including Ms. Brianna Sexton, Ms. Cayla Eckley, and Captain Christopher Bellanova. Lastly, I would like to thank my wife for her patience and encouragement during my time of study at AFIT.

James M. Gunderson

## Table of Contents

I. Introduction.....	1
1.1 General Issue .....	1
1.2 Problem Statement .....	1
1.3 Research Questions .....	2
1.4 Approach.....	3
1.5 Assumptions .....	4
1.6 Preview .....	4
II. Background and Literature Review.....	6
2.1 Chapter Overview .....	6
2.2 Material Background .....	6
2.3 Material Issues.....	9
2.4 Additive Manufacturing Background.....	9
2.5 Additive Manufacturing Advantages .....	11
2.6 Additive Manufacturing Disadvantages.....	12
2.7 Current Research Efforts .....	13
2.8 Summary .....	16
III. Methodology .....	17
3.1 Chapter Overview .....	17
3.2 Manufacturing of Parts used in Research.....	17
3.3 Sample Preparation .....	26
3.4 Three Point Bend Testing.....	28
3.5 Compression Testing.....	32
3.6 Tensile Testing .....	34

3.7 Data Processing .....	37
3.8 Microscopy .....	39
3.9 Summary .....	43
IV. Analysis and Results .....	45
4.1 Chapter Overview .....	45
4.2 Ground Room Temperature Three Point Bend Results .....	45
4.3 Unground Room Temperature Three Point Bend Results .....	49
4.4 Ground High Temperature Three Point Bend Results .....	53
4.5 Comparison Between the Ground and Unground Room Temperature Three Point Bend Tests .....	57
4.6 Comparison Between the Ground Room and High Temperature Three Point Bend Tests .....	63
4.7 Comparison of Ground Room Temperature Three Point Bend Tests and Traditionally Manufactured Ti 6-4.....	65
4.8 Comparison of Yield and Ultimate Stress Results for Three Point Bend Samples	67
4.9 Ground Room Temperature Compression Results .....	72
4.10 Unground Room Temperature Compression Results .....	76
4.11 Comparison of Ground and Unground Room Temperature Compression Tests ..	80
4.12 Comparison of Ground Room Temperature Compression Tests and Traditionally Manufactured Ti 6-4.....	82
4.13 Comparison of Yield and Ultimate Stress Results for Compression Samples .....	83
4.14 Ground Room Temperature Tensile Results .....	86
4.15 Comparison of Ground Room Temperature Tensile Tests and Traditionally Manufactured Ti 6-4.....	90
4.16 Comparison of Yield and Ultimate Stress Results for Tensile Samples .....	91

4.17 Microscopy .....	94
4.18 Summary .....	108
V. Conclusions and Recommendations .....	109
5.1 Chapter Overview .....	109
5.2 Research Conclusions .....	109
5.3 Significance of Research.....	111
5.4 Recommendations for Future Research .....	112
5.5 Summary .....	113

## List of Figures

Figure 1. DMLS Process [8] .....	10
Figure 2. DMLS Manufacturing Setup Diagram [9] .....	11
Figure 3. EOS M400-4 Printing Machine [22] .....	18
Figure 4. 30 and 60 Micron Build Height Sample Build Plate [24] .....	22
Figure 5. Build Directions of Samples Printed .....	23
Figure 6. Compression Cube Dimensions .....	25
Figure 7. Tensile Bar Dimensions .....	25
Figure 8. Three Point Bend Bar Dimensions .....	26
Figure 9. Buehler Ecomet 300 Grinding and Polishing Machine .....	27
Figure 10. Ground and Unground Three Point Bend Specimens .....	28
Figure 11. MTS 22 kip Load Frame used for Three Point Bend Tests .....	29
Figure 12. Room Temperature Three Point Bend Test Sample during Testing .....	30
Figure 13. High Temperature Three Point Bend Test Sample during Testing .....	31
Figure 14. MTS 110 kip Load Frame used for Compression Tests .....	32
Figure 15. Room Temperature Compression Test Sample during Testing .....	34
Figure 16. MTS 11 kip Load Frame used for Tensile Tests .....	35
Figure 17. Room Temperature Tensile Test Sample during Testing .....	37
Figure 18. Tescan MAIA3 SEM .....	40
Figure 19. Metpress A Automatic Mounting Press .....	41
Figure 20. Zeiss Inverted Optical Microscope .....	43
Figure 21. 30 Micron/0 Degrees/Room Temperature .....	47
Figure 22. 30 Micron/45 Degrees/Room Temperature .....	47

Figure 23. 30 Micron/90 Degrees/Room Temperature .....	47
Figure 24. 60 Micron/0 Degrees/Room Temperature .....	48
Figure 25. 60 Micron/45 Degrees/Room Temperature .....	48
Figure 26. 60 Micron/90 Degrees/Room Temperature .....	48
Figure 27. 30 Micron/0 Degrees/Room Temperature .....	51
Figure 28. 30 Micron/45 Degrees/Room Temperature .....	51
Figure 29. 30 Micron/90 Degrees/Room Temperature .....	51
Figure 30. 60 Micron/0 Degrees/Room Temperature .....	52
Figure 31. 60 Micron/45 Degrees/Room Temperature .....	52
Figure 32. 60 Micron/90 Degrees/Room Temperature .....	52
Figure 33. 30 Micron/0 Degrees/High Temperature .....	55
Figure 34. 30 Micron/45 Degrees/High Temperature .....	55
Figure 35. 30 Micron/90 Degrees/High Temperature .....	55
Figure 36. 60 Micron/0 Degrees/High Temperature .....	56
Figure 37. 60 Micron/45 Degrees/High Temperature .....	56
Figure 38. 60 Micron/90 Degrees/High Temperature .....	56
Figure 39. Ground Three Point Bend Room Temperature 30 Micron 0 Degree Sample #1 .....	59
Figure 40. Unground Three Point Bend Room Temperature 30 Micron 0 Degree Sample #1.....	59
Figure 41. Unground Three Point Bend Room Temperature 30 Micron 0 Degree Sample #1.....	61

Figure 42. Ground Three Point Bend Room Temperature 30 Micron 0 Degree Sample #1 .....	61
Figure 43. Ground Room and High Temperature Three Point Bend Samples Post Testing .....	65
Figure 44. Yield Stress Comparison for Room Temperature Three Point Bend Samples	68
Figure 45. Yield Stress Comparison for High Temperature Three Point Bend Samples .	69
Figure 46. Ultimate Stress Comparison for Room Temperature Three Point Bend Samples .....	70
Figure 47. Ultimate Stress Comparison for High Temperature Three Point Bend Samples .....	71
Figure 48. 30 Micron/0 Degrees/Room Temperature .....	74
Figure 49. 30 Micron/90 Degrees/Room Temperature .....	74
Figure 50. 60 Micron/0 Degrees/Room Temperature .....	75
Figure 51. 60 Micron/90 Degrees/Room Temperature .....	75
Figure 52. 30 Micron/0 Degrees/Room Temperature .....	78
Figure 53. 30 Micron/90 Degrees/Room Temperature .....	78
Figure 54. 60 Micron/0 Degrees/Room Temperature .....	79
Figure 55. 60 Micron/90 Degrees/Room Temperature .....	79
Figure 56. Yield Stress Comparison for Room Temperature Compression Samples .....	84
Figure 57. Ultimate Stress Comparison for Room Temperature Compression Samples .	85
Figure 58. 30 Micron/0 Degrees/Room Temperature .....	88
Figure 59. 30 Micron/45 Degrees/Room Temperature .....	88
Figure 60. 30 Micron/90 Degrees/Room Temperature .....	88

Figure 61. 60 Micron/0 Degrees/Room Temperature .....	89
Figure 62. 60 Micron/45 Degrees/Room Temperature .....	89
Figure 63. 60 Micron/90 Degrees/Room Temperature .....	89
Figure 64. Yield Stress Comparison for Room Temperature Tensile Samples .....	92
Figure 65. Ultimate Stress Comparison for Room Temperature Tensile Samples .....	93
Figure 66. 30 Micron/0 Degrees/RT/Tensile .....	95
Figure 67. 30 Micron/45 Degrees/RT/Tensile .....	95
Figure 68. 30 Micron/90 Degrees/Room Temperature/Tensile .....	95
Figure 69. 60 Micron/0 Degrees/ RT/Tensile .....	97
Figure 70. 60 Micron/45 Degrees/ RT/Tensile .....	97
Figure 71. 60 Micron/90 Degrees/Room Temperature/Tensile .....	97
Figure 72. 30 Micron/0 Degrees/RT/Compressive .....	98
Figure 73. 30 Micron/90 Degrees/RT/Compressive .....	98
Figure 74. 30 Micron/0 Degrees/RT/Compressive .....	99
Figure 75. 30 Micron/90 Degrees/RT/Compressive .....	99
Figure 76. Failed Compression Sample .....	100
Figure 77. Sample Powder Distribution.....	102
Figure 78. Sample Powder .....	103
Figure 79. Unground Room Temperature Three Point Bend Sample .....	105
Figure 80. Fracture Surface for an Unground Room Temperature Three Point Bend Sample.....	105
Figure 81. Ground Room Temperature Three Point Bend Sample .....	106
Figure 82. Ground High Temperature Three Point Bend Sample .....	107

## List of Tables

Table 1. Chemical and Mechanical Properties of Titanium, Aluminum, and Vanadium [4] [5].....	8
Table 2. EOS M400-4 Additive Manufacturing Printer Specifications [23] .....	19
Table 3. 30 Micron Build Height Print Parameters [24].....	20
Table 4. 60 Micron Build Height Print Parameters [24].....	21
Table 5. Sample Characteristics for 30 and 60 Micron Powder Build Height Samples ...	24
Table 6. Values for Ground Room Temperature Three Point Bend Tests.....	46
Table 7. Values for Unground Room Temperature Three Point Bend Tests.....	49
Table 8. Values for Ground High Temperature Three Point Bend Tests .....	53
Table 9. Comparison of Means Between the Ground Room Temperature Three Point Bend Tests and the Unground Room Temperature Three Point Bend Tests .....	57
Table 10. Comparison of Means Between the Ground Room Temperature Three Point Bend Tests and the Ground High Temperature Three Point Bend Tests .....	63
Table 11. Largest Percent Differences for Ground Room Temperature Three Point Bend Tests .....	66
Table 12. Smallest Percent Differences for Ground Room Temperature Three Point Bend Tests .....	66
Table 13. Values for Ground Room Temperature Compression Tests.....	73
Table 14. Values for Unground Room Temperature Compression Tests.....	76
Table 15. Comparison of Means Between the Ground Room Temperature Compression Tests and the Unground Room Temperature Compression Tests .....	80

Table 16. Largest Percent Differences for Ground Room Temperature Compressive Tests .....	82
Table 17. Smallest Percent Differences for Ground Room Temperature Compressive Tests .....	82
Table 18. Values for Ground Room Temperature Tensile Tests .....	87
Table 19. Largest Percent Differences for Ground Room Temperature Tensile Tests ....	90
Table 20. Smallest Percent Differences for Ground Room Temperature Tensile Tests...	90
Table 21. 30 Micron Build Height Sample Elemental Makeup.....	101
Table 22. 60 Micron Build Height Sample Elemental Makeup.....	101
Table 23. Large Sample Powder Elemental Makeup.....	104
Table 24. Small Sample Powder Elemental Makeup.....	104

## **I. Introduction**

### **1.1 General Issue**

Additively manufactured titanium is a strong, ductile, heat resistant, and light weight material that has the potential to serve in a variety of high temperature structural applications under complex load states. This is important in the aerospace industry as high temperatures and complex load states are common such as in gas turbines and aircraft structures. Research into additively manufactured Ti 6-4 is important, especially in the aerospace field since “titanium has the highest strength-to-weight ratio of any metal. Its high corrosion resistance, fatigue resistance, and ability to withstand high temperatures make it an ideal substance for the aerospace and military industries [1].” Titanium even has the advantage over steel as it has similar strength properties but is about 45 percent lighter [2].

### **1.2 Problem Statement**

Traditionally manufactured Grade 5 (Ti 6Al-4V) is readily found throughout the aerospace field. Ti 6-4 contains 90 percent titanium, 6 percent aluminum, and 4 percent vanadium. The potential for additively manufactured materials like additively manufactured Ti 6-4 to replace their traditionally manufactured counterparts is great due to additive manufacturing’s ability to print complex shapes and geometries traditional methods cannot make or manufacture. Even with this advantage over traditional manufacturing methods, understanding the behavior and response of additively

manufactured materials under different loading conditions is vital for designing parts that will safely and effectively execute their designed mission. In addition, knowing how the material fails allows proper care to be taken to ensure that components are properly maintained and removed from service before ultimate failure happens based on design parameters and predictive models. The mechanical response of additively manufactured Ti 6-4 under different loading conditions was investigated to look into the mechanical properties and failure response of the material.

### **1.3 Research Questions**

The main question asked during this research effort was to find out if build direction, surface finish, powder build height size, and temperature had any effect on the mechanical response of additively manufactured Ti 6-4 in tension, compression, and three point bend testing scenarios. This would be answered by conducting tensile tests, compression tests, and three point bend tests and recording the load and displacement values as the test was conducted. From this, stress and strain values for the three samples tested for each test case would be calculated and plotted on the same stress-strain graph for comparison. From here, relationships could be found regarding how temperature, surface finish, sample build height, and print orientation affected the materials response, look for trends, and draw conclusions from the results. The different test cases would be compared to see if:

- A certain print orientation had a superior mechanical response and greater resistance to failure compared to the other print directions for all the different tests
- To research if surface grinding was necessary for additively manufactured Ti 6-4 parts or if the part could be left unprepared after printing
- To see how the build height of the samples affected the mechanical properties of the samples
- To see the effects of elevated temperatures on the mechanical responses of the different samples

Focus was given to conducting testing on ground and unground room temperature samples with remaining time spent on high temperature conditions. Any high temperature conditions investigated were only considered using ground samples due to sample number limitations.

#### **1.4 Approach**

To better predict failure for additively manufactured Ti 6-4, tensile tests, compression tests, and three point bend tests were undertaken to investigate the mechanical response of the material. Samples were printed with a 30 micron and 60 micron build height with varying print orientations and tested with varying surface finishes and under different temperatures using the above test scenarios. From these experiments, data was collected and analyzed. In addition, tensile and compression samples were inspected using Scanning Electron Microscopy (SEM) to look at fracture

surfaces. The samples and sample powder were also inspected using Energy Dispersive X-ray Spectroscopy (EDS) to look at the elemental makeup of the Ti 6-4 samples and sample powder. In addition, the sample powder was investigated with the SEM to look at powder size and distribution. Lastly, the three point bend samples were ground and etched to compare the grain growth in the different build directions and under different temperatures.

### **1.5 Assumptions**

Additively manufactured materials experience anisotropic behavior due to the material being printed in one direction. Ti 6-4 is also an inherently anisotropic material. Based on these two reasons, the material was assumed to be anisotropic. Another major assumption made was that grinding the samples left no scratches that significantly contributed to crack generation and propagation. The ground samples were ground using a 220 grit grinding sheet but it was assumed further grinding using finer grit sizes would have no significant benefits to preventing crack generation and propagation from scratches introduced during the grinding process.

### **1.6 Preview**

Four subsequent chapters are discussed throughout the rest of this paper. Chapter two deals with the background and literature review of additively manufactured Ti 6-4. Chapter three presents the methodology of the research conducted. Chapter four looks at

analysis and presents results. Lastly, chapter five provides conclusions and offers recommendations.

## **II. Background and Literature Review**

### **2.1 Chapter Overview**

This chapter will review existing background and literature surrounding Ti 6-4 and additive manufacturing, specifically the additive manufacturing process known as direct metal laser sintering (DMLS). An analysis pertaining to the background of titanium and issues surrounding the metal will be conducted. In addition, the process by which metals are printed using DMLS, advantages of DMLS, and disadvantages of DMLS will be discussed. Lastly, current research surrounding additively manufactured Ti 6-4 will be investigated.

### **2.2 Material Background**

Titanium was discovered in the late 18<sup>th</sup> century. The material was first discovered in its natural “black sand” state which is a form of titanium oxide. Titanium oxide was not processed into pure titanium until the early 20<sup>th</sup> century. It was processed in small batches in the lab until 1932 when William Kroll was able to produce pure titanium by reducing titanium tetrachloride with calcium. He eventually tuned the process by using magnesium and sodium. This process became known as the Kroll process and was used as the main method to extract pure titanium from raw titanium ore. This process is still in use today. By the end of World War Two, the United States government started to pour money into research looking at titanium due to its potential use in the emerging aerospace field. Eventually, Grade 5 (Ti 6Al-4V) was developed [3]. This alloy continues

to be the predominant alloy used in the aerospace field due to its corrosion resistance, high strength to density ratio, and high temperature resistance. Ti 6-4 contains 90 percent titanium, 6 percent aluminum, and 4 percent vanadium. Chemical and mechanical properties of titanium, aluminum, and vanadium can be found below in Table 1 [4] [5].

**Table 1. Chemical and Mechanical Properties of Titanium, Aluminum, and Vanadium [4] [5]**

	Titanium	Aluminum	Vanadium
<b>Symbol</b>	Ti	Al	V
<b>Atomic Number</b>	22	13	23
<b>Atomic Mass (g/mol)</b>	47.867	26.982	50.941
<b>Density (g/cm<sup>3</sup>)</b>	4.51	2.7	6.1
<b>Melting Point (°C)</b>	1660	660	1910
<b>Boiling Point (°C)</b>	3287	2467	3407
<b>Vickers Hardness</b>	60	15	170
<b>Ultimate Strength (MPa)</b>	220	90	800
<b>Yield Strength (MPa)</b>	140	30	776
<b>Modulus of Elasticity (GPa)</b>	116	68.0	125.5
<b>Poissons Ratio</b>	0.34	0.36	0.36
<b>Electrical Resistivity (ohm-cm)</b>	0.0000554	0.00000270	0.0000248
<b>Magnetic Susceptibility</b>	0.00000125	6.0e-7	0.0000014
<b>Specific Heat Capacity (J/g-°C)</b>	0.528	0.900	0.502
<b>Thermal Conductivity (W/m-K)</b>	17.0	210	31.0

## **2.3 Material Issues**

Titanium has many desirable qualities, but some of the biggest challenges surrounding the material is the ability to safely work with it and machine it. Titanium is a reactive powder. This is an inherent concern when working with titanium powder as it can easily combust or explode. Titanium is also known to react with cutting tools making it difficult to work with while machining. Due to titanium's low thermal conductivity, excessive amounts of heat can build up on the cutting tool. This usually is not an issue in other materials like steel and aluminum due to the chips that form during the cutting process that absorb the heat. Titanium does not produce chips easily so all the heat is absorbed by the cutting tool. This requires the cutting tool to be made of a material that can withstand the high temperatures that are a byproduct of the cutting process. These issues lead to titanium's machining costs to account for 40-50 percent of the total cost to manufacture titanium [3].

## **2.4 Additive Manufacturing Background**

These issues, in addition to issues arising in manufacturing certain titanium parts and shapes using traditional manufacturing methods, are why additive manufacturing is an important new manufacturing method to research. Opportunities in which it may be able to supplement and potentially one day dominate the manufacturing methods commonly used to create Ti 6-4 today is one of the main reasons such research is important. One common method used to additively manufacture parts is direct metal laser sintering (DMLS). This method is commonly used because almost any metal alloy can be

printed. The process works by having a sliding arm spread a fine metal powder layer out on a print surface. A laser travels across the print surface and sinters, or fuses, the powder together that follows the shape of the part being manufactured. The shape is determined by uploading a computer aided design (CAD) drawing to the printer. This CAD drawing is sliced into numerous two dimensional layers by slicing software. These layers are then fed into the printer. The printer builds the part based of this input one layer at a time [6]. After the first layer is completed, the part is lowered, another layer of powder is spread out on the print surface, and the process is repeated many times until the part is completed [7]. Once the build is completed, the part is removed from the build plate typically using wire electrical discharge machining (EDM). Figure 1 below displays the process followed to create a part using DMLS [8] and Figure 2 shows a diagram of the DMLS manufacturing setup [9].

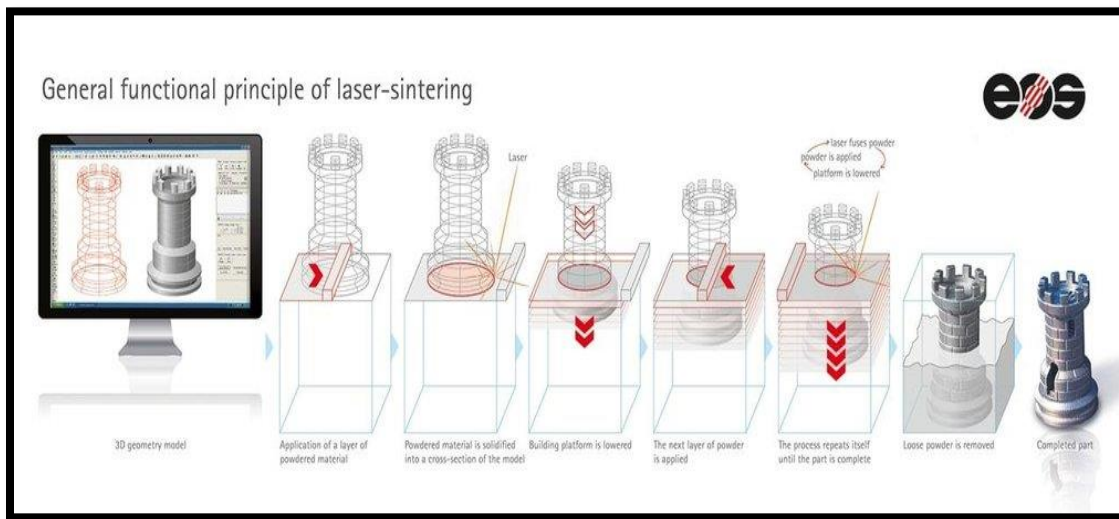


**Figure 1. DMLS Process [8]**

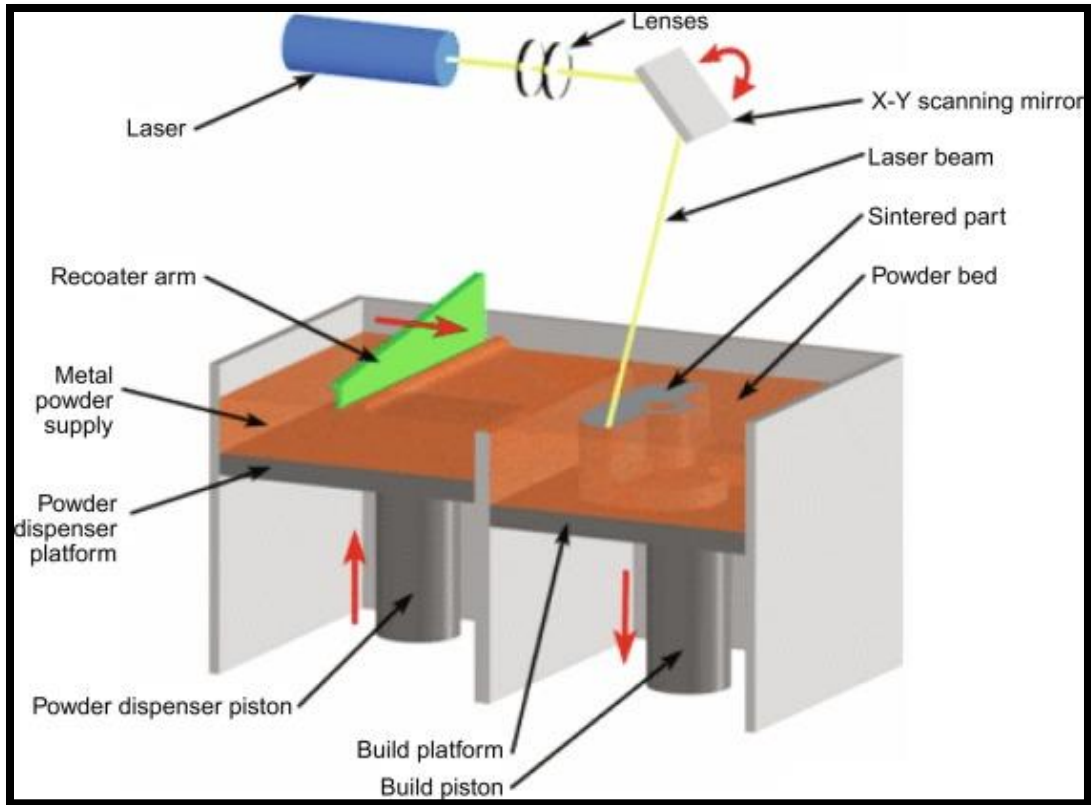


**Figure 2. DMLS Manufacturing Setup Diagram [9]**

### **2.5 Additive Manufacturing Advantages**

During the printing process, the metal powder is not melted, it is sintered. Sintering is defined as “the process of forming a solid mass of material through heat and pressure without melting to the point of liquefaction [10].” This is advantageous since materials can be printed with multiple elements that have different melting temperatures. Another advantage to sintering is that the metal powder is not fully melted, it only heats the powder enough to cause the layers to weld together. This requires less energy during the printing process [11]. DMLS also prints parts that limit residual stresses and internal defects [6]. Due to the repetitive nature of the fusing process used in DMLS, the part has

a 99.9% uniform density throughout the entire structure. In addition, the parts quick solidification rate after the metal powder is fused to another layer produces a fine crystalline structure with a higher strength value when compared to other manufacturing methods [7]. Additive manufacturing also has the advantage over traditionally manufactured materials since the process can create internal structures that cannot be traditionally manufactured. Lastly, an additively manufactured part can be pre-fabricated and finished by a machinist which saves fabrication time.

## **2.6 Additive Manufacturing Disadvantages**

Even with additive manufacturing's advantages, there are some shortcomings. The biggest downfall to additive manufacturing is the cost associated. DMLS is less expensive when compared to other additive manufacturing methods but the upfront costs to buy printing machines and the recurring costs of metal powders is very expensive. This is one of the main reasons only small parts and prototypes are currently produced using additive manufacturing techniques. Another big issue with additive manufacturing is that printed parts are more susceptible to porosity when compared to traditionally manufactured parts. These internal defects can lead to premature part failure due to cracks developing and propagating with less resistance when compared to traditionally manufactured parts. Next, additive manufacturing is size restricted. Small build plate sizes limit the dimensions of parts to usually not much larger than one foot cubed. This limits the scale of parts that can be printed and put into service throughout different industries. Lastly, additive manufacturing requires post-processing. Parts need to be wire

EDM cut from build plates since parts are directly welded to the build plate. Sharp rough edges from the manufacturing process also need to be removed. Some materials, like titanium, print with a rough surface that potentially needs to be removed to create a smooth surface. All this just adds to the cost and time associated with additive manufacturing [12].

## 2.7 Current Research Efforts

There is an abundance of research right now looking into additively manufactured Ti 6-4 and the best ways to print the material. One of the biggest concerns while printing the material is the presence of acicular  $\alpha'$  martensite caused by certain additive manufacturing methods when the metal powder is melted. This is seen in manufacturing methods like selective laser melting. The acicular  $\alpha'$  martensite develops in the material due to the rapid cooling of the melted pool during manufacturing. This cooling rate is in the range of 1000 to 100,000 K/s. This is above the 410 K/s critical cooling rate needed for martensitic transformation. On top of this, a thermal gradient in the 10,000 to 100,000 K/cm range exists in the build direction. This leads to columnar prior- $\beta$  grains, which cause intergranular failure when near acicular  $\alpha'$  martensitic grains. This issue also leads to reduced ductility when compared to other additive manufacturing methods. It has been found that variables used in the selective laser melting process like energy density, layer thickness, and focal offset distance have a large impact on the ability for equilibrium  $\alpha$  and  $\beta$  phases to form during manufacturing [13].

Research is also looking into how the surface finish of the additively manufactured part affects its surface and subsurface. It was found that the postproduction, such as different turning actions, has a large impact on the surface integrity of the final part. The results found that machining processes used for traditionally manufactured materials are not well suited for additively manufactured materials and need to be modified [14]. As stated by the authors, “the presented work demonstrates that the machining process leads to differing percentages of microstructural, topographical, and mechanical alterations on the surface due to the initial production techniques [14].”

Research has also shown that components have distinct areas with differing microstructures that lead to non-uniform mechanical responses. This shows that additively manufactured parts have randomly scattered defects [15] [16]. It was found that additively manufactured parts had a large difference compared to traditionally manufactured materials when considering the mechanical response and characteristics of the microstructure. The severity of the thermal gradient that develops during manufacturing also has a large impact on the microstructure of the material such as grain sizes [15].

The effects of surface roughness on the fatigue life of the material is also very important and is an area of high interest and study. Researchers are considering how different grinding and polishing methods affect the surface roughness and the fatigue life of additively manufactured Ti 6-4 parts. A few researches investigated how blasting, micro machining, milling, and vibratory grinding affected the fatigue behavior of Ti 6-4 samples. It was found that surface roughness depends greatly on the build direction of the

part. This rough surface leads to a fatigue performance with a stress amplitude of 300 MPa over  $3 \times 10^7$  cycles. The best results were seen with a milled surface. This led to the stress amplitude increasing to 775 MPa over  $3 \times 10^7$  cycles. The next best results were seen in the blasted samples that showed fatigue performance could be improved to a stress amplitude of 525 MPa after  $3 \times 10^7$  cycles when compared to unground samples. This was due to a rougher surface present for the blasted samples after polishing when compared to the milled samples (surface roughness of  $10.1 \mu\text{m}$  versus a surface roughness of  $0.3 \mu\text{m}$  respectively). The researchers were unable to find any direct correlation between surface roughness and fatigue life, even though a general relationship was seen. This was due to certain polishing processes affecting the intrinsic material properties and internal stresses [17]. Other research efforts have also looked into this phenomenon and found similar results [18] [19].

Lastly, researchers investigated post processing heat treatment options to remove the fine, acicular, fully martensitic microstructure  $\alpha'$  phase. This phase has a high ultimate strength and a high yield strength but exhibits lower ductility. The researchers attempted to remove this thin brittle layer while limiting the loss of ductility in the material. They found that the size of the  $\alpha'$  phase had a major impact on the initial microstructure and heating temperature needed when concerned with the post production heat treatment. The size of the  $\alpha'$  phase did not change after a heat treatment of  $600^\circ\text{C}$  over two hours or  $730^\circ\text{C}$  over two hours. Only above  $900^\circ\text{C}$  over two hours was growth in the  $\alpha'$  phase seen. They also found that the cooling rate did not have a large effect on the mechanical properties of the heat treated samples [20].

## **2.8 Summary**

In this chapter, background pertaining to the material, specifically titanium, and the overall additive manufacturing process for DMLS was discussed. The advantages and disadvantages of additive manufacturing were investigated, specifically looking at DMLS. Lastly, current research looking into additively manufactured Ti 6-4 was discussed.

### **III. Methodology**

#### **3.1 Chapter Overview**

The purpose of this chapter is to discuss the methodology and processes used during the material printing, preparation, testing, data processing, and microscopy for the additively manufactured Ti 6-4 samples. Discussion will focus on these few areas and will go into detail regarding the processes and procedures followed.

#### **3.2 Manufacturing of Parts used in Research**

The parts used throughout this research effort were manufactured by i3DMFG based in Redmond, Oregon. The powder used to manufacture the parts was 20-40 micron sized powder that was fused together with 400 W lasers in one of the nine print machines the company currently uses [7]. The company uses DMLS machines to print parts for customers. They have a variety of different printing machines including two EOS M400-4 machines to print parts [21]. Figure 3 below shows an example of these machines [22].



**Figure 3. EOS M400-4 Printing Machine [22]**

These machines are very versatile and can print a multitude of materials into complex geometries. Table 2 below shows the technical data associated with these machines [23].

**Table 2. EOS M400-4 Additive Manufacturing Printer Specifications [23]**

<b>Construction Volume</b>	400 x 400 x 400 mm (height includes build plate)
<b>Laser Type</b>	Yb-fiber laser; 4 x 400 W
<b>Precision Optics</b>	4 F-theta-lenses; 4 high-speed scanners
<b>Scan Speed</b>	up to 7.0 m/s
<b>Focus Diameter</b>	approximately 100 $\mu\text{m}$
<b>Power Supply</b>	3 x 50 A
<b>Power Consumption</b>	max 45 kW / typical 22 kW
<b>compressed air supply</b>	7000 hPa; 20 m <sup>3</sup> /h
<b>Machine Dimensions (W x D x H)</b>	4181 x 1613 x 2355 mm
<b>Recommended Installation Space</b>	min 6.500 x 6.000 x 3.300 mm
<b>Weight</b>	approximately 4835 kg
<b>Software</b>	EOSPRINT 2, EOSTATE PowderBed, EOSCONNECT Core, EOSCONNECT MachinePark, Materialise Magics Metal Package and modules

During the additive manufacturing process used to manufacture the parts for the experiments, the printing machines were set to specific print parameters. These print parameters varied for the 30 and 60 micron build height samples. Table 3-Table 4 below shows the print parameters used to print the 30 and 60 micron build height samples [24].

**Table 3. 30 Micron Build Height Print Parameters [24]**

<b>Options Under Stripes</b>		<b>Options Under Up Down</b>	
<b>Distance (mm)</b>	0.14	<b>Upskin Distance (mm)</b>	0.14
<b>Speed (mm/s)</b>	1200	<b>Upskin Speed (mm/s)</b>	1200
<b>Power (W)</b>	280	<b>Upskin Powder (W)</b>	280
<b>Beam Offset (mm)</b>	0.015	<b>Upskin Thickness (mm)</b>	0.09
<b>Stripe Width (mm)</b>	5.0	<b>Downskin Distance (mm)</b>	0.10
<b>Stripes Overlap (mm)</b>	0	<b>Downskin Speed (mm/s)</b>	1000
<b>Hatching X</b>	On	<b>Downskin Powder (W)</b>	120
<b>Hatching Y</b>	Off	<b>Downskin Thickness (mm)</b>	0.06
<b>Skywriting</b>	On	<b>Upskin and Downskin X</b>	On
<b>Offset</b>	On	<b>Upskin and Downskin Y</b>	On
<b>Altering</b>	Off	<b>Upskin and Downskin Altering</b>	Off
<b>Rotated</b>	On	<b>Skywriting</b>	On
		<b>Overlap with Inskin (mm)</b>	0
		<b>Min Length (mm)</b>	0.30

**Table 4. 60 Micron Build Height Print Parameters [24]**

<b>Options Under Stripes</b>		<b>Options Under Up Down</b>	
<b>Distance (mm)</b>	0.12	<b>Upskin Distance (mm)</b>	0.12
<b>Speed (mm/s)</b>	1250	<b>Upskin Speed (mm/s)</b>	1250
<b>Power (W)</b>	340	<b>Upskin Powder (W)</b>	340
<b>Beam Offset (mm)</b>	0.025	<b>Upskin Thickness (mm)</b>	0.12
<b>Stripe Width (mm)</b>	5.0	<b>Downskin Distance (mm)</b>	0.07
<b>Stripes Overlap (mm)</b>	0	<b>Downskin Speed (mm/s)</b>	1100
<b>Hatching X</b>	On	<b>Downskin Powder (W)</b>	160
<b>Hatching Y</b>	Off	<b>Downskin Thickness (mm)</b>	0.12
<b>Skywriting</b>	On	<b>Upskin and Downskin X</b>	On
<b>Offset</b>	On	<b>Upskin and Downskin Y</b>	On
<b>Altering</b>	Off	<b>Upskin Altering</b>	Off
<b>Rotated</b>	On	<b>Downskin Altering</b>	On
		<b>Skywriting</b>	On
		<b>Overlap with Inskin (mm)</b>	0
		<b>Min Length (mm)</b>	0.30

All the 30 micron build height samples were manufactured together on one build plate. This is also true for the 60 micron build height samples. Figure 4 below displays the layout of the build plate with the location of all the samples manufactured [24].

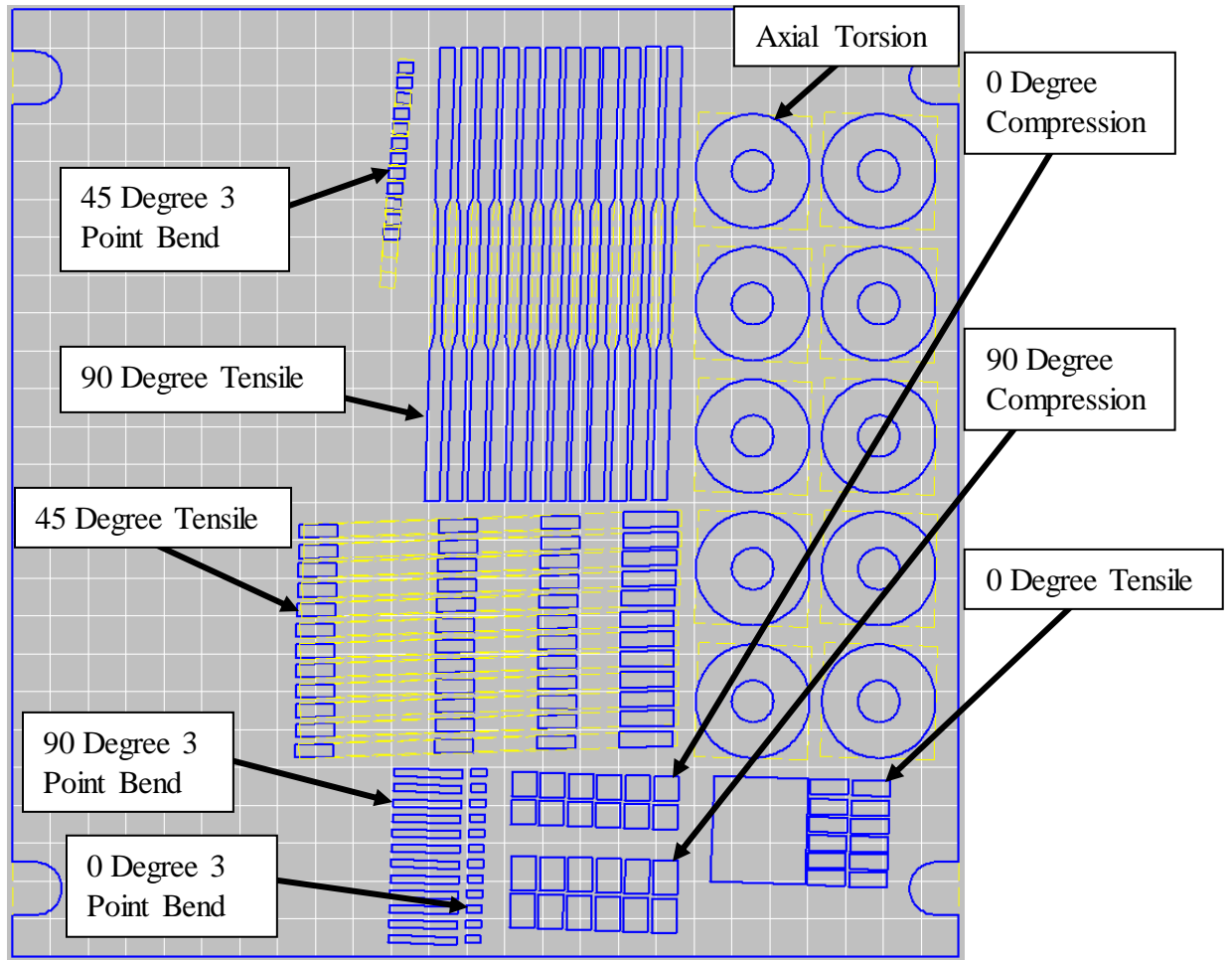


**Figure 4. 30 and 60 Micron Build Height Sample Build Plate [24]**

As seen above in Figure 4, the samples are slightly angled. This is so the wiper does not move over a long surface all at once. The yellow areas shown above are thin webs that were added to support the samples during the printing process. The samples above were printed in 0 degree, 45 degree, and 90 degree orientations. Figure 5 below displays the directions of the different print orientations.

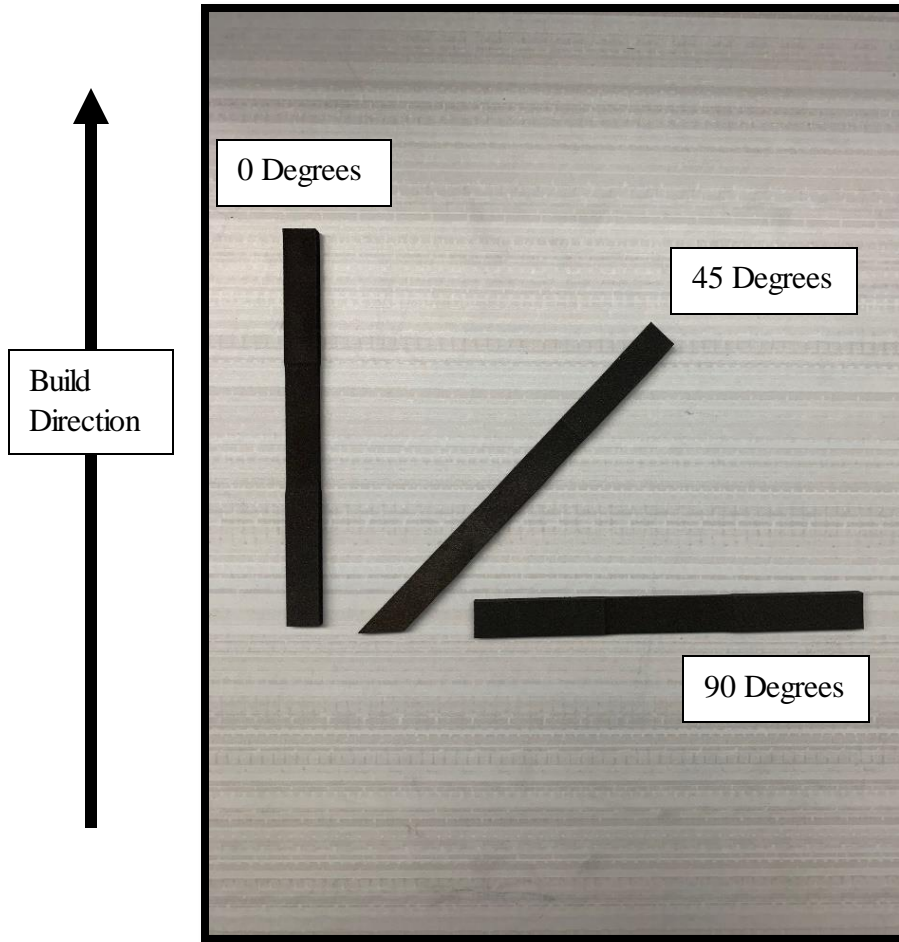


**Figure 5. Build Directions of Samples Printed**

Once the samples were received from the manufacturer, they were sorted based on certain parameters. These parameters were test type, print direction, temperature, surface finish, and sample build height. Table 5 shown below illustrates the test types, print directions, temperatures, surface finishes, and number of samples tested for the 30 and 60 micron build height samples.

**Table 5. Sample Characteristics for 30 and 60 Micron Powder Build Height Samples**

	<b>Test Temperatures</b>	<b>Surface Finishes</b>	<b>Number of Samples Tested For Each Test</b>
<b>Three Point Bend 0 Degree</b>	Room Temperature	Ground	3
<b>Three Point Bend 45 Degree</b>	Room Temperature	Ground	3
<b>Three Point Bend 90 Degree</b>	Room Temperature	Ground	3
<b>Three Point Bend 0 Degree</b>	Room Temperature	Unground	3
<b>Three Point Bend 45 Degree</b>	Room Temperature	Unground	3
<b>Three Point Bend 90 Degree</b>	Room Temperature	Unground	3
<b>Three Point Bend 0 Degree</b>	800 °C	Ground	3
<b>Three Point Bend 45 Degree</b>	800 °C	Ground	3
<b>Three Point Bend 0 Degree</b>	800 °C	Ground	3
<b>Compression 0 Degree</b>	Room Temperature	Ground	3
<b>Compression 90 Degree</b>	Room Temperature	Ground	3
<b>Compression 0 Degree</b>	Room Temperature	Unground	3
<b>Compression 90 Degree</b>	Room Temperature	Unground	3
<b>Tensile 0 Degree</b>	Room Temperature	Edges Ground	3
<b>Tensile 45 Degree</b>	Room Temperature	Edges Ground	3
<b>Tensile 90 Degree</b>	Room Temperature	Edges Ground	3

All the samples for the same test type had the same dimensions in the CAD drawing that was sliced and input into the printer. Figure 6-Figure 8 below show the dimensions of the compression cubes, tensile bars, and three point bend bars. The compression cubes were printed with a square cross section instead of a circular cross section due to the printability advantages of the square cross section parts.

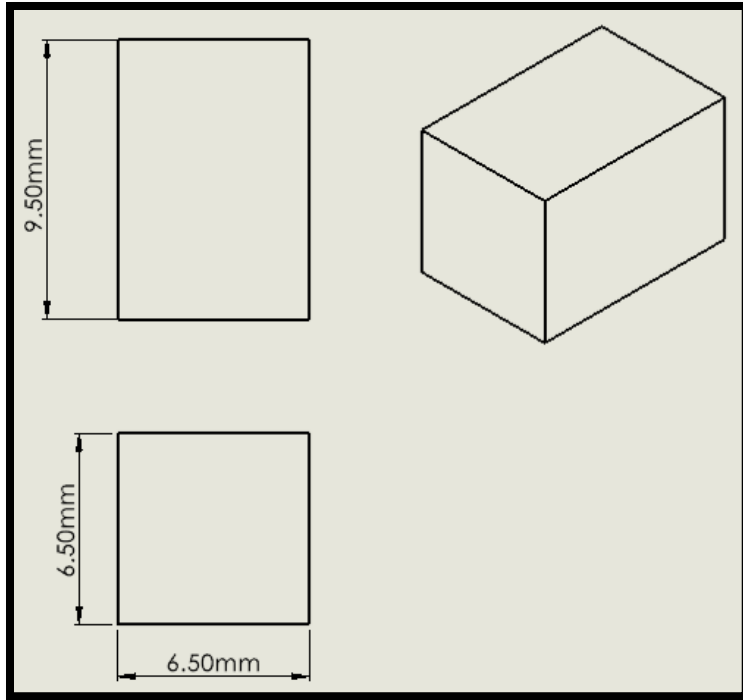


**Figure 6. Compression Cube Dimensions**

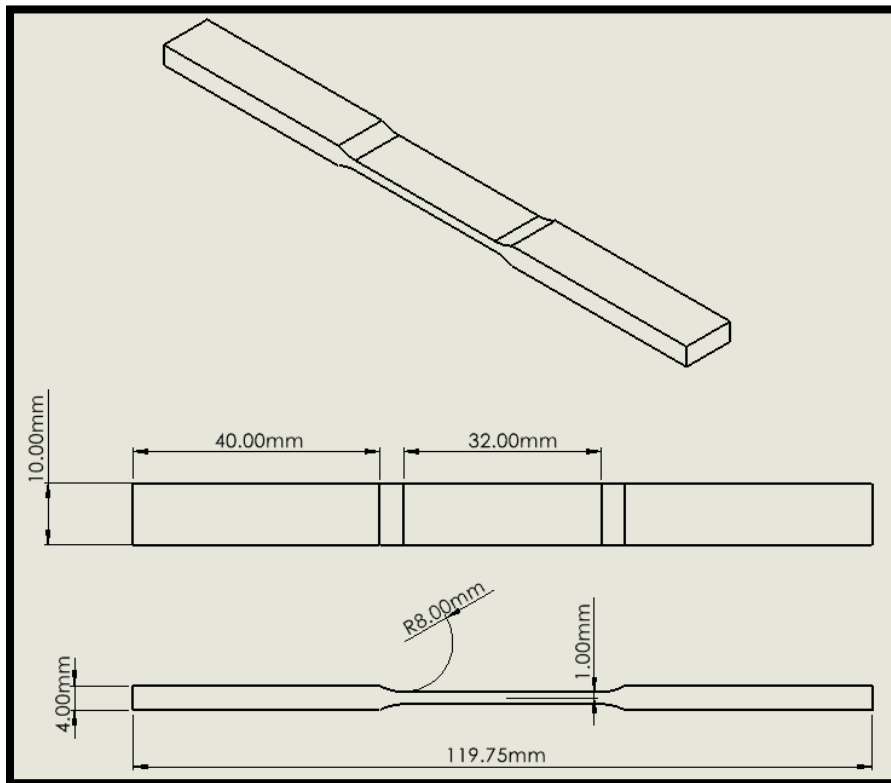


**Figure 7. Tensile Bar Dimensions**

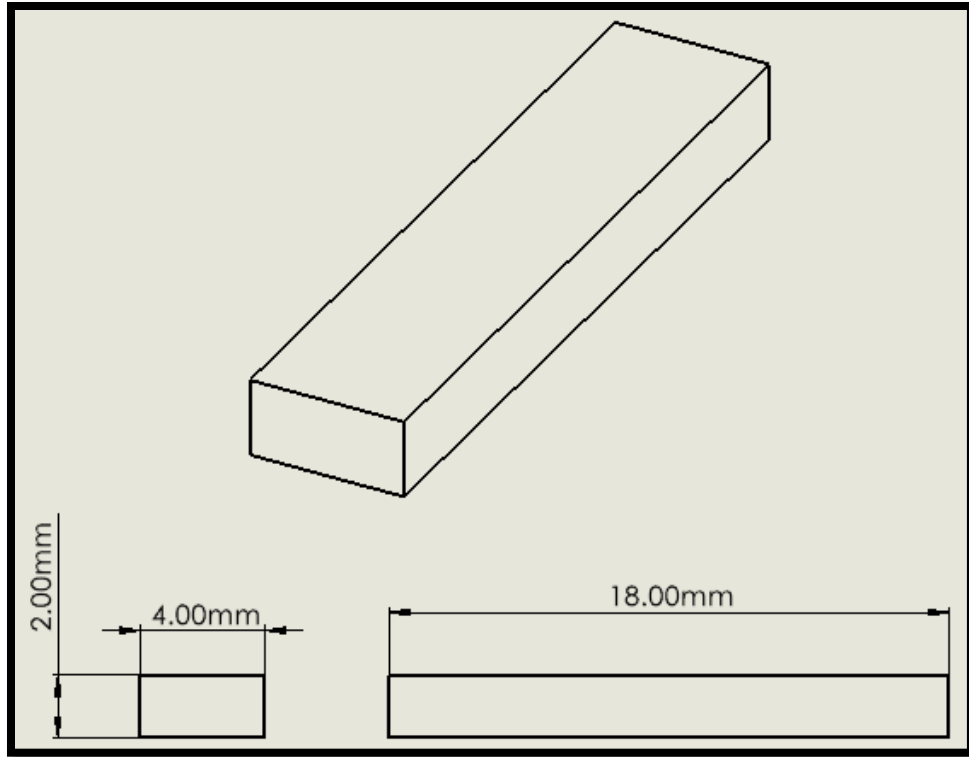


**Figure 8. Three Point Bend Bar Dimensions**

### **3.3 Sample Preparation**

All the samples were measured after printing and grinding (unground samples were measured after printing only) to record accurate dimensions for use in analysis and calculations due to small variations in the specimen dimensions resulting from the manufacturing process (these dimensions are presented in Appendix A). After the measurements were taken, the samples marked for grinding were ground using a Buehler Ecomet 300 grinding and polishing machine. Figure 9 below shows the machine used for grinding.



**Figure 9. Buehler Ecomet 300 Grinding and Polishing Machine**

The machine was set to a rotating speed of 180 revolutions per minute (rpm) for the tensile bars while the three point bend bars and compression cubes were set to a speed of 120 rpm. This was due to the smaller compression and three point bend samples being harder to grip during grinding at higher rotational speeds. The samples were ground using 240 grit silicon carbide sandpaper sheets. The samples were ground until all the rough surface from the manufacturing process was removed and no rough surfaces remained. Once this was done, the ground samples were cleaned with tap water and dried with a paper towel. An example of the surface finish for the unground and ground samples can be seen in Figure 10 below. Both the 30 and 60 micron ground and unground build samples had this finish to the naked eye.

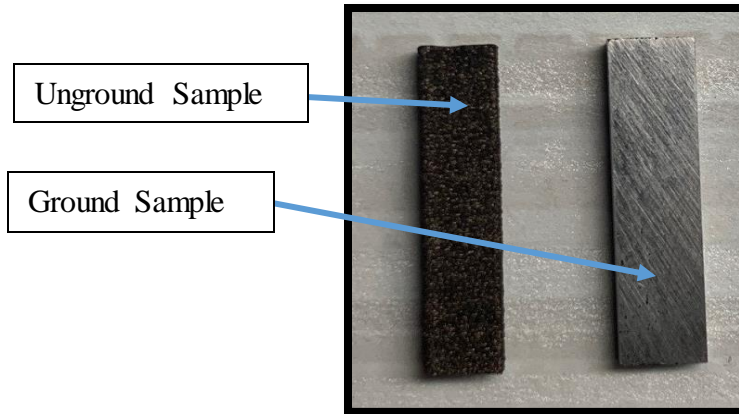


**Figure 10. Ground and Unground Three Point Bend Specimens**

### **3.4 Three Point Bend Testing**

Once the samples were prepped, three point bend tests were conducted at room temperature and at 800 degrees Celsius. A temperature of 800 degrees Celsius was chosen since the high temperature limit commonly used when working with Ti 6-4 is around 800 to 850 degrees Celsius. To conduct a three point bend test, the middle of a test specimen is pushed down with a point or roller while the two ends of the sample are not allowed to translate due to the ends being simply supported. The head displacement, force applied to the sample, and test run time are usually recorded during the test. The head displacement and force applied to the sample allows for flexural stress and flexural strain to be calculated. The three point bend tests were conducted using an MTS 22 kip servo-hydraulic load frame shown in Figure 11 below.

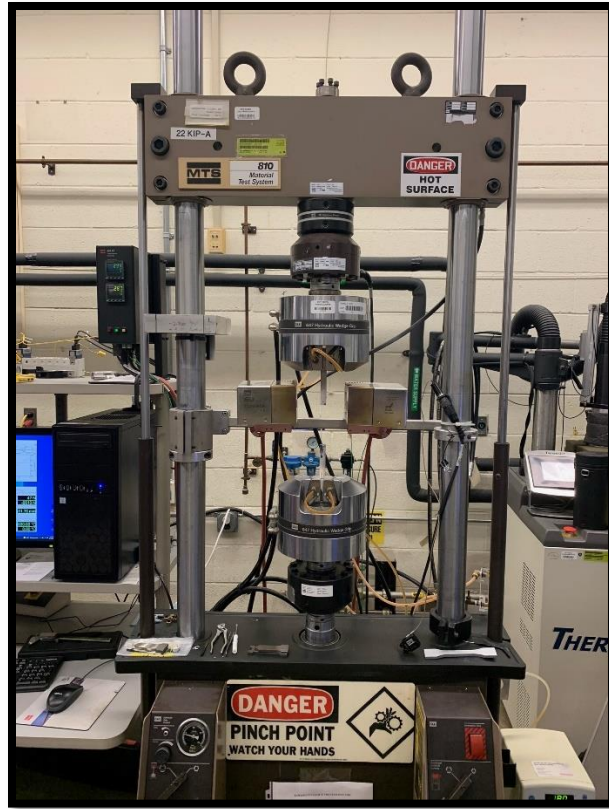


**Figure 11. MTS 22 kip Load Frame used for Three Point Bend Tests**

The samples were tested using specialty fabricated three point bend test fixtures machined by the Air Force Institute of Technology (AFIT) machine shop. These Inconel fixtures were used due to their high melting temperature since room and high temperature tests were conducted. Once these test fixtures were loaded into the machine, a test sample was loaded into a slot in the test fixture that resisted the sample from displacing down at the edges but allowed movement in the middle of the sample. The gap between the ends of the fixture was 14 mm. This was the span used throughout the testing and analysis process for all the three point bend specimens. Once the specimen was loaded, the force offset was set to zero and the bottom fixture was brought up until the control computer registered a jump in force from the fixture point coming in contact with the test specimen.

The displacement and force offsets were set to zero again and the test was conducted. The bottom fixture was brought up at a rate of 0.009 mm per second until the sample fractured and could not bear anymore load. Displacement of the bottom head moving up, force applied to the sample, and test run time were recorded during the test. This process was repeated for the ground and unground three point bend test samples at room temperature for the 0, 45, and 90 degree print orientations for both the 30 and 60 micron build height samples. Figure 12 shown below shows an example of one of the room temperature three point bend samples during testing.



Three Point Bend Test Specimen

**Figure 12. Room Temperature Three Point Bend Test Sample during Testing**

For the high temperature samples, a furnace was used to heat the individual samples to 800 degrees Celsius. Each sample was heated for 25 minutes until it reached a steady temperature of 800 degrees Celsius. Once this was done, the test was run the same way as for the room temperature samples. 0, 45, and 90 degree print orientation ground samples were tested at 800 degrees Celsius for both the 30 and 60 micron build height samples. None of the samples broke due to the high temperature causing the samples to experience more ductility so the test was terminated after the bottom fixture displaced up 3.6 mm. Figure 13 shown below shows an example of one of the high temperature three point bend samples during testing.

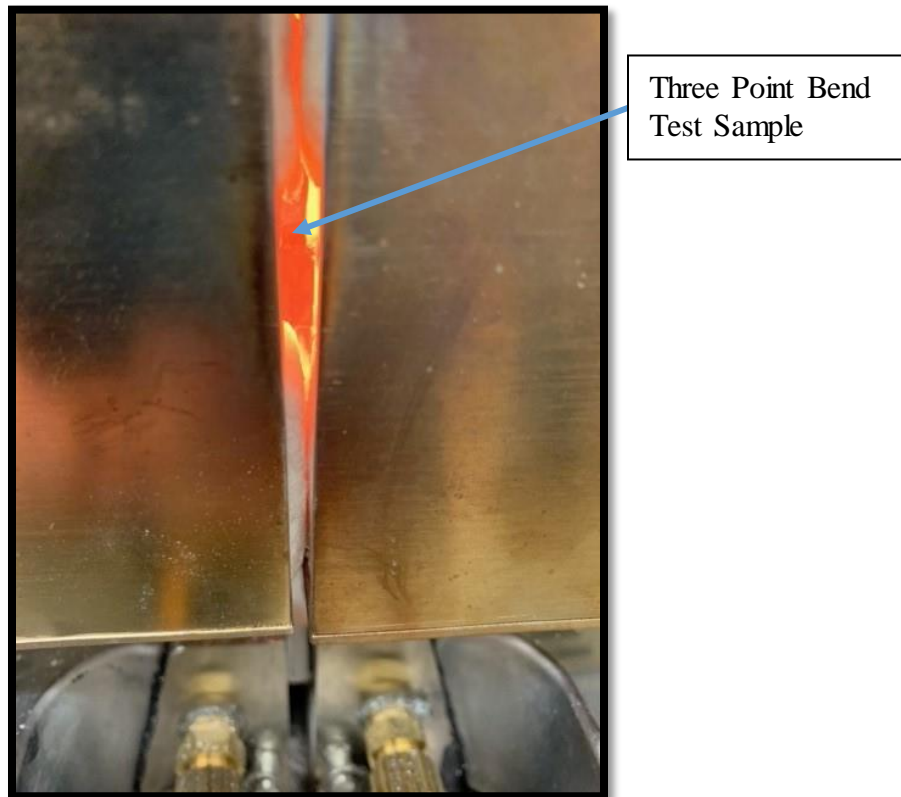


**Figure 13. High Temperature Three Point Bend Test Sample during Testing**

### 3.5 Compression Testing

The next samples to be tested were the compression cubes at room temperature. A compression test works by holding the sample flat on a bottom platen and bringing up a large bottom platen to compress the sample. The head displacement, force applied to the sample, and test run time are usually recorded during the test. The head displacement and force applied to the sample allows for compressive stress and compressive strain to be calculated. The compression tests were conducted using an MTS 110 kip servo-hydraulic load frame shown in Figure 14 below.



**Figure 14. MTS 110 kip Load Frame used for Compression Tests**

All the compression cubes were tested at room temperature. 0 degree and 90 degree print orientation samples were tested. No 45 degree print orientation samples were manufactured or tested due to complexities associated with printing a thick cube at 45 degrees and being able to support the sample with support material during printing. Both ground and unground samples were tested for both the 30 and 60 micron build height samples.

To test a sample, one specimen was centered on the bottom platen in the compression test frame. The force offset was reset to zero on the control computer and the bottom platen was raised towards the top platen until the top platen came into contact with the specimen. This was detected by a jump in the force being applied to the sample. Once a force was detected, the force and displacement offsets were reset to zero and the test was run. The bottom platen was brought up at a rate of 0.009 mm per second until the sample fractured and could not bear anymore load. Displacement of the bottom head moving up, force applied to the sample, and test run time were recorded during the test. This process was repeated for the ground and unground compression test samples at room temperature in the 0 and 90 degree print orientations for both the 30 and 60 micron build height samples. Figure 15 shown below shows an example of one of the room temperature compression samples during testing.

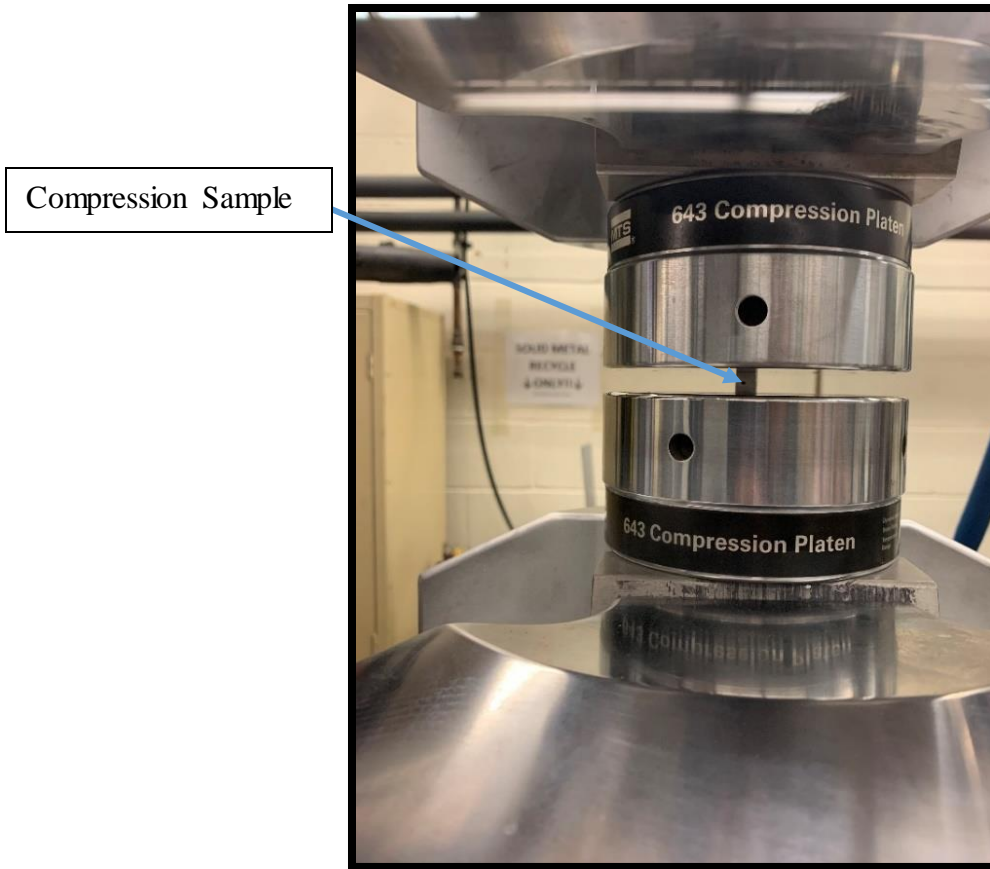


**Figure 15. Room Temperature Compression Test Sample during Testing**

### **3.6 Tensile Testing**

The next samples to be tested were the tensile test samples at room temperature. A tensile test works by holding the top and bottom of the test sample in the test machine's grips and pulling the sample apart until it fractures. The head displacement, force applied to the sample, and test run time are usually recorded during the test. An extensometer can also be used to measure the strain more accurately since the head displacement is not a very accurate measure of strain due to the fact that a load train deflects when a load is applied [25]. The head displacement or extensometer measured strain and force applied

to the sample allows for uniaxial tensile stress and uniaxial tensile strain to be calculated. The tensile tests were conducted using an MTS 11 kip servohydraulic load frame shown in Figure 16 below.

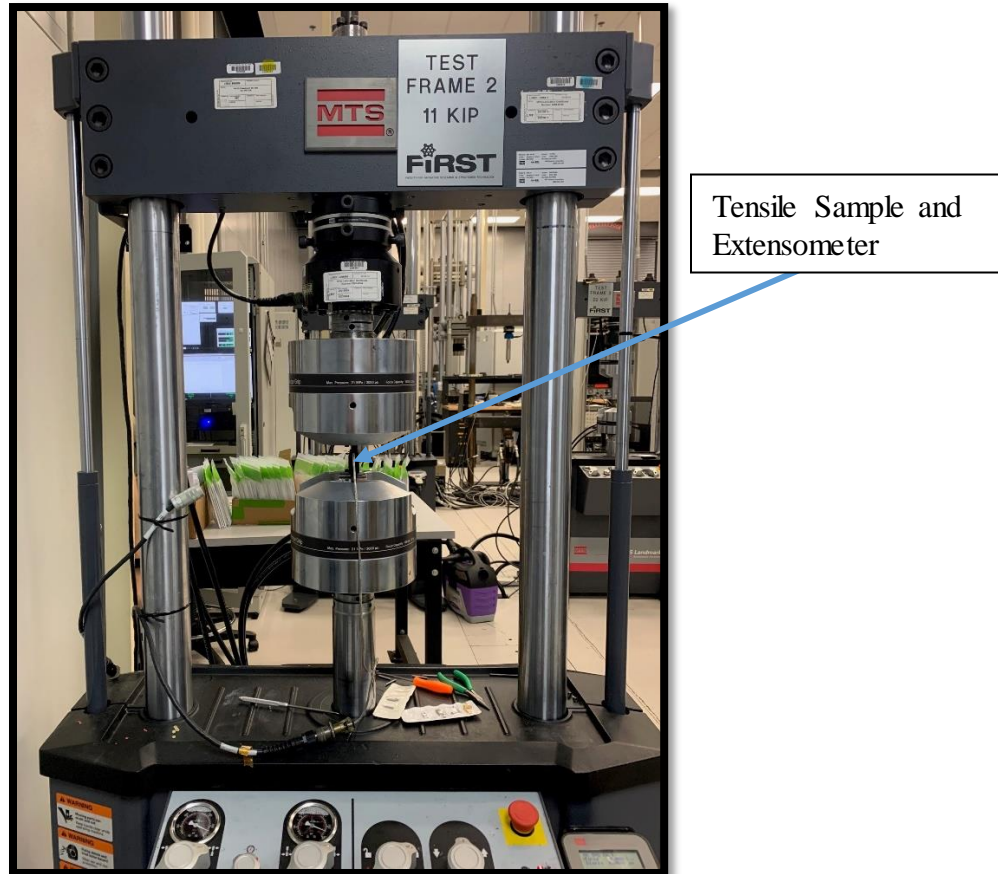


**Figure 16. MTS 11 kip Load Frame used for Tensile Tests**

The samples were printed as flat specimens with a necked down area in the center section of the samples. All the tensile samples were tested at room temperature. 0, 45, and 90 degree orientation print direction samples were tested for both the 30 and 60 micron build height samples. Only unground samples with the sides ground were tested.

The sides were ground on all the tensile samples to remove material left over from the cutting process used to detach the samples from each other after they were manufactured. To test a sample, the test frame was set back to the zero offset displacement position and one specimen was loaded into the top grip. Any force offset on the control computer was reset to zero and the control computer was verified to be in displacement control. The bottom grip was then closed while simultaneously putting the software into force control. This ensured that no force was imparted into the sample from the bottom grip closing which would introduce a force into the sample if the grip was just closed without putting the machine into force control at the same time. After this, the extensometer was attached to the front side of the sample with two springs to keep the extensometer in place. The extensometer was also rocked back and forth to make sure it was sitting flush on the sample. The force and displacement offsets was reset to zero on the control computer, the extensometer pin was pulled out, and the test was run. The bottom grip was brought down at a rate of 0.01 mm per second until the sample broke and could not bear anymore load. Displacement of the bottom grip moving down, force applied to the sample, and test run time were recorded during the test. This process was repeated for the remaining samples at room temperature in the 0, 45, and 90 degree print orientations for both the 30 and 60 micron build height samples. Figure 17 shown below shows an example of one of the room temperature tensile samples during testing.

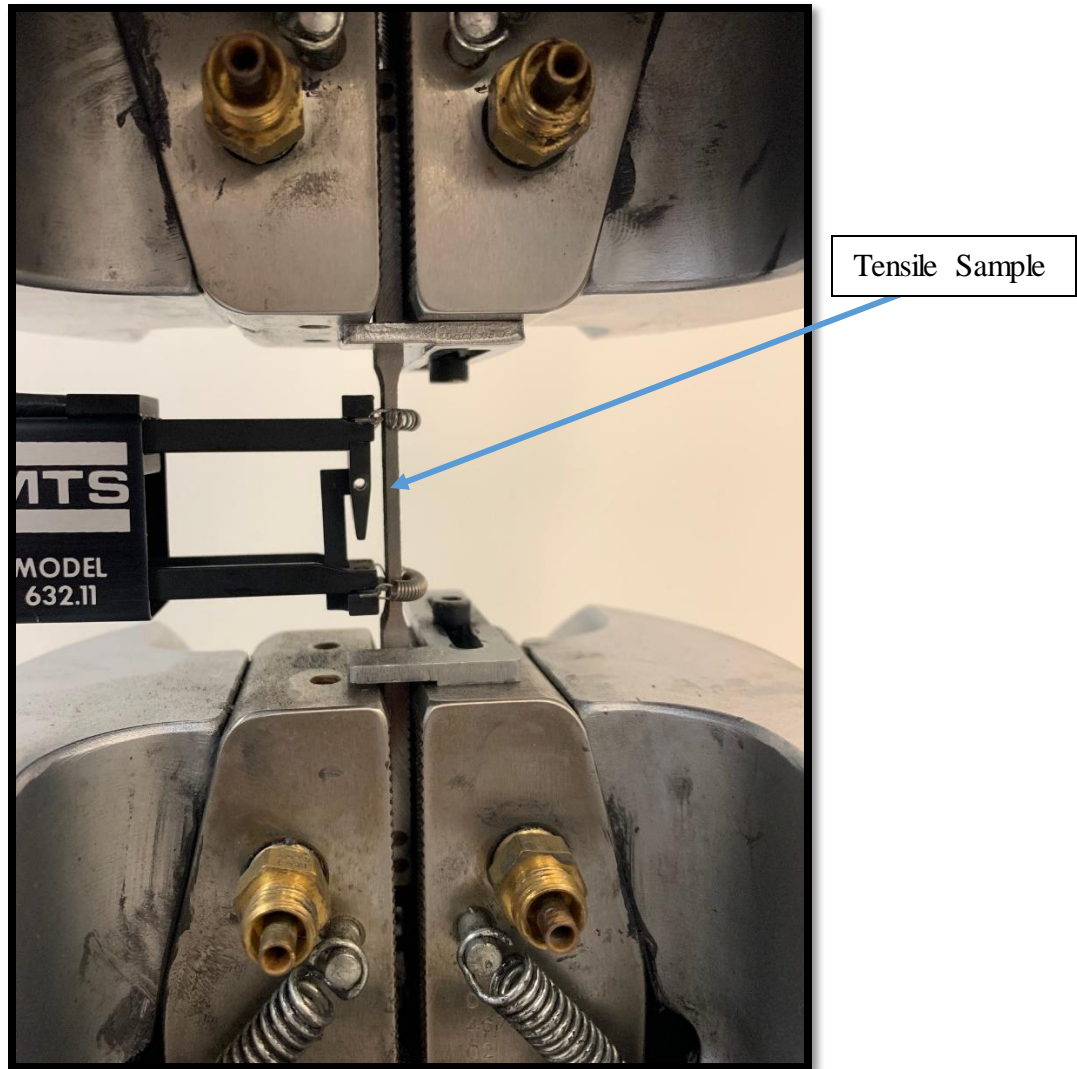


**Figure 17. Room Temperature Tensile Test Sample during Testing**

### **3.7 Data Processing**

To find the flexural stress from the three point bend tests, the axial force (kN), span (mm), width (mm), and thickness (mm) were found. Equation 1 [26] shows how flexural stress (MPa) is calculated. In the equation,  $\sigma$  is the flexural stress, F is the axial force, L is the span, w is the width, and t is the thickness.

$$\sigma = \frac{3FL}{2wt^2} \quad (1)$$

To find the flexural strain from the three point bend tests, the span (mm), axial displacement (mm), and thickness (mm) were found. Equation 2 [26] shows how flexural strain (mm/mm) is calculated. In the equation,  $\varepsilon$  is the flexural strain,  $D$  is the axial displacement,  $L$  is the span, and  $t$  is the thickness.

$$\varepsilon = \frac{6Dt}{L^2} \quad (2)$$

To find the compressive and tensile stress from the compressive and tensile tests, the axial force (kN) and area (mm<sup>2</sup>) were found. Equation 3 [27] shows how compressive and tensile stress (MPa) is calculated. In the equation,  $\sigma$  is the compressive and tensile stress,  $F$  is the axial force, and  $A$  is the cross sectional area.

$$\sigma = \frac{F}{A} \quad (3)$$

To find the compressive and tensile strain from the compressive and tensile tests, the change in length (mm) and original length (mm) were found. Equation 4 [27] shows how compressive and tensile strain (mm/mm) is calculated. In the equation,  $\varepsilon$  is the axial strain,  $\Delta L$  is the change in length, and  $L_o$  is the original length.

$$\varepsilon = \frac{\Delta L}{L_o} \quad (4)$$

Matlab code was created to take in the load or stress and displacement or strain data in any combination from the different tests. The code calculated stress and strain values while also creating stress-strain plots for all the tests. The code had the ability to smooth noisy data and downsample data when the collection rate was too high during testing to ensure efficient computation time. The code could pull information from the stress-strain data such as ultimate stress/strain, fracture stress/strain, modulus of elasticity, yield stress/strain, and others just to name a few while also having the ability to omit certain data points not needed or that were not relevant. The code also generated average values, standard deviations, and confidence intervals for multiple iterations of the same type of test with different samples.

### **3.8 Microscopy**

The next step was to perform microscopy on the samples. The first samples investigated were the tensile samples and the compression samples in the SEM. The fracture surfaces were looked at and photos were taken to determine fracture mechanisms for the different test samples. Both the 30 and 60 micron build height tensile and compression samples were investigated with the Tescan MAIA3 SEM/EDS shown below in Figure 18.



**Figure 18. Tescan MAIA3 SEM**

Once this was done, 30 and 60 micron build height tensile samples were investigated using EDS to determine the elemental makeup of the samples to verify the elemental percentages in the Ti 6-4 samples were correct. After this, the powder used to manufacture the samples was investigated in the SEM to look at the size and distribution of the powder. The powder was also investigated using EDS to verify the elemental makeup of the powder. In addition, the powder was looked at to see if any impurities were present in the powder.

The next task undertaken was to puck, grind, and etch the three point bend samples. One three point bend sample from each build height, surface finish, print direction, and temperature was pucked in multiple carbon pucks using a Metpress A

Automatic mounting press manufactured by MetLab Corporation shown below in Figure 19.

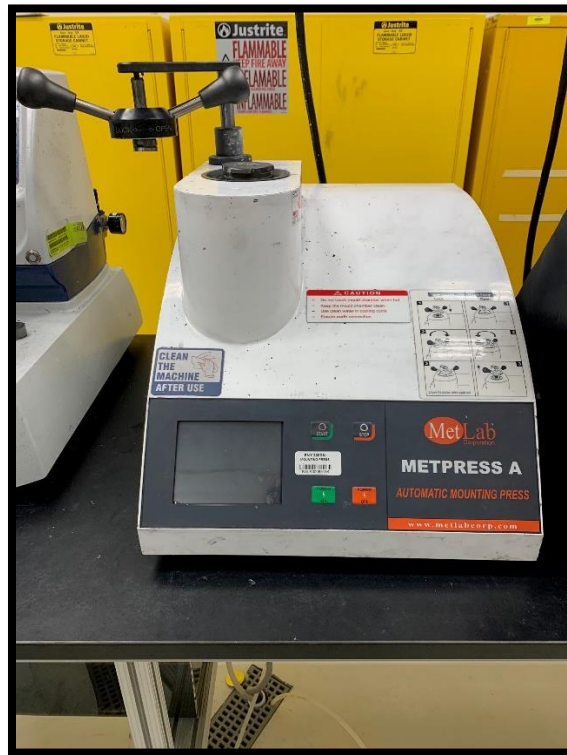


**Figure 19. Metpress A Automatic Mounting Press**

After the samples were pucked, they were ground using the Buehler Ecomet 300 grinding and polishing machine. Three 240 grit, three 320 grit, three 400 grit, three 600 grit, and three 800 grit silicon carbide sandpaper sheets were used to grind the samples. Each abrasive sheet was run for one minute then replaced. The polisher was run at 260 rpm and 25 N for each grinding step. In the future, using only two grinding sheets for each grinding step would be better since using three sheets completely ground through some of the samples and those samples had to be re-pucked and re-ground. Next, the

samples were ground for ten minutes using MetaDi Supreme polycrystalline diamond suspension nine micron polishing solution and a Buehler microfloc polishing cloth. This stage was run at 260 rpm and 20 N of applied force. After this step was completed, the samples were put into vibration table holders and placed on a Saphir Vibro vibration polishing table for 30 minutes. A Colloidal silica suspension polishing fluid with 30% hydrogen peroxide was used on the polishing table. In the future, it is recommended to leave the samples on the vibration table for 24 hours since it works very well to produce a mirror finish while barely removing any material.

After this, the samples were etched. The samples were etched using Kroll's agent which consisted of 93% distilled water, 6% nitric acid, and 1% hydrofluoric acid [28]. Each sample was etched for 20 seconds with Kroll's agent and then submerged in a solution of baking soda and water to stop the reaction. Once this was done, the samples were checked to make sure they were sufficiently etched using an optical microscope. Under the microscope, the samples were sufficiently etched after 20 seconds so longer periods of etching were not needed. Once this was done, the samples were investigated further using a Zeiss Inverted Optical Microscope. Under this microscope, grain growth in the different build directions was investigated to see how each print direction affected the grain growth and changed with varying build heights, surface finishes, and temperatures during the three point bend tests. Pictures of the results using the optical microscope were taken. Figure 20 below shows the optical microscope used.

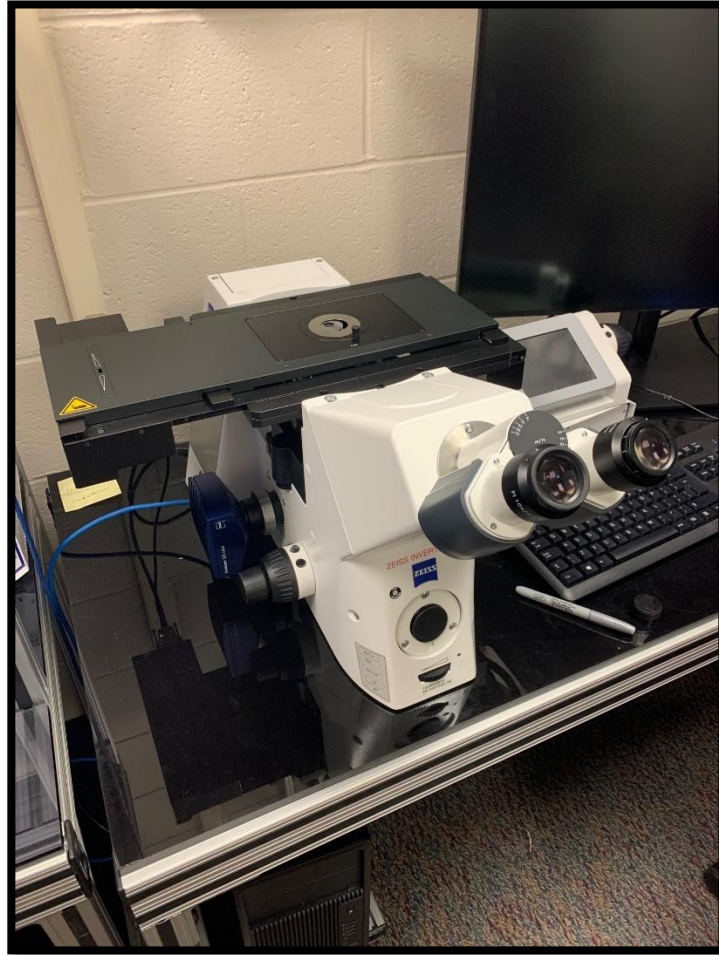


**Figure 20. Zeiss Inverted Optical Microscope**

### **3.9 Summary**

This chapter detailed the methodology and processes used throughout the sample printing, preparation, testing, data processing, and microscopy efforts for the additively manufactured Ti 6-4 samples. Focus was given to the sample manufacturing process in addition to the steps needed for grinding the samples during material preparation. The room temperature and high temperature three point bend test procedures were examined in detail. The room temperature compression and tensile test procedures were also

discussed. Next, the equations and Matlab code used to process the data to generate accurate results were reviewed in detail. Lastly, the procedures to prepare the samples for microscopy and the steps to perform the different types of microscopy used in this research effort were discussed.

## **IV. Analysis and Results**

### **4.1 Chapter Overview**

This chapter will examine the data produced from the three point bend tests, compression tests, and tensile tests. Results including stress-strain plots, important points and characteristics from the stress-strain plots, statistical significance of the results, and comparison of the results from the different tests will be discussed. Reasoning behind the results will be explained to gain an understanding of how print direction, surface finish, size of build height, and temperature affect the mechanical response of the additively manufactured Ti 6-4 samples under compressive, tensile, and bending loads. In addition, SEM and EDS were performed on the samples and sample powder to learn more about the fracture mechanisms and elemental makeup. Lastly, some samples were ground and etched to look at grain growth in the different build directions.

### **4.2 Ground Room Temperature Three Point Bend Results**

Room temperature three point bend tests were performed on 0, 45, and 90 degree print orientation samples for both 30 and 60 micron build heights. Table 6 below shows average data values in the three print directions for each build height. Each orientation and build height was tested using three samples. Statistical analysis was also conducted for the experimental results. Since each test variant was conducted three times, standard deviations and 95% confidence intervals based on a Student's t-distribution were

determined for all the different tests to examine the validity of the data and to look for any outliers.

**Table 6. Values for Ground Room Temperature Three Point Bend Tests**

	<b>30 Micron/ 0 Degrees</b>	<b>30 Micron/ 45 Degrees</b>	<b>30 Micron/ 90 Degrees</b>	<b>60 Micron/ 0 Degrees</b>	<b>60 Micron/ 45 Degrees</b>	<b>60 Micron/ 90 Degrees</b>
<b>Modulus of Elasticity (MPa)</b>	97400 SD (7780) CI [90200-105000]	85200 SD (8440) CI [77400-93000]	103000 SD (3250) CI [100000-106000]	109000 SD (1300) CI [106000- 112000]	104000 SD (5700) CI [98900-109000]	108000 SD (8380) CI [99800-115000]
<b>Yield Stress (MPa)</b>	1710 SD (8.32) CI [1710-1720]	1580 SD (82.6) CI [1500-1650]	1770 SD (56.8) CI [1720-1820]	1800 SD (16.5) CI [1790-1820]	1710 SD (15.2) CI [1670-1750]	1780 SD (21.8) CI [1760-1800]
<b>Yield Strain (mm/mm)</b>	0.020 SD (0.0014) CI [0.018-0.021]	0.021 SD (0.00090) CI [0.020-0.021]	0.019 SD (0.00034) CI [0.018-0.020]	0.018 SD (0.00012) CI [0.018-0.019]	0.018 SD (0.00090) CI [0.018-0.019]	0.019 SD (0.0012) CI [0.017-0.020]
<b>Ultimate Stress (MPa)</b>	2250 SD (34.6) CI [2220-2290]	2140 SD (96.8) CI [1900-2380]	2310 SD (30.8) CI [2290-2340]	2280 SD (50.3) CI [2230-2320]	2200 SD (18.4) CI [2180-2220]	2260 SD (50.8) CI [2130-2390]
<b>Ultimate Strain (mm/mm)</b>	0.086 SD (0.00075) CI [0.085-0.087]	0.093 SD (0.0022) CI [0.091-0.095]	0.081 SD (0.0049) CI [0.076-0.085]	0.061 SD (0.011) CI [0.051-0.072]	0.082 SD (0.013) CI [0.070-0.093]	0.065 SD (0.0056) CI [0.060-0.070]
<b>Fracture Stress (MPa)</b>	2200 SD (32.7) CI [2160-2230]	2050 SD (127) CI [1930-2170]	2270 SD (35.7) CI [2180-2360]	2200 SD (90.7) CI [2110-2280]	2110 SD (43.8) CI [2070-2150]	2170 SD (77.9) CI [2100-2240]
<b>Fracture Strain (mm/mm)</b>	0.097 SD (0.0062) CI [0.091-0.10]	0.107 SD (0.0036) CI [0.104-0.110]	0.088 SD (0.0045) CI [0.083-0.092]	0.074 SD (0.015) CI [0.060-0.087]	0.102 SD (0.019) CI [0.084-0.120]	0.072 SD (0.0049) CI [0.068-0.077]

The data points shown in Table 6 were taken from stress-strain curves generated from the test data. Figure 21-Figure 26 below show the stress-strain curves for the ground room temperature three point bend tests. The 0, 45, and 90 degree print directions for both the 30 and 60 micron build heights are shown.

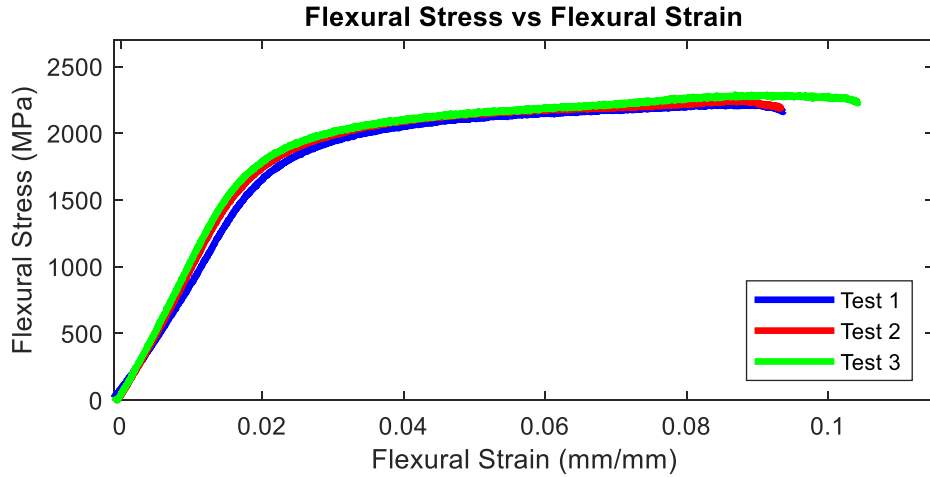


**Figure 21. 30 Micron/0 Degrees/Room Temperature**

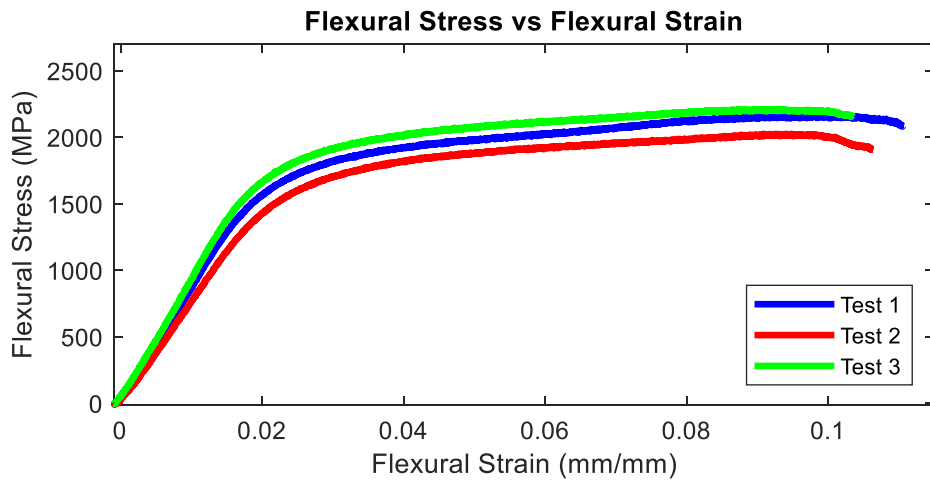


**Figure 22. 30 Micron/45 Degrees/Room Temperature**

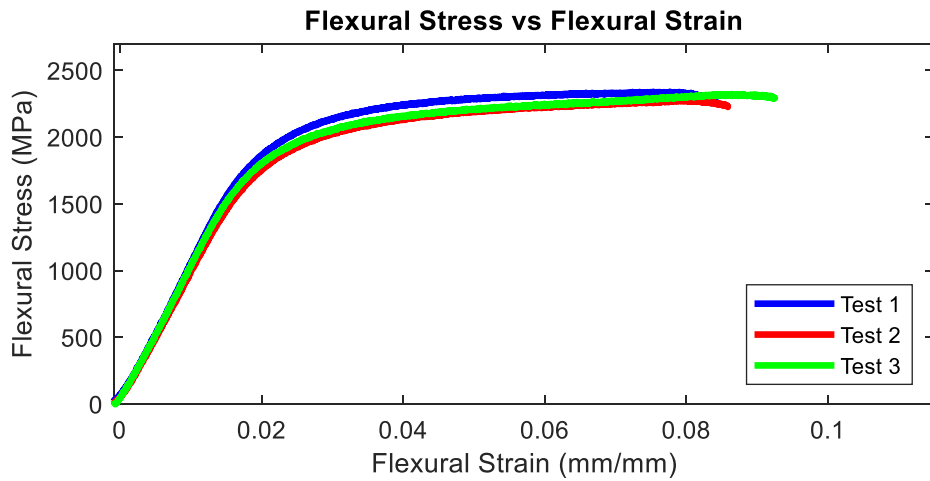


**Figure 23. 30 Micron/90 Degrees/Room Temperature**

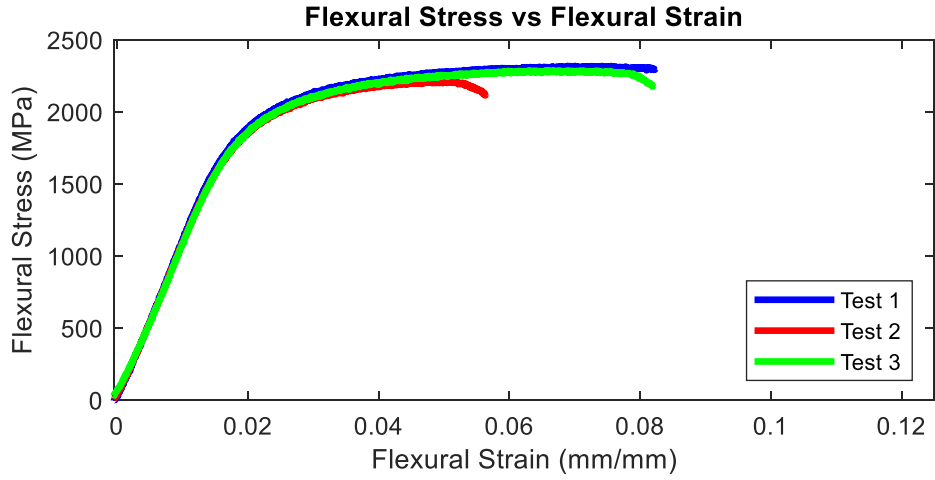


**Figure 24. 60 Micron/0 Degrees/Room Temperature**

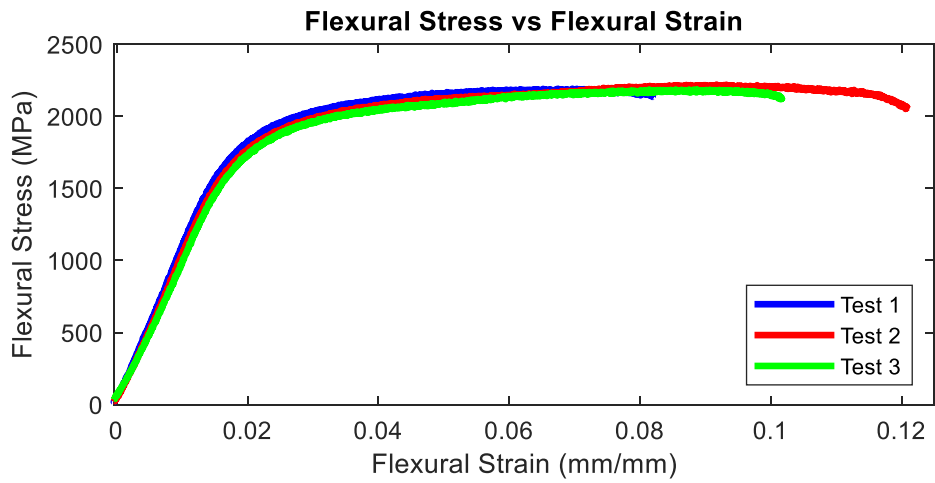


**Figure 25. 60 Micron/45 Degrees/Room Temperature**

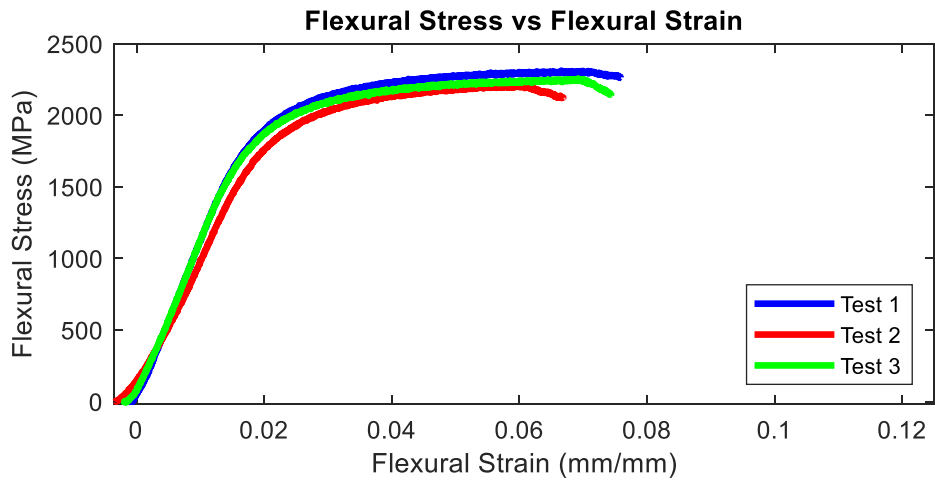


**Figure 26. 60 Micron/90 Degrees/Room Temperature**

### 4.3 Unground Room Temperature Three Point Bend Results

Room temperature three point bend tests were performed on 0, 45, and 90 degree print orientation samples for both 30 and 60 micron build heights. Table 7 below shows average data values in the three print directions for each build height. Each orientation and build height was tested using three samples. Statistical analysis was also conducted for the experimental results. Since each test variant was conducted three times, standard deviations and 95% t-test confidence intervals were determined for all the different tests to examine the validity of the data and to look for any outliers.

**Table 7. Values for Unground Room Temperature Three Point Bend Tests**

	<b>30 Micron/ 0 Degrees</b>	<b>30 Micron/ 45 Degrees</b>	<b>30 Micron/ 90 Degrees</b>	<b>60 Micron/ 0 Degrees</b>	<b>60 Micron/ 45 Degrees</b>	<b>60 Micron/ 90 Degrees</b>
<b>Modulus of Elasticity (MPa)</b>	59900 SD (9030) CI [51600-68200]	61300 SD (3130) CI [58500-64200]	57200 SD (4260) CI [53300-61200]	67600 SD (2420) CI [65300-69800]	50000 SD (2980) CI [47200-52700]	72500 SD (5300) CI [67600-77400]
<b>Yield Stress (MPa)</b>	1370 SD (83.2) CI [1300-1450]	1370 SD (37.9) CI [1330-1400]	1400 SD (28.4) CI [1380-1430]	1470 SD (18.3) CI [1450-1480]	1230 SD (46.7) CI [1190-1280]	1530 SD (46.5) CI [1490-1580]
<b>Yield Strain (mm/mm)</b>	0.025 SD (0.0021) CI [0.023-0.027]	0.024 SD (0.00054) CI [0.024-0.025]	0.027 SD (0.0013) CI [0.025-0.028]	0.024 SD (0.00054) CI [0.023-0.024]	0.027 SD (0.00081) CI [0.026-0.027]	0.023 SD (0.0010) CI [0.021-0.026]
<b>Ultimate Stress (MPa)</b>	1780 SD (124) CI [1660-1890]	1800 SD (40.3) CI [1760-840]	1800 SD (41.1) CI [1700-1910]	1830 SD (65.2) CI [1770-1890]	1570 SD (56.6) CI [1520-1620]	1930 SD (58.8) CI [1870-1980]
<b>Ultimate Strain (mm/mm)</b>	0.075 SD (0.0037) CI [0.072-0.079]	0.094 SD (0.024) CI [0.072-0.116]	0.076 SD (0.0014) CI [0.074-0.077]	0.058 SD (0.011) CI [0.048-0.068]	0.071 SD (0.0053) CI [0.058- .085]	0.063 SD (0.0048) CI [0.051-0.075]
<b>Fracture Stress (MPa)</b>	1740 SD (128) CI [1420-2060]	1710 SD (54.5) CI [1660-1760]	1740 SD (42.0) CI [1700-1780]	1770 SD (60.3) CI [1710-1820]	1500 SD (58.1) CI [1440-1550]	1880 SD (73.5) CI [1810-1950]
<b>Fracture Strain (mm/mm)</b>	0.084 SD (0.0053) CI [0.079-0.089]	0.111 SD (0.030) CI [0.084-0.139]	0.090 SD (0.0047) CI [0.086-0.094]	0.067 SD (0.013) CI [0.054-0.079]	0.092 SD (0.017) CI [0.077-0.108]	0.074 SD (0.010) CI [0.064-0.083]

The data points shown in Table 7 were taken from stress-strain curves generated from the test data. Figure 27-Figure 32 below show the stress-strain curves for the unground room temperature three point bend tests. The 0, 45, and 90 degree print directions for both the 30 and 60 micron build heights are shown.

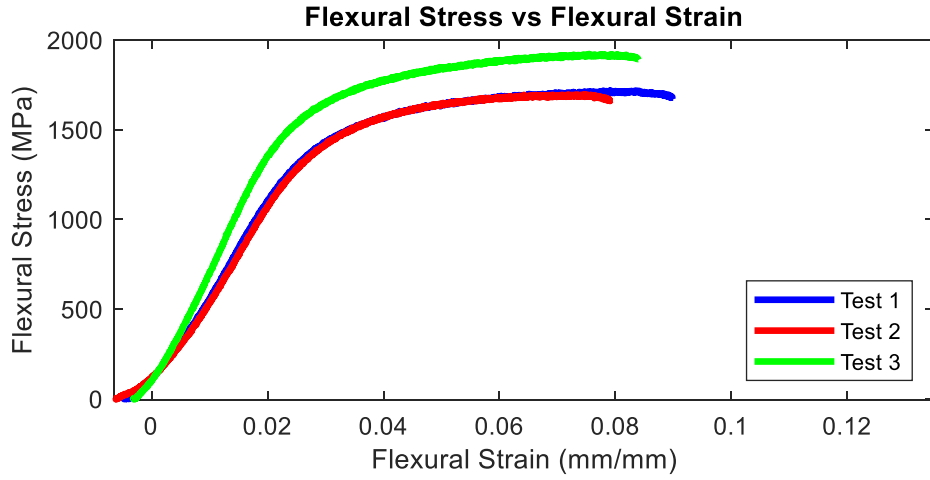


**Figure 27. 30 Micron/0 Degrees/Room Temperature**

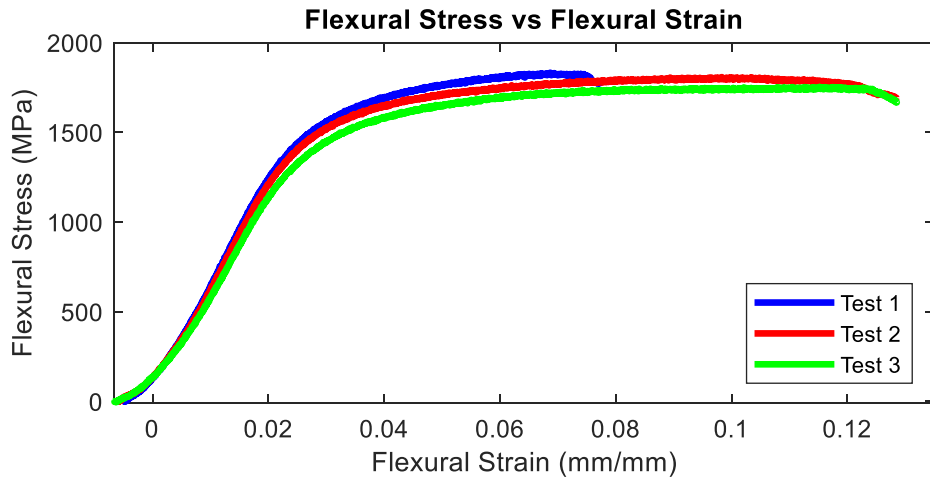


**Figure 28. 30 Micron/45 Degrees/Room Temperature**

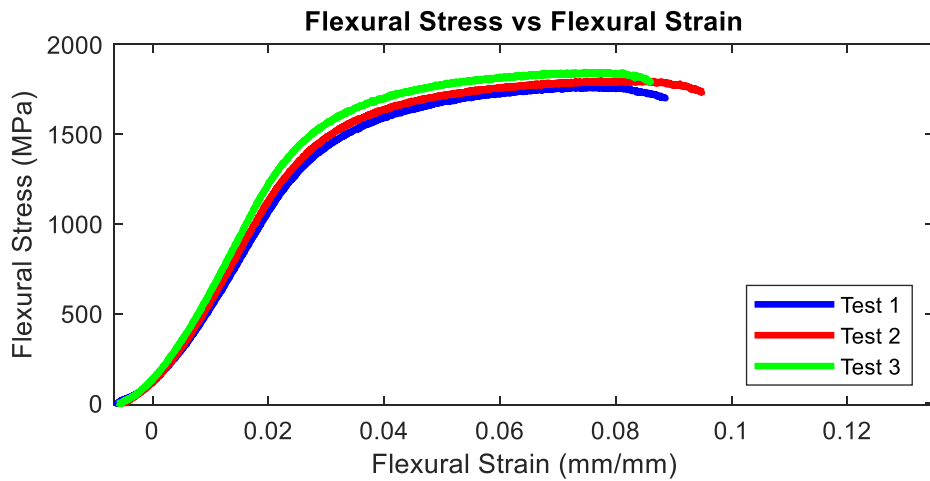


**Figure 29. 30 Micron/90 Degrees/Room Temperature**

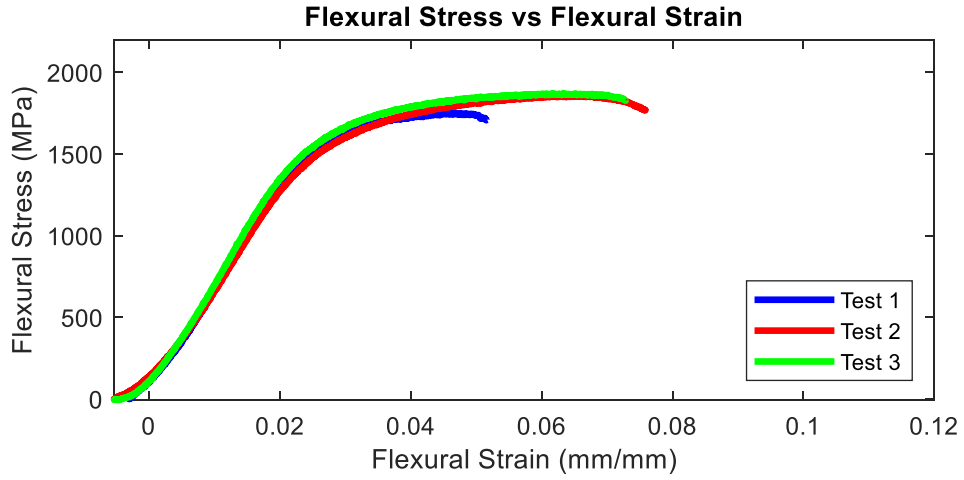


**Figure 30. 60 Micron/0 Degrees/Room Temperature**

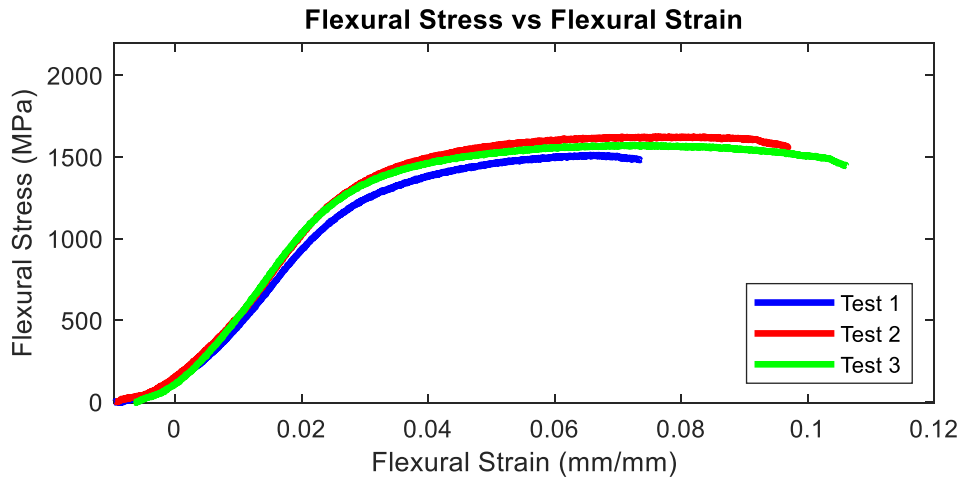


**Figure 31. 60 Micron/45 Degrees/Room Temperature**

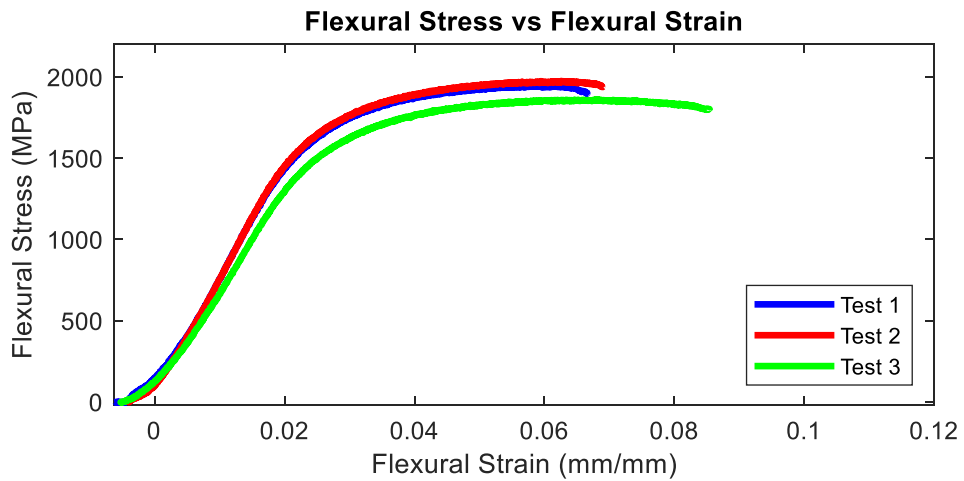


**Figure 32. 60 Micron/90 Degrees/Room Temperature**

#### 4.4 Ground High Temperature Three Point Bend Results

High temperature three point bend tests were performed on 0, 45, and 90 degree print orientation samples for both 30 and 60 micron build heights at a temperature of 800 degrees Celsius. Table 8 below shows average data values in the three print directions for each build height. Each orientation and build height was tested using three samples. Statistical analysis was also conducted for the experimental results. Since each test variant was conducted three times, standard deviations and 95% confidence intervals were determined for all the different tests to examine the validity of the data and to look for any outliers. Fracture stress and fracture strain are not shown since the samples were not taken to fracture due to the high ductility experienced by the material at elevated temperatures.

**Table 8. Values for Ground High Temperature Three Point Bend Tests**

	<b>30 Micron/ 0 Degrees</b>	<b>30 Micron/ 45 Degrees</b>	<b>30 Micron/ 90 Degrees</b>	<b>60 Micron/ 0 Degrees</b>	<b>60 Micron/ 45 Degrees</b>	<b>60 Micron/ 90 Degrees</b>
<b>Modulus of Elasticity (MPa)</b>	7350 SD (662) CI [674-796]	6010 SD (2440) CI [63.6-12100]	6730 SD (1200) CI [5630-7820]	5970 SD (1150) CI [4900-7030]	10100 SD (1810) CI [8470-11800]	4780 SD (855) CI [3990-5570]
<b>Yield Stress (MPa)</b>	95.5 SD (3.32) CI [92.4-98.6]	82.6 SD (5.50) CI [77.5-87.7]	89.4 SD (7.45) CI [82.5-96.3]	89.7 SD (3.62) CI [86.4-93.1]	78.7 SD (20.2) CI [60.3-97.1]	77.8 SD (23.3) CI [56.4-99.3]
<b>Yield Strain (mm/mm)</b>	0.015 SD (0.00076) CI [0.014-0.016]	0.018 SD (0.0071) CI [0.011-0.024]	0.016 SD (0.0035) CI [0.012-0.019]	0.017 SD (0.0031) CI [0.015-0.020]	0.0097 SD (0.00078) CI [0.0090-0.010]	0.019 SD (0.0077) CI [0.012-0.026]
<b>Ultimate Stress (MPa)</b>	118 SD (4.31) CI [114-122]	102 SD (15.3) CI [87.5-116]	116 SD (1.15) CI [114-117]	107 SD (5.98) CI [101-112]	102 SD (29.7) CI [75.3-128]	109 SD (13.9) CI [96.6-122]
<b>Ultimate Strain (mm/mm)</b>	0.112 SD (0.0081) CI [0.104-0.119]	0.091 SD (0.043) CI [0.051-0.130]	0.112 SD (0.0050) CI [0.107-0.117]	0.097 SD (0.064) CI [0.039-0.156]	0.052 SD (0.046) CI [0.0094-0.094]	0.108 SD (0.014) CI [0.074-0.142]

The data points shown in Table 8 were taken from stress-strain curves generated from the test data. Figure 33-Figure 38 below show the stress-strain curves for the ground high temperature three point bend tests. The 0, 45, and 90 degree print directions for both the 30 and 60 micron build heights are shown.

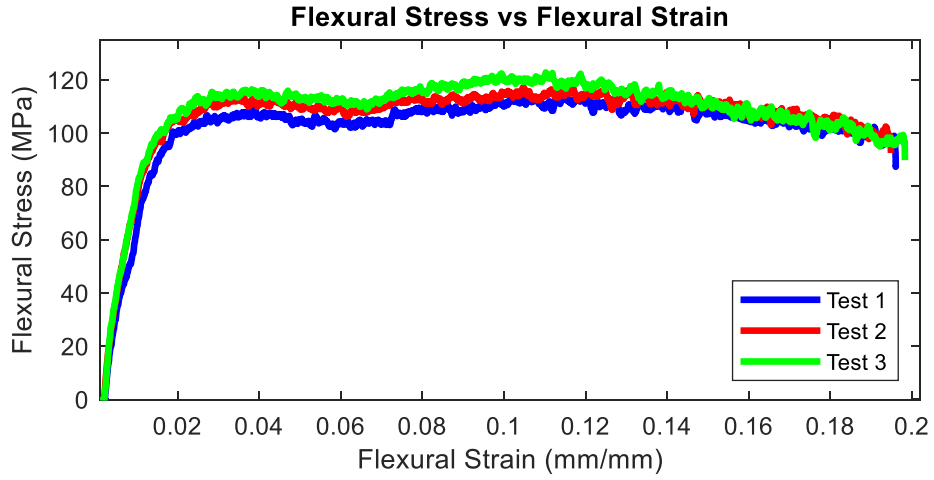


**Figure 33. 30 Micron/0 Degrees/High Temperature**

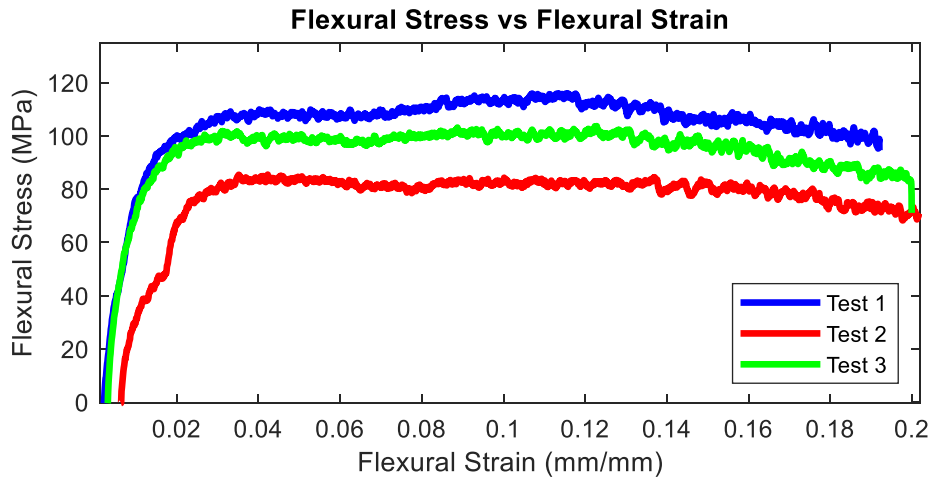


**Figure 34. 30 Micron/45 Degrees/High Temperature**

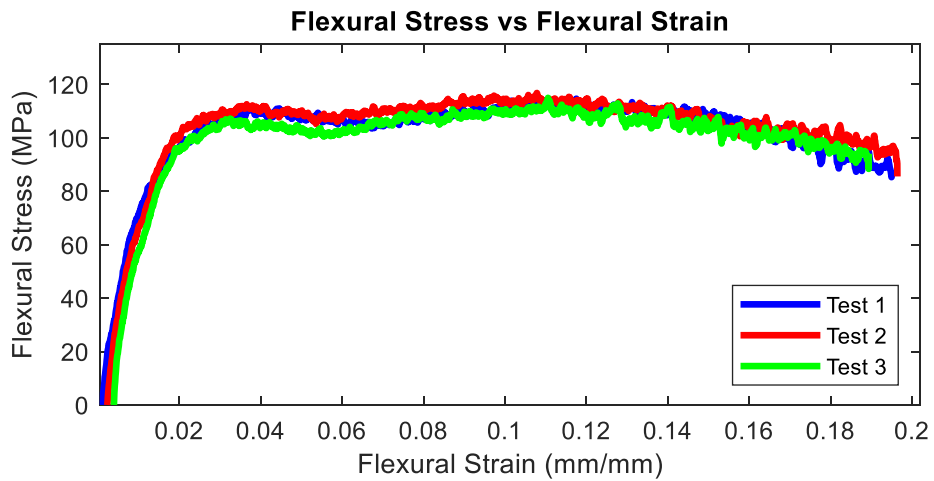


**Figure 35. 30 Micron/90 Degrees/High Temperature**

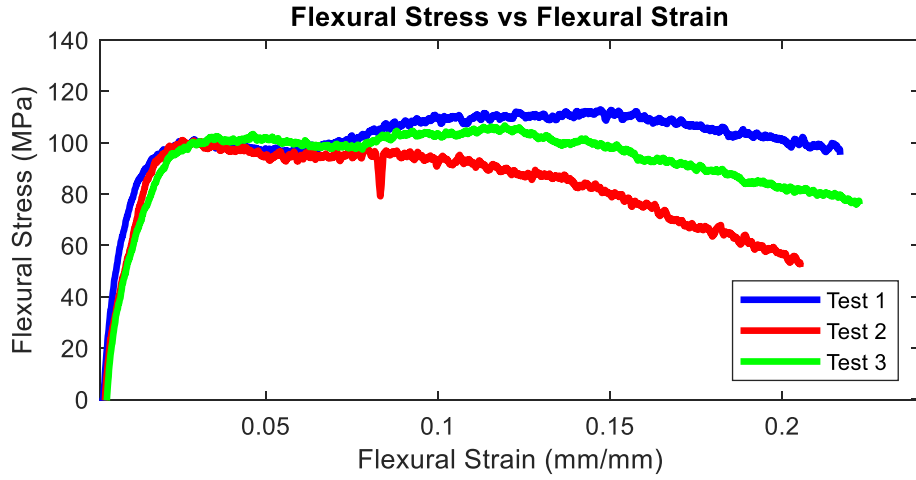


**Figure 36. 60 Micron/0 Degrees/High Temperature**

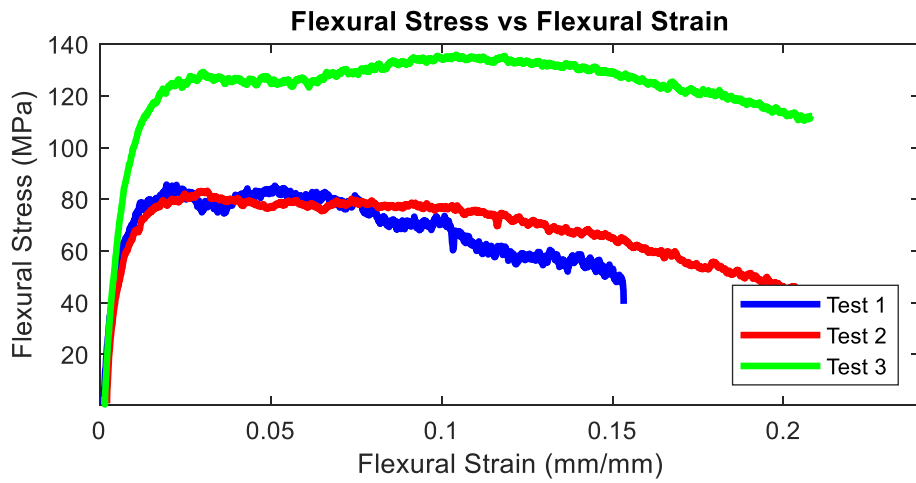


**Figure 37. 60 Micron/45 Degrees/High Temperature**

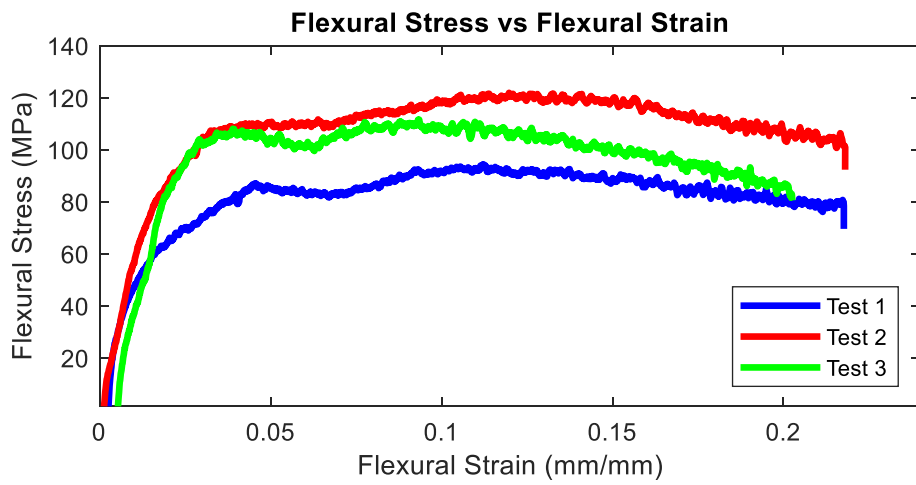


**Figure 38. 60 Micron/90 Degrees/High Temperature**

#### 4.5 Comparison Between the Ground and Unground Room Temperature Three Point Bend Tests

As shown above in Table 7, the unground room temperature three point bend tests had significantly lower mechanical response values when compared to the ground room temperature three point bend tests in Table 6. Table 9 below demonstrates this by conducting a comparison of means between the two sample types using a t-test.

**Table 9. Comparison of Means Between the Ground Room Temperature Three Point Bend Tests and the Unground Room Temperature Three Point Bend Tests**

	<b>30 Micron/ 0 Degrees</b>	<b>30 Micron/ 45 Degrees</b>	<b>30 Micron/ 90 Degrees</b>	<b>60 Micron/ 0 Degrees</b>	<b>60 Micron/ 45 Degrees</b>	<b>60 Micron/ 90 Degrees</b>
<b>Modulus of Elasticity (MPa)</b>	0.0055	0.0100	0.0001	< 0.0001	0.0003	0.0034
<b>Yield Stress (MPa)</b>	0.0021	0.0161	0.0005	< 0.0001	0.0001	0.0011
<b>Yield Strain (mm/mm)</b>	0.0265	0.0161	0.0005	< 0.0001	0.0001	0.0011
<b>Ultimate Stress (MPa)</b>	0.0032	0.0049	0.0001	0.0007	0.0001	0.0018
<b>Ultimate Strain (mm/mm)</b>	0.0072	0.9462	0.1645	0.7551	0.2463	0.6631
<b>Fracture Stress (MPa)</b>	0.0038	0.0130	0.0001	0.0024	0.0001	0.0094
<b>Fracture Strain (mm/mm)</b>	0.0508	0.8299	0.6227	0.5743	0.5342	0.7713

In Table 9 above, p-values are presented to compare the means between the two sample types. Any p-value less than 0.05 indicates that the two sample means are significantly different [29]. Differences that are unique are shown in white cells, while differences that are not conclusively unique are shown in blue cells. Most of the values in the table above have a p-value less than 0.05. This indicates that the ground and

unground three point bend samples are generally significantly different and the surface finish has an important part in determining the mechanical response of the material. The majority of the strain values presented above were found not to be significantly different.

Some theories as to why the unground samples had a lower mechanical response compared to the ground samples is a combination of the formation of cracks resulting from the rough surface of the unground samples left from the manufacturing process and the rough surface not being able to support any load on the unground samples. Figure 39- Figure 40 shown below show the load-displacement curves for the ground and unground room temperature three point bend tests looking at the 30 micron, 0 degree sample number one.

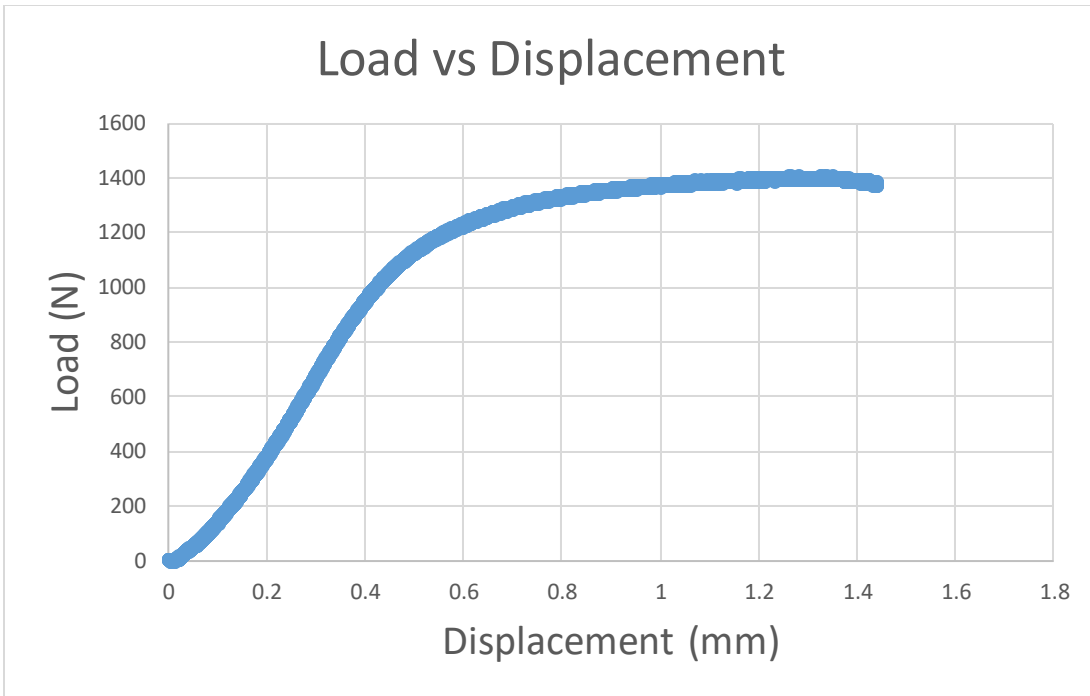


**Figure 39. Ground Three Point Bend Room Temperature 30 Micron 0 Degree Sample #1**

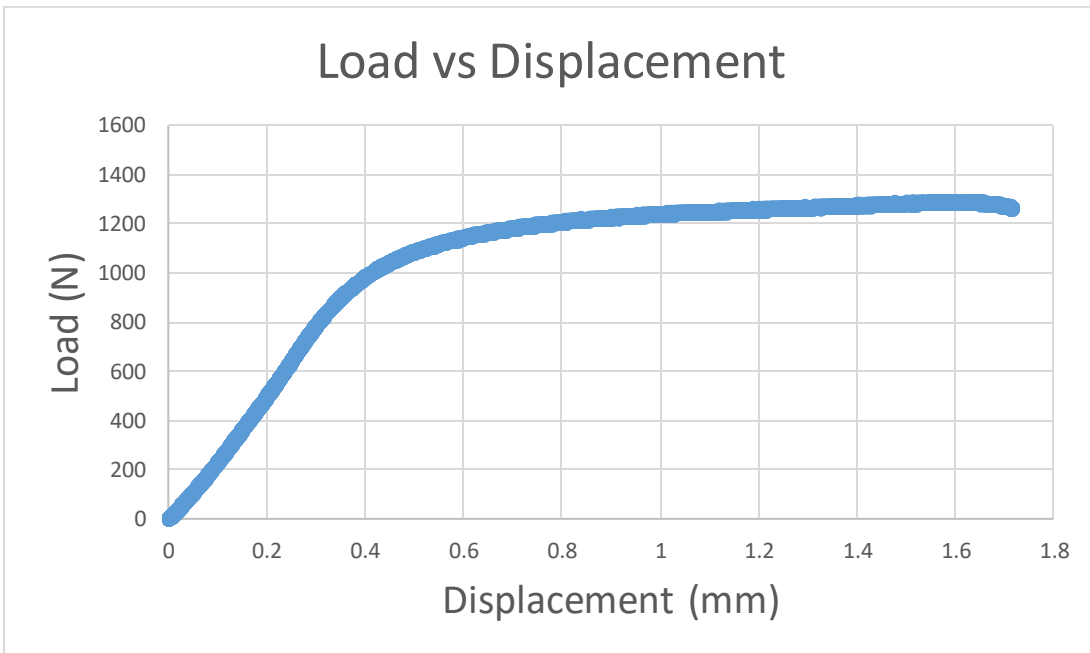


**Figure 40. Unground Three Point Bend Room Temperature 30 Micron 0 Degree Sample #1**

As seen from Figure 39-Figure 40, the ground samples were able to support a larger load before fracture. This lends to the theory that the lower mechanical response in the unground samples vs the ground samples was due to cracks initiating in the unground samples because of the rough surface which lead to a lower mechanical response for the unground samples. The response seen in the above graphs is also seen in samples two and three, in the 60 micron samples, and in the other print directions.

The other theory, that the rough surface did not support any load on the unground samples, is supported when looking at Figure 41-Figure 42 below.

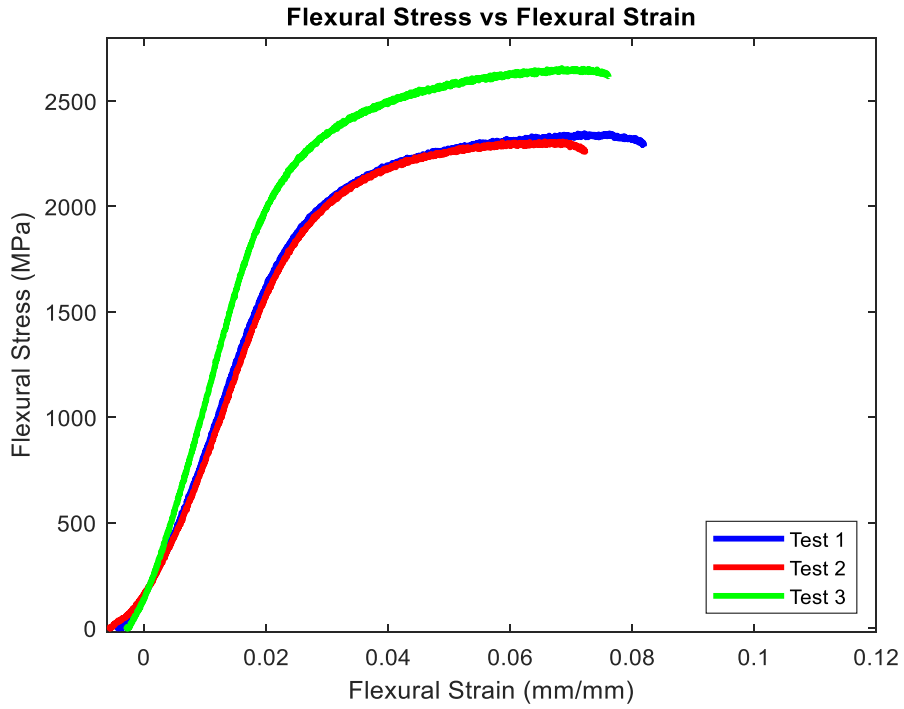


**Figure 41. Unground Three Point Bend Room Temperature 30 Micron 0 Degree Sample #1**

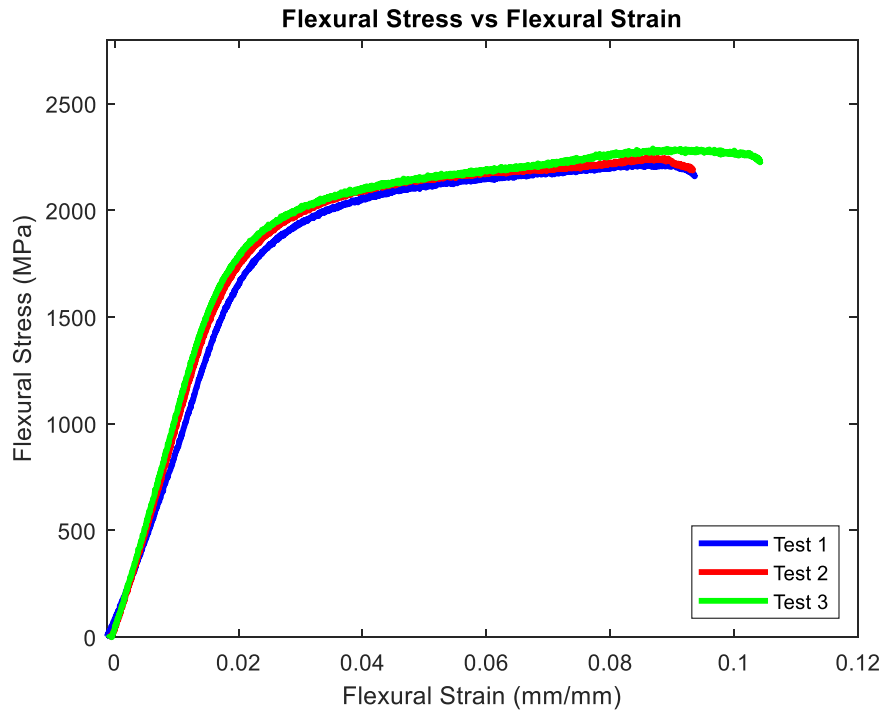


**Figure 42. Ground Three Point Bend Room Temperature 30 Micron 0 Degree Sample #1**

In the above figures, the unground samples were corrected using the thickness of the outside rough surface, which was measured to be 130 microns, and subtracting it off twice from all the dimensions of the sample to get the dimensions minus the rough surface. This represented the samples useful cross section that supported load. As seen in Figure 41-Figure 42, the ultimate stress values that the ground and unground samples could withstand were very close to each other, minus test three for the unground samples. The response seen in the above graphs is also seen in samples two and three, in the 60 micron samples, and in the other print directions. This supports the theory that the rough surface on the unground samples does not support any load and the difference in mechanical response seen in the ground versus unground samples was due to the unground samples rough surface not supporting any load. In the end, the difference seen in the ground versus unground three point bend samples mechanical response is due to a combination of these two theories presented above.

When looking at the individual flexural stress-flexural strain graphs for the ground room temperature three point bend results in Figure 21-Figure 26, the three samples had similar mechanical responses when looking at the 30 micron samples while the fracture strain varied more for the 60 micron samples. The overall response of the entire material was similar for all the print directions in the 30 micron samples but more variance was seen in the 60 micron samples, especially in the fracture strains. Even so, the Ti 6-4 samples followed a similar mechanical response when comparing the 30 micron and 60 micron build height samples and all the 30, 45, and 90 degree print directions.

The unground room temperature three point bend test graphs presented above in Figure 27-Figure 32 do not show much difference between the 30 micron and 60 micron build height samples. The different build directions also generally show similar results with the 60 micron/90 degree samples exhibiting slightly higher ultimate stress values but only 20.6% higher than the lowest ultimate stress seen in the 60 micron/45 degree sample.

#### **4.6 Comparison Between the Ground Room and High Temperature Three Point Bend Tests**

As seen above in Table 8, the ground high temperature three point bend tests results were much lower than the ground room temperature three point bend tests results seen in Table 6. Table 10 below demonstrates this by conducting a comparison of means between the two sample types using a t-test.

**Table 10. Comparison of Means Between the Ground Room Temperature Three Point Bend Tests and the Ground High Temperature Three Point Bend Tests**

	<b>30 Micron/ 0 Degrees</b>	<b>30 Micron/ 45 Degrees</b>	<b>30 Micron/ 90 Degrees</b>	<b>60 Micron/ 0 Degrees</b>	<b>60 Micron/ 45 Degrees</b>	<b>60 Micron/ 90 Degrees</b>
<b>Modulus of Elasticity (MPa)</b>	< 0.0001	0.0001	< 0.0001	< 0.0001	< 0.0001	< 0.0001
<b>Yield Stress (MPa)</b>	< 0.0001	< 0.0001	< 0.0001	< 0.0001	< 0.0001	< 0.0001
<b>Yield Strain (mm/mm)</b>	0.0056	0.5080	0.2136	0.6064	0.0003	1.0000
<b>Ultimate Stress (MPa)</b>	< 0.0001	< 0.0001	< 0.0001	< 0.0001	< 0.0001	< 0.0001
<b>Ultimate Strain (mm/mm)</b>	0.0052	0.9397	0.0016	0.3913	0.3381	0.0078

In Table 10 above, p-values are presented to compare the means between the two sample types. Any p-value less than 0.05 indicates that the two sample means are significantly different [29]. Differences that are unique are shown in white cells, while differences that are not conclusively unique are shown in blue cells. All of the values for the modulus of elasticity and the stress values have a p-value less than 0.05. This shows that the ground high temperature three point bend tests results and the ground room temperature three point bend tests results had very different results for the modulus and stress values. This is because as ductile metals are heated, they lose strength compared to room temperature ductile metals. When looking at the strain values, for the most part, they are significantly similar across most of the print build directions and sample build heights.

When looking at the ground high temperature three point bend test graphs in Figure 33-Figure 38, some variance was seen between the different sample print directions and between the sample build heights. The greatest variance was seen in the 60 micron/45 degree test #3. This sample had a much higher ultimate stress compared to the other samples tested at 60 micron/45 degree. The 60 micron/0 degree sample also had a wide range in stress values in the plastic region. All the ground high temperature three point bend test samples were brought out to 0.2 mm/mm strain unless they bent to a point where the test could not be continued. None of the samples fractured due to the increased ductility of ductile metals at elevated temperatures. With Ti 6-4 being known for its ductile properties in general, it would have been very difficult to get the samples to fracture. Figure 43 below shows an example of a room temperature and high temperature

three point bend sample after testing. The significant bend seen in the high temperature sample demonstrates Ti 6-4s excellent ductility under high temperatures.

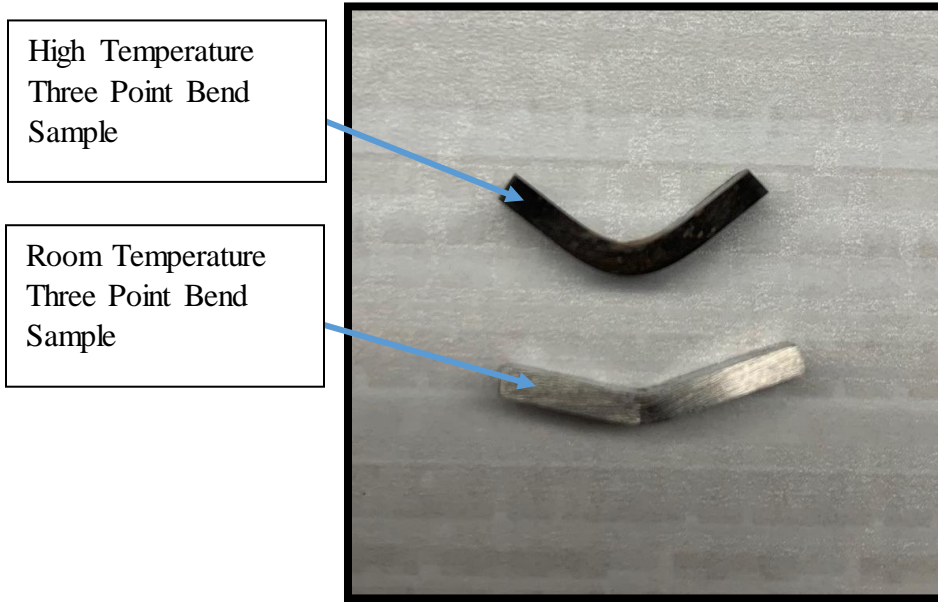


**Figure 43. Ground Room and High Temperature Three Point Bend Samples Post Testing**

#### **4.7 Comparison of Ground Room Temperature Three Point Bend Tests and Traditionally Manufactured Ti 6-4**

To check if the additively manufactured three point bend samples had a different mechanical response when compared to traditionally manufactured Ti 6-4, the results in Table 6 were compared to wrought Ti 6-4 data [30] using percentage differences. Table 11-Table 12 shown below displays the percent difference results.

**Table 11. Largest Percent Differences for Ground Room Temperature Three Point Bend Tests**

	<b>Largest Percent Difference (%)</b>	<b>Sample Compared</b>
<b>Flexural Modulus of Elasticity</b>	25.4	30 Micron/45 Degrees
<b>Ultimate Flexural Stress</b>	43.9	30 Micron/90 Degrees

**Table 12. Smallest Percent Differences for Ground Room Temperature Three Point Bend Tests**

	<b>Smallest Percent Difference (%)</b>	<b>Sample Compared</b>
<b>Flexural Modulus of Elasticity</b>	0.93	60 Micron/0 Degrees
<b>Ultimate Flexural Stress</b>	36.6	30 Micron/45 Degrees

As seen from Table 11-Table 12, the ground room temperature three point bend samples lined up well with the wrought Ti 6-4 data for the flexural modulus of elasticity but a larger difference was seen between the ultimate flexural stress values. The largest percent difference for the ultimate flexural stress was still under 50% but the smallest percent difference seen for the ultimate flexural stress was over 30%.

## **4.8 Comparison of Yield and Ultimate Stress Results for Three Point Bend Samples**

To compare all the print orientations, sample build heights, and surface finishes from the three point bend tests, plots were created to compare all the three point bend test yield stress values. The room and high temperature tests were broken up onto separate graphs since the magnitudes of the yield stresses were vastly different. Figure 44-Figure 45 shown below display the room and high temperature yield stress results for the three point bend samples. On the graphs, filled shapes represent ground samples while open shapes represent unground samples. Triangles represent a build height of 30 microns while circles represent a build height of 60 microns.

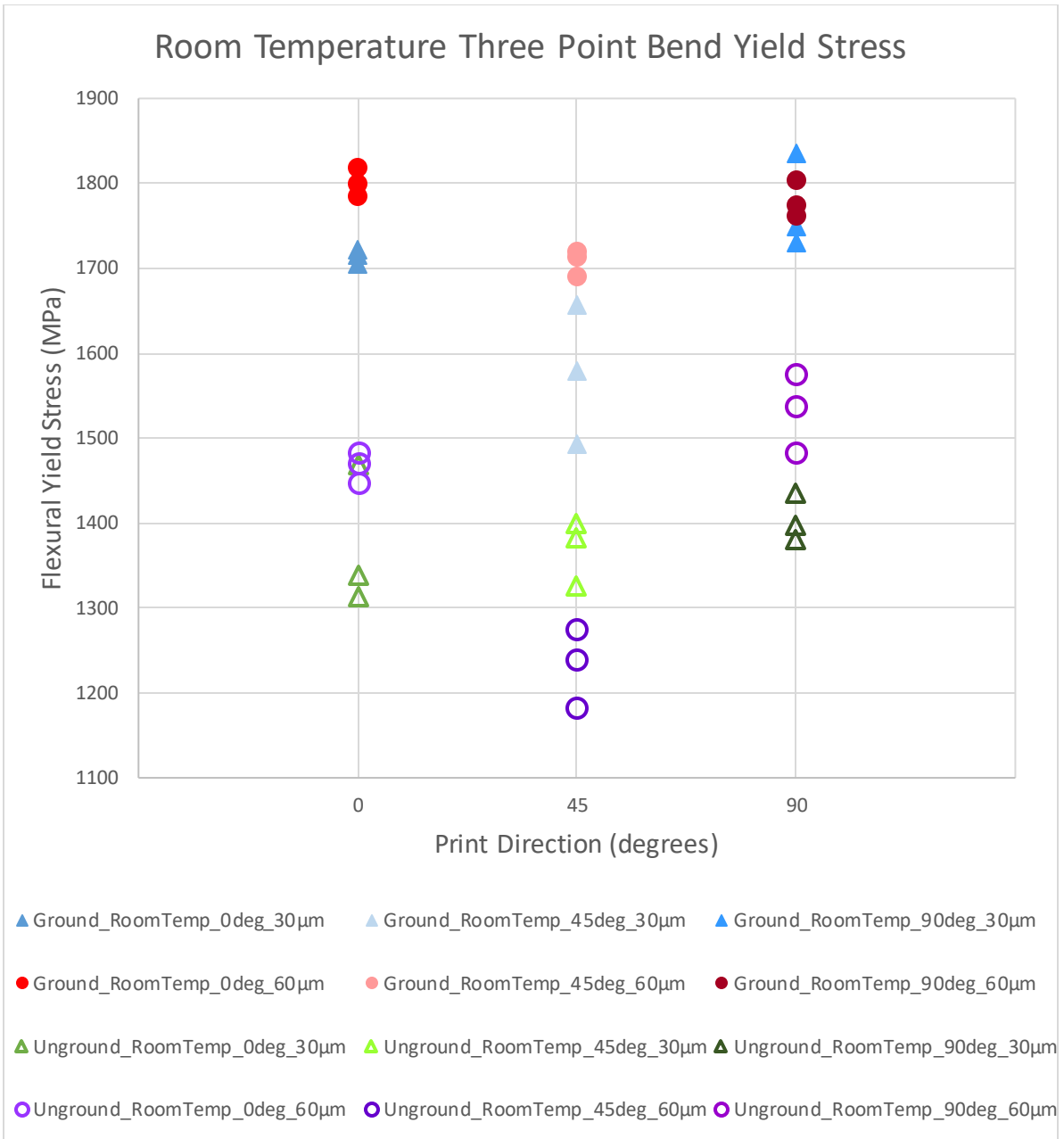


**Figure 44. Yield Stress Comparison for Room Temperature Three Point Bend Samples**

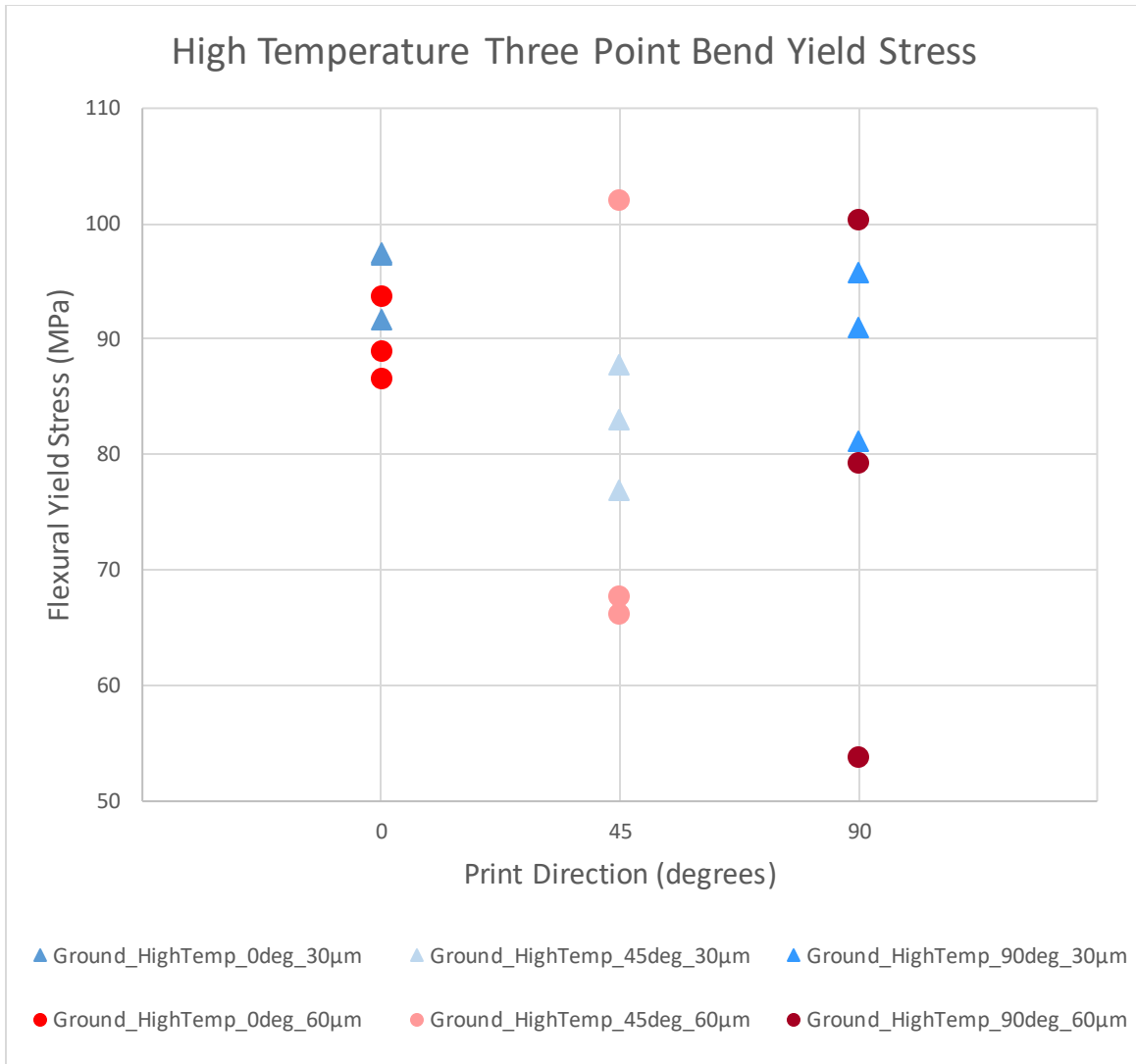


**Figure 45. Yield Stress Comparison for High Temperature Three Point Bend Samples**

To compare all the print orientations, sample build heights, and surface finishes from the three point bend tests, plots were created to compare all the three point bend test ultimate stress values. The room and high temperature tests were broken up onto separate graphs since the magnitudes of the ultimate stresses were vastly different. Figure 46- Figure 47 shown below displays the room and high temperature ultimate stress results for

the three point bend samples. On the graphs, filled shapes represent ground samples while open shapes represent unground samples. Triangles represent a build height of 30 micron while circles represent a build height of 60 micron.

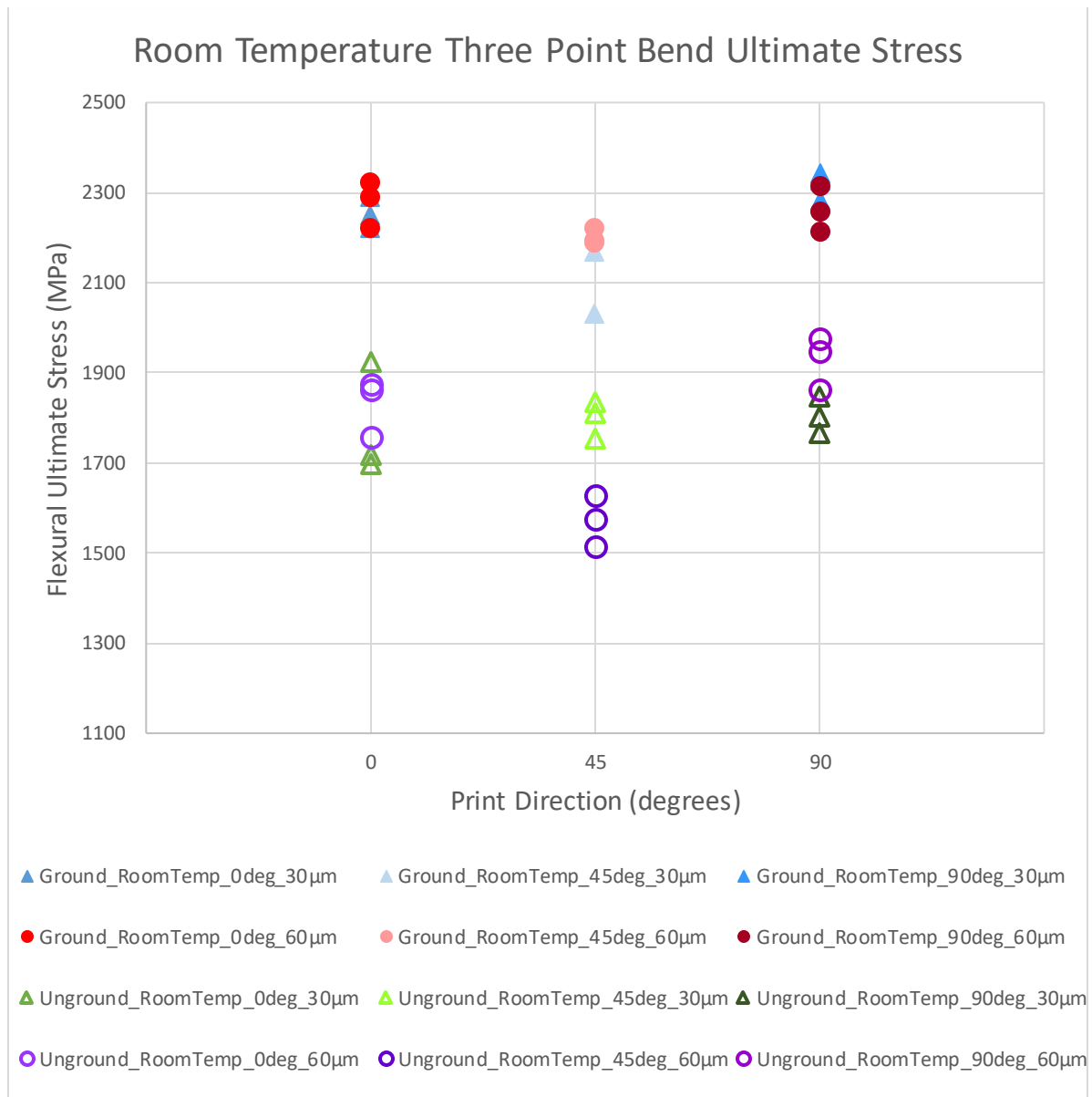


**Figure 46. Ultimate Stress Comparison for Room Temperature Three Point Bend Samples**

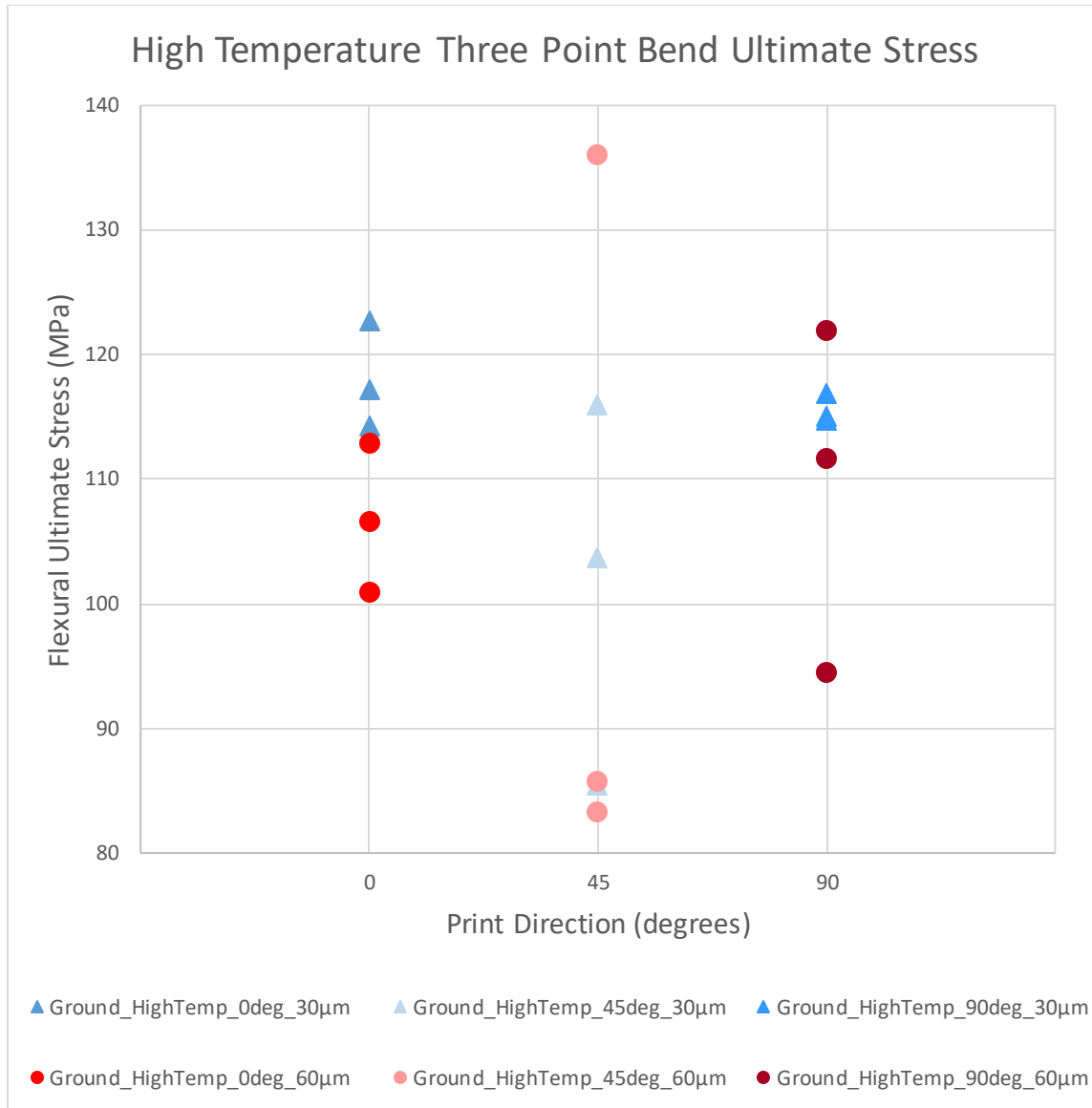


**Figure 47. Ultimate Stress Comparison for High Temperature Three Point Bend Samples**

As seen in Figure 44 and Figure 46, the ground samples had a higher yield stress compared to the unground samples. This is due to the unground samples having crack initiation points that develop cracks easier when compared to the ground samples. This lowers the yield and ultimate stresses seen in the unground samples. The sample build

height had little effect on the yield and ultimate stress values for the different print directions. The 45 degree samples had a slightly lower yield and ultimate stress when compared to the other print directions for a given test. The yield and ultimate stress values were still close to the 0 and 90 degree print orientation yield and ultimate stress values for a given test type.

When looking at Figure 45-Figure 47, the yield and ultimate stress values seen for the high temperature samples was much lower than the values seen for the room temperature tests. There was also little difference between the yield and ultimate stress values for the different sample build heights and print directions when comparing the different high temperature three point bend tests. No discernable pattern could be seen since all these yield and ultimate stress values were so close.

#### **4.9 Ground Room Temperature Compression Results**

Room temperature compression tests were performed on 0 and 90 degree print orientation samples for both 30 and 60 micron build heights. Table 13 below shows average data values in the two print directions for each build height. Each orientation and build height was tested using three samples. Statistical analysis was also conducted for the experimental results. Since each test variant was conducted three times, standard deviations and 95% t-test confidence intervals were determined for all the different tests to examine the validity of the data and to look for any outliers.

**Table 13. Values for Ground Room Temperature Compression Tests**

	<b>30 Micron/ 0 Degrees</b>	<b>30 Micron/ 90 Degrees</b>	<b>60 Micron/ 0 Degrees</b>	<b>60 Micron/ 90 Degrees</b>
<b>Modulus of Elasticity (MPa)</b>	25200 SD (4330) CI [21200-29100]	24600 SD (3420) CI [21400-27700]	32000 SD (909) CI [31200-32900]	28900 SD (2890) CI [26200-31500]
<b>Yield Stress (MPa)</b>	1120 SD (118) CI [1010-1230]	1190 SD (56.9) CI [1140-1240]	1220 SD (5.76) CI [1220-1230]	1190 SD (34.2) CI [1110-1280]
<b>Yield Strain (mm/mm)</b>	0.048 SD (0.012) CI [0.018-0.078]	0.051 SD (0.0075) CI [0.044-0.058]	0.040 SD (0.0011) CI [0.039-0.041]	0.043 SD (0.0032) CI [0.040-0.046]
<b>Ultimate Stress (MPa)</b>	1650 SD (27.0) CI [1620-1670]	1760 SD (58.4) CI [1710-1820]	1790 SD (59.7) CI [1650-1940]	1720 SD (30.2) CI [1690-1750]
<b>Ultimate Strain (mm/mm)</b>	0.26 SD (0.011) CI [0.204-0.225]	0.23 SD (0.026) CI [0.206-0.253]	0.22 SD (0.026) CI [0.200-0.248]	0.21 SD (0.015) CI [0.192-0.220]
<b>Fracture Stress (MPa)</b>	1640 SD (29.0) CI [1610-1670]	1760 SD (59.7) CI [1700-1810]	1790 SD (64.2) CI [1730-1850]	1710 SD (36.4) CI [1680-1750]
<b>Fracture Strain (mm/mm)</b>	0.22 SD (0.010) CI [0.208-0.227]	0.23 SD (0.025) CI [0.211-0.257]	0.23 SD (0.025) CI [0.206-0.252]	0.21 SD (0.012) CI [0.179-0.240]

The data points shown in Table 13 were taken from stress-strain curves generated from the test data. Figure 48-Figure 51 below show the stress-strain curves for the ground room temperature compression tests. The 0 and 90 degree print directions for both the 30 and 60 micron build heights are shown.

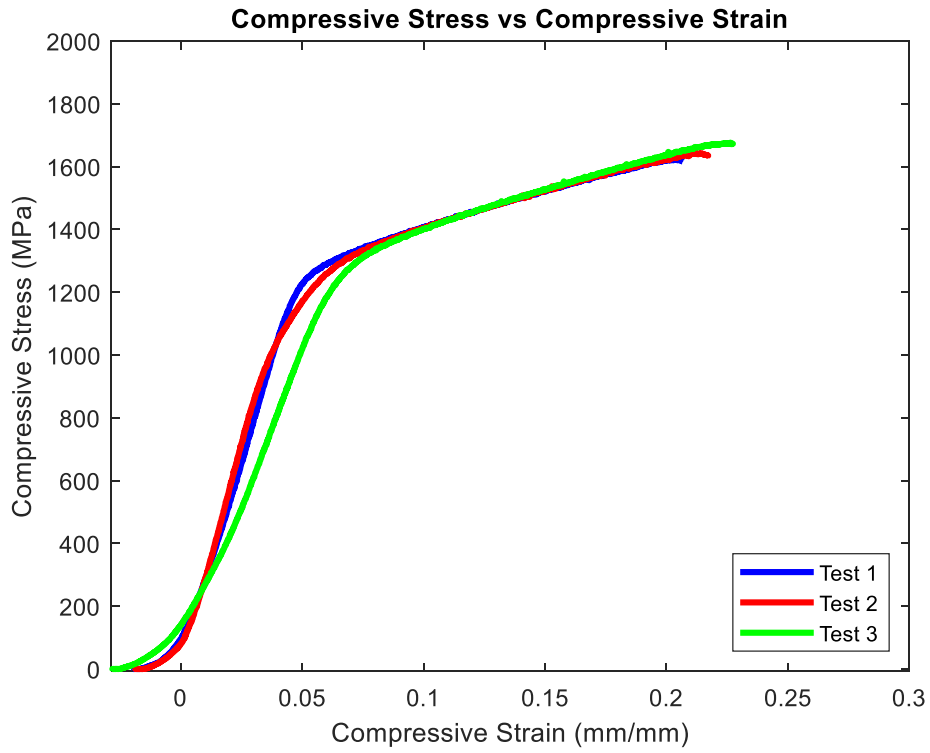


**Figure 48. 30 Micron/0 Degrees/Room Temperature**

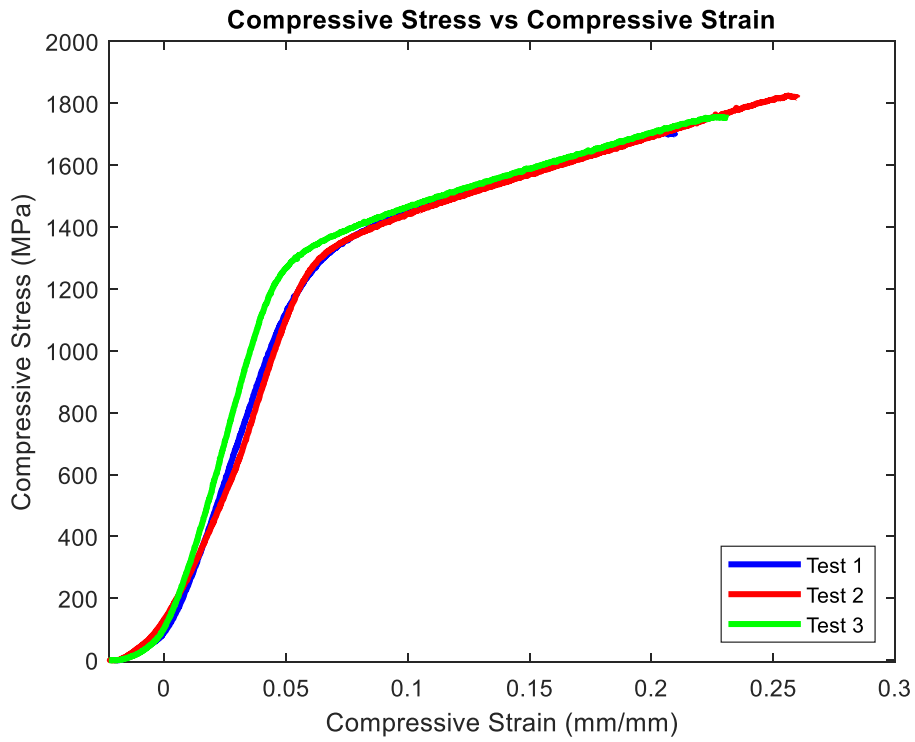


**Figure 49. 30 Micron/90 Degrees/Room Temperature**

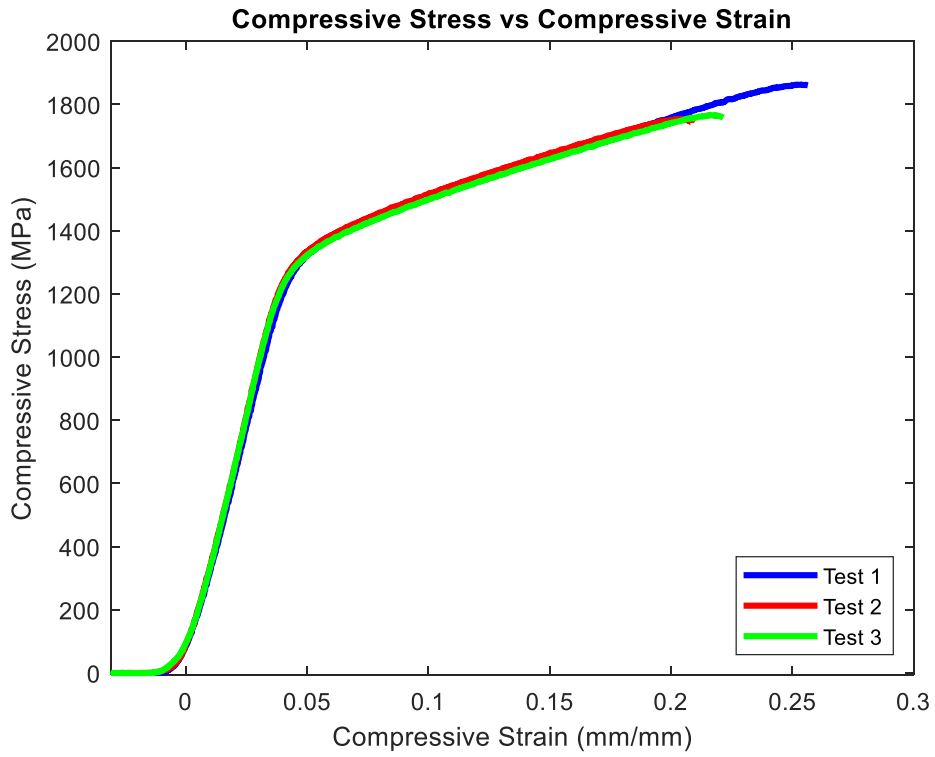


**Figure 50. 60 Micron/0 Degrees/Room Temperature**

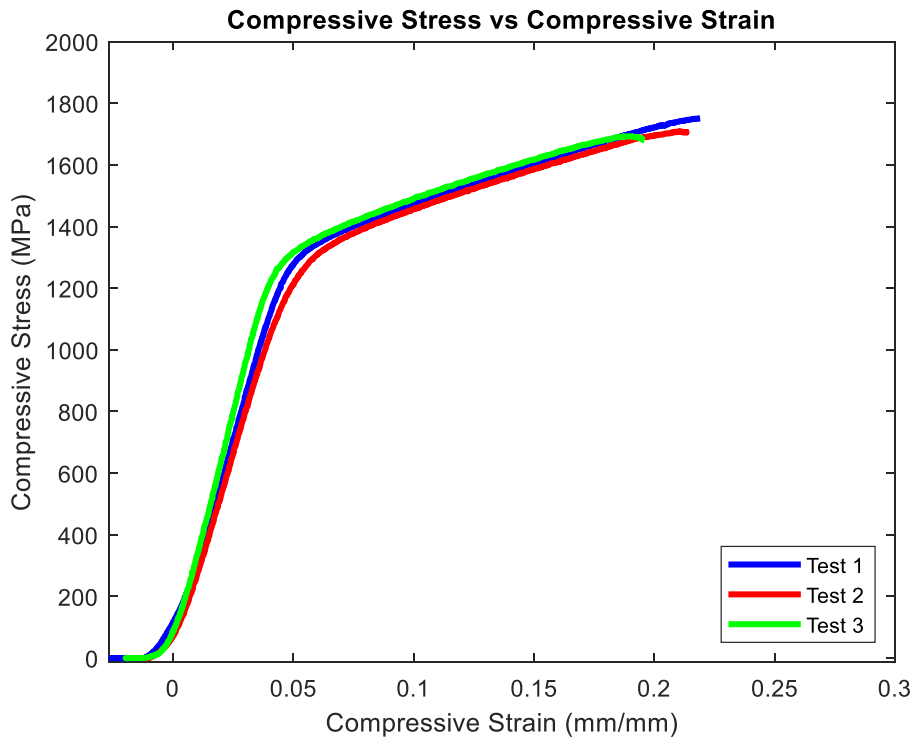


**Figure 51. 60 Micron/90 Degrees/Room Temperature**

#### 4.10 Unground Room Temperature Compression Results

Room temperature compression tests were performed on 0 and 90 degree print orientation samples for both the 30 and 60 micron build heights. Table 14 below shows average data values in the two print directions for each build height. Each orientation and build height was tested using three samples. Statistical analysis was also conducted for the experimental results. Since each test variant was conducted three times, standard deviations and 95% t-test confidence intervals were determined for all the different tests to examine the validity of the data and to look for any outliers.

**Table 14. Values for Unground Room Temperature Compression Tests**

	<b>30 Micron/ 0 Degrees</b>	<b>30 Micron/ 90 Degrees</b>	<b>60 Micron/ 0 Degrees</b>	<b>60 Micron/ 90 Degrees</b>
<b>Modulus of Elasticity (MPa)</b>	21500 SD (2980) CI [18700-24200]	24400 SD (1860) CI [22700-26100]	29200 SD (5230) CI [16200-42200]	26000 SD (3420) CI [22800-29100]
<b>Yield Stress (MPa)</b>	1040 SD (55.1) CI [990-1090]	1100 SD (13.6) CI [1070-1130]	1080 SD (37.3) CI [1040-1110]	1060 SD (48.3) CI [1010-1100]
<b>Yield Strain (mm/mm)</b>	0.0513 SD (0.0090) CI [0.043-0.060]	0.047 SD (0.0032) CI [0.044-0.050]	0.040 SD (0.0062) CI [0.034-0.045]	0.043 SD (0.0035) CI [0.040-0.046]
<b>Ultimate Stress (MPa)</b>	1550 SD (83.3) CI [1480-1630]	1590 SD (64.6) CI [1530-1650]	1570 SD (42.4) CI [1530-1610]	1600 SD (61.1) CI [1450-1750]
<b>Ultimate Strain (mm/mm)</b>	0.221 SD (0.024) CI [0.199-0.243]	0.204 SD (0.028) CI [0.134-0.275]	0.205 SD (0.022) CI [0.150-0.260]	0.208 SD (0.019) CI [0.190-0.226]
<b>Fracture Stress (MPa)</b>	1550 SD (85.9) CI [1470-1630]	1580 SD (69.0) CI [1510-1640]	1570 SD (44.9) CI [1530-1610]	1590 SD (57.4) CI [1540-1650]
<b>Fracture Strain (mm/mm)</b>	0.224 SD (0.023) CI [0.166-0.283]	0.212 SD (0.027) CI [0.186-0.237]	0.207 SD (0.021) CI [0.187-0.227]	0.215 SD (0.019) CI [0.197-0.233]

The data points shown in Table 14 were taken from stress-strain curves generated from the test data. Figure 52-Figure 55 below show the stress-strain curves for the unground room temperature compression tests. The 0 and 90 degree print directions for both the 30 and 60 micron build heights are shown.

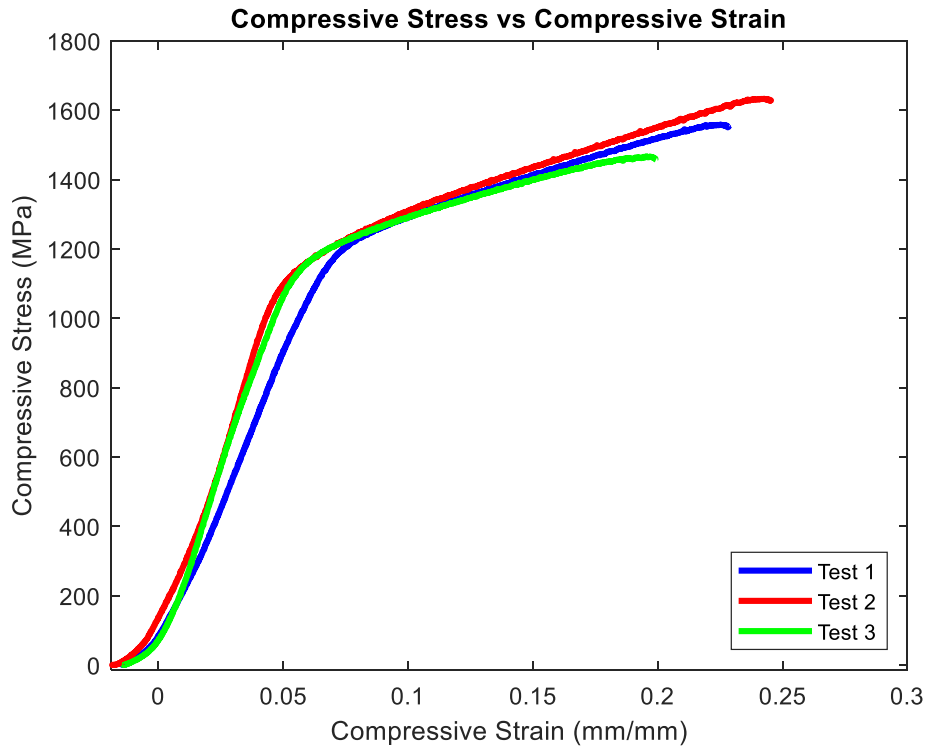


**Figure 52. 30 Micron/0 Degrees/Room Temperature**

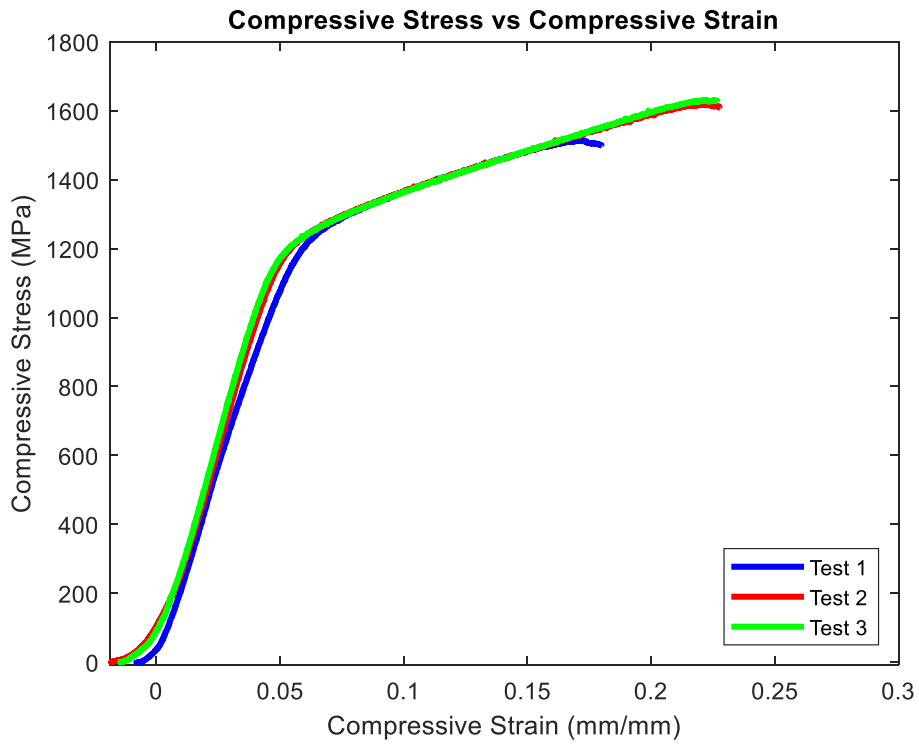


**Figure 53. 30 Micron/90 Degrees/Room Temperature**

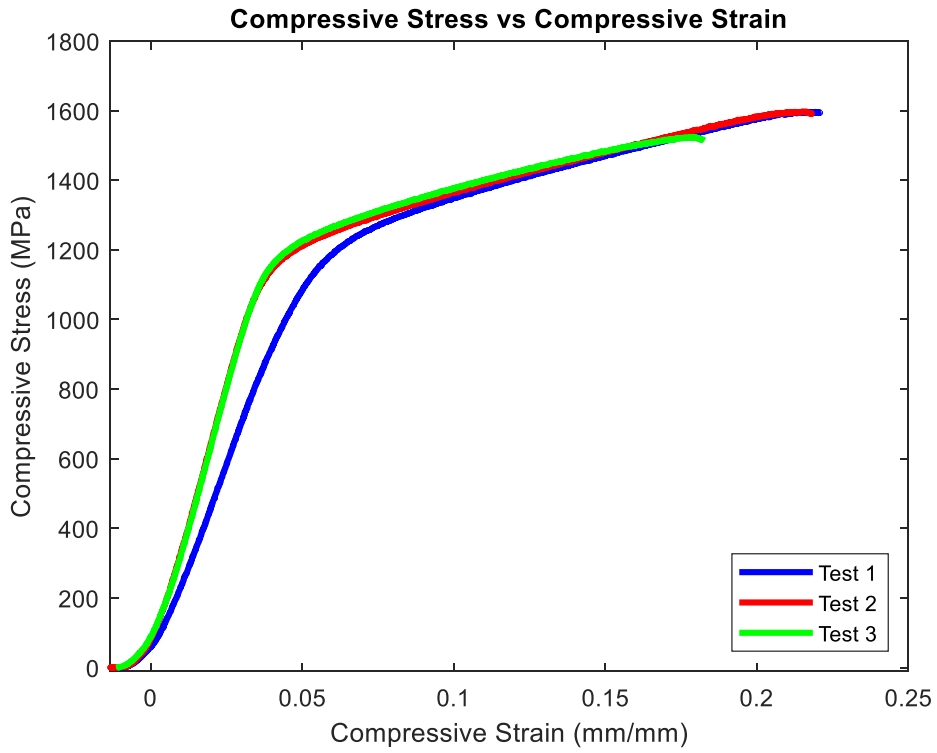


**Figure 54. 60 Micron/0 Degrees/Room Temperature**

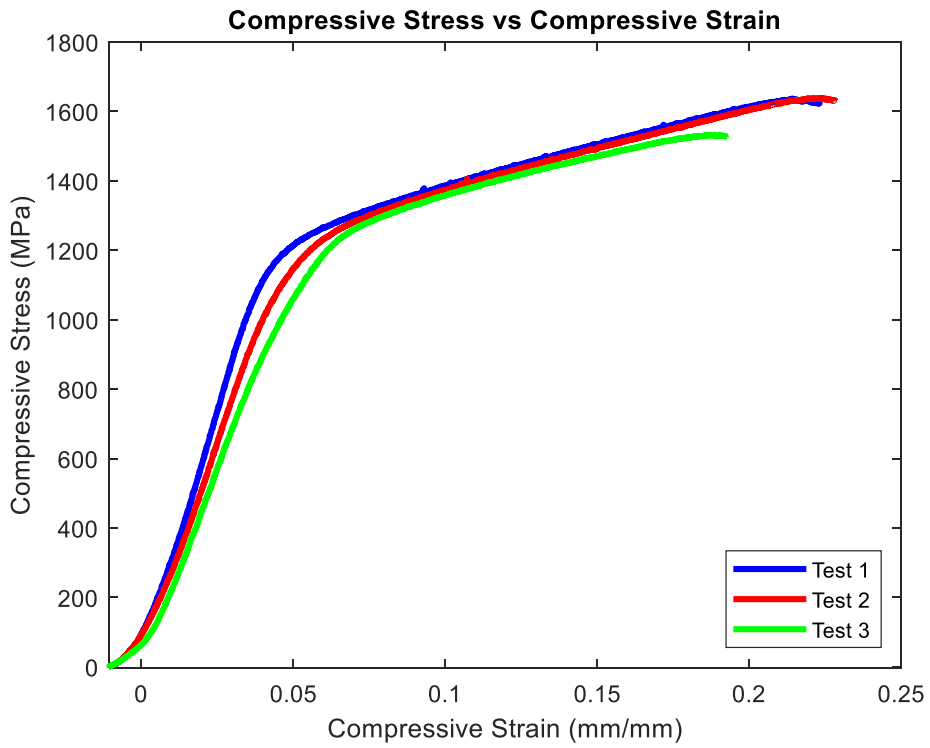


**Figure 55. 60 Micron/90 Degrees/Room Temperature**

#### 4.11 Comparison of Ground and Unground Room Temperature Compression Tests

As seen above in Table 14, the results are not much different when they are compared to the ground room temperature compression test results in Table 13. To check if the results were significantly different or similar, a comparison of means using a t-test was run on the ground and unground room temperature compression tests. Table 15 below shows the results.

**Table 15. Comparison of Means Between the Ground Room Temperature Compression Tests and the Unground Room Temperature Compression Tests**

	<b>30 Micron/ 0 Degrees</b>	<b>30 Micron/ 90 Degrees</b>	<b>60 Micron/ 0 Degrees</b>	<b>60 Micron/ 90 Degrees</b>
<b>Modulus of Elasticity (MPa)</b>	0.2897	0.9334	0.4126	0.3247
<b>Yield Stress (MPa)</b>	0.3473	0.0561	0.0030	0.0190
<b>Yield Strain (mm/mm)</b>	0.7225	0.4434	1.0000	1.0000
<b>Ultimate Stress (MPa)</b>	0.1519	0.0286	0.0077	0.0553
<b>Ultimate Strain (mm/mm)</b>	0.0627	0.3039	0.4881	0.8931
<b>Fracture Stress (MPa)</b>	0.1607	0.0269	0.0083	0.0377
<b>Fracture Strain (mm/mm)</b>	0.7960	0.4446	0.2894	0.7196

In Table 15 above, p-values are presented to compare the means between the two sample types. Any p-value less than 0.05 indicates that the two sample means are significantly different [29]. Differences that are unique are shown in white cells, while differences that are not conclusively unique are shown in blue cells. As is seen, most of the values in the table are above the 0.05 threshold indicating the unground and ground room temperature compression tests are not significantly different. The only parameter that has more than one value that is significantly different is the yield stress. All other parameters show a very strong agreement in their results.

As seen above in Figure 48-Figure 51, the ground room temperature compression results show very little variance between the build directions and sample build heights. This is expected since compression tests close crack initiation points so varying print directions and sample build heights will not have an impact on the overall mechanical response of the material. The samples are also sufficiently thick so the rough surface that does not support load will not contribute to the overall response of the material. Lastly, the only differences seen in the graphs were the fracture stress and fracture strain values observed in some of the tests.

As seen above in Figure 52-Figure 55, the three tests on the individual graphs match up very well. The only value that does not line up very well is the fracture strain. This is expected since the unground sides give cracks an easier and somewhat unpredictable place to initiate propagation through the sample which eventually leads to failure. Other than this, the two print directions and the different sample build heights match up very well with each other.

#### 4.12 Comparison of Ground Room Temperature Compression Tests and Traditionally Manufactured Ti 6-4

To check if the additively manufactured compressive samples had a different mechanical response when compared to traditionally manufactured Ti 6-4, the results in Table 13 were compared to wrought Ti 6-4 data [31] [32] using percentage differences. Table 16-Table 17 shown below displays the percent difference results.

**Table 16. Largest Percent Differences for Ground Room Temperature Compressive Tests**

	<b>Largest Percent Difference (%)</b>	<b>Sample Compared</b>
<b>Compressive Yield Stress</b>	22.8	60 Micron/0 Degrees
<b>Ultimate Compressive Stress</b>	60.0	60 Micron/0 Degrees

**Table 17. Smallest Percent Differences for Ground Room Temperature Compressive Tests**

	<b>Smallest Percent Difference (%)</b>	<b>Sample Compared</b>
<b>Compressive Yield Stress</b>	14.4	30 Micron/0 Degrees
<b>Ultimate Compressive Stress</b>	52.5	30 Micron/0 Degrees

As seen from Table 16-Table 17, the ground room temperature compressive samples lined up well with the wrought Ti 6-4 data for the compressive yield stress but a larger difference was seen between the ultimate compressive stress values and the

traditionally manufactured Ti 6-4 data. The smallest percent difference for the ultimate compressive stress was over 50% but the largest percent difference seen for the ultimate compressive stress was at 60%.

#### **4.13 Comparison of Yield and Ultimate Stress Results for Compression Samples**

To compare all the print orientations, sample build heights, and surface finishes from the compression tests, a plot was created to compare all the compression test yield stress values. Figure 56 shown below displays the room temperature yield stress results for the compression samples. On the graph, filled shapes represent ground samples while open shapes represent unground samples. Triangles represent a build height of 30 micron while circles represent a build height of 60 micron.

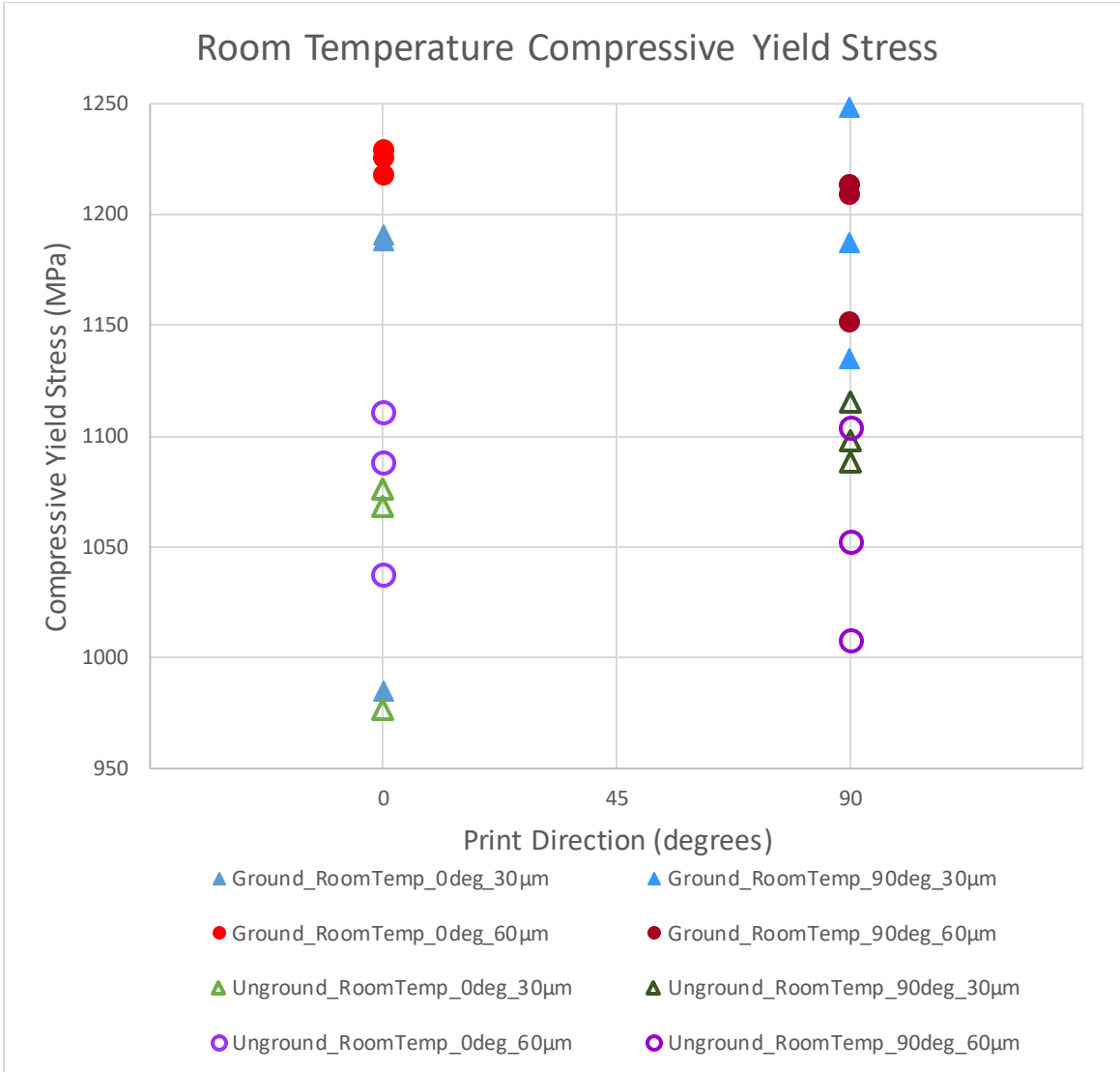


**Figure 56. Yield Stress Comparison for Room Temperature Compression Samples**

To compare all the print orientations, sample build heights, and surface finishes from the compression tests, a plot was created to compare all the compression test ultimate stress values. Figure 57 shown below displays the room temperature ultimate stress results for the compression samples. On the graph, filled shapes represent ground samples while open shapes represent unground samples. Triangles represent a build height of 30 micron while circles represent a build height of 60 micron.

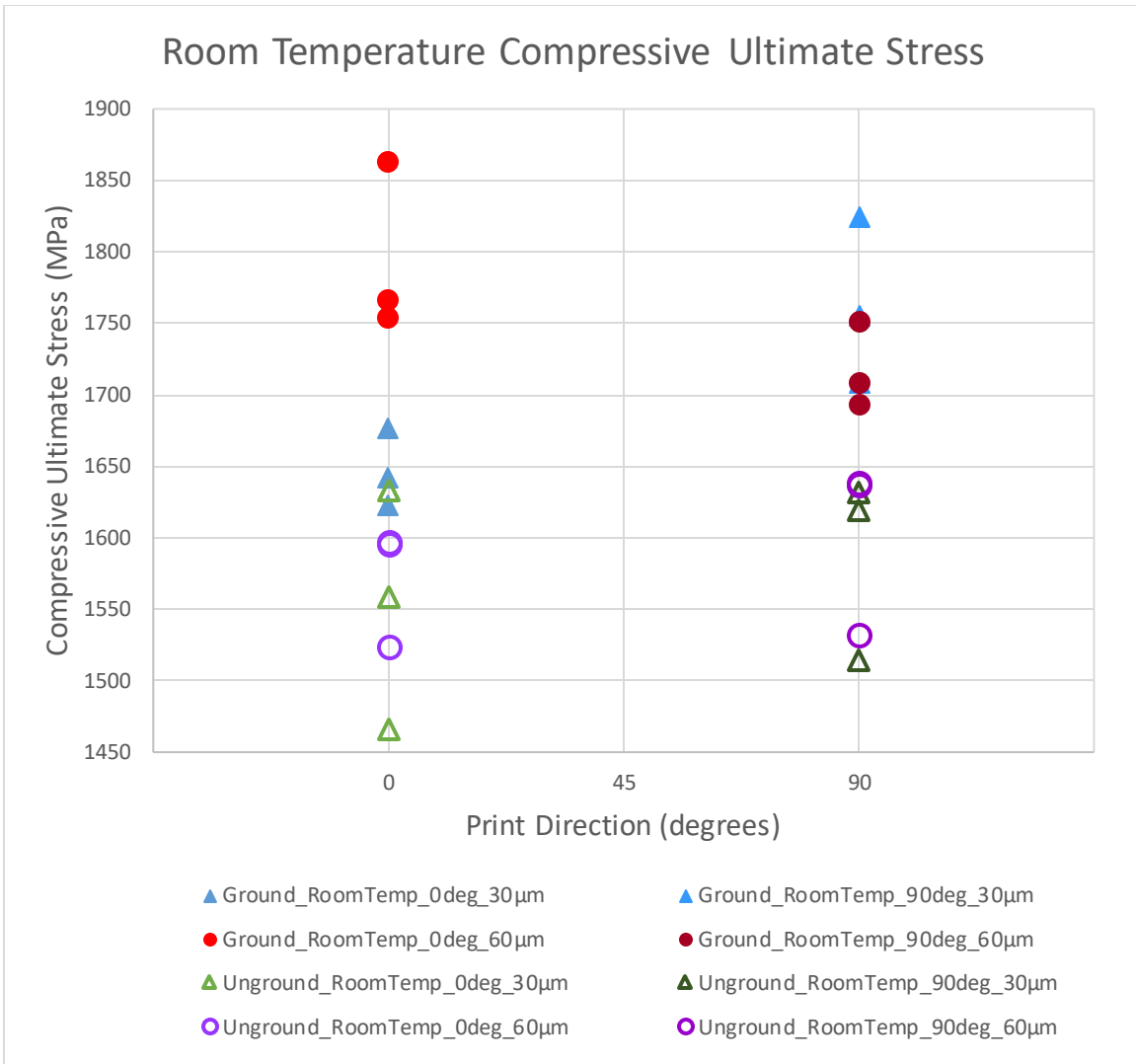


**Figure 57. Ultimate Stress Comparison for Room Temperature Compression Samples**

As seen above in Figure 56-Figure 57, the ground samples had slightly higher yield and ultimate stress values when compared to the unground samples, but the values were very close to each other and only a small spread was seen. The different sample build heights had similar results when looking at the different print directions for a given grinding type for the different compression tests. The print directions also did not seem to

play a role in the yield or ultimate stress responses of the material in compression as the 0 and 90 degree print orientations had similar yield and ultimate stress responses for a given compression test.

#### **4.14 Ground Room Temperature Tensile Results**

Room temperature tensile tests were performed on 0, 45, and 90 degree print orientation samples for both the 30 and 60 micron build heights. Table 18 below shows average data values in the three print directions for each build height. Each orientation and build height was tested using three samples. Statistical analysis was also conducted for the experimental results. Since each test variant was conducted three times, standard deviations and 95% t-test confidence intervals were determined for all the different tests to examine the validity of the data and to look for any outliers.

**Table 18. Values for Ground Room Temperature Tensile Tests**

	<b>30 Micron/ 0 Degrees</b>	<b>30 Micron/ 45 Degrees</b>	<b>30 Micron/ 90 Degrees</b>	<b>60 Micron/ 0 Degrees</b>	<b>60 Micron/ 45 Degrees</b>	<b>60 Micron/ 90 Degrees</b>
<b>Modulus of Elasticity (MPa)</b>	100000 SD (1520) CI [98600-101000]	127000 SD (43200) CI [87400-166000]	102000 SD (2160) CI [100000-104000]	113000 SD (21000) CI [94000-133000]	103000 SD (1330) CI [102000-104000]	98700 SD (1870) CI [97000-100000]
<b>Yield Stress (MPa)</b>	837 SD (16.9) CI [794-879]	892 SD (11.2) CI [882-903]	911 SD (1.35) CI [910-913]	874 SD (15.7) CI [860-889]	915 SD (9.57) CI [907-924]	887 SD (4.80) CI [883-892]
<b>Yield Strain (mm/mm)</b>	0.010 SD (0.00024) CI [0.0098-0.011]	0.0096 SD (0.0022) CI [0.0075-0.012]	0.011 SD (0.00020) CI [0.010-0.011]	0.0099 SD (0.0014) CI [0.0086-0.011]	0.011 SD (.000034) CI [0.011-0.011]	0.011 SD (0.00013) CI [0.011-0.011]
<b>Ultimate Stress (MPa)</b>	889 SD (18.1) CI [872-906]	927 SD (11.7) CI [917-938]	960 SD (2.8) CI [957-962]	927 SD (14.2) CI [914-941]	957 SD (9.66) CI [948-966]	938 SD (5.78) CI [923-952]
<b>Ultimate Strain (mm/mm)</b>	0.041 SD (0.0028) CI [0.038-0.043]	0.045 SD (0.0053) CI [0.040-0.050]	0.045 SD (0.0015) CI [0.044-0.047]	0.044 SD (0.0053) CI [0.039-0.049]	0.045 SD (0.00095) CI [0.044-0.046]	0.041 SD (0.0027) CI [0.039-0.044]
<b>Fracture Stress (MPa)</b>	850 SD (30.4) CI [774-925]	872 SD (29.5) CI [798-945]	896 SD (34.0) CI [864-927]	908 SD (10.4) CI [882-934]	908 SD (41.4) CI [870-947]	897 SD (4.45) CI [893-901]
<b>Fracture Strain (mm/mm)</b>	0.092 SD (0.0080) CI [0.072-0.111]	0.089 SD (0.011) CI [0.078-0.099]	0.097 SD (0.0085) CI [0.090-0.105]	0.071 SD (0.012) CI [0.061-0.082]	0.079 SD (0.012) CI [0.068-0.091]	0.078 SD (0.0060) CI [0.073-0.084]

The data points shown in Table 18 were taken from stress-strain curves generated from the test data. Figure 58-Figure 63 below show the stress-strain curves for the ground room temperature tensile tests. The 0, 45, and 90 degree print directions for both the 30 and 60 micron build heights are shown.

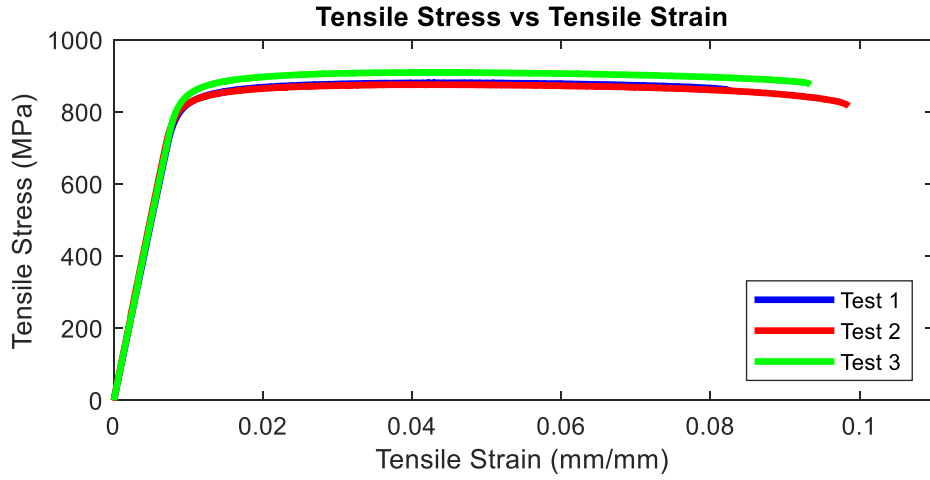


**Figure 58. 30 Micron/0 Degrees/Room Temperature**

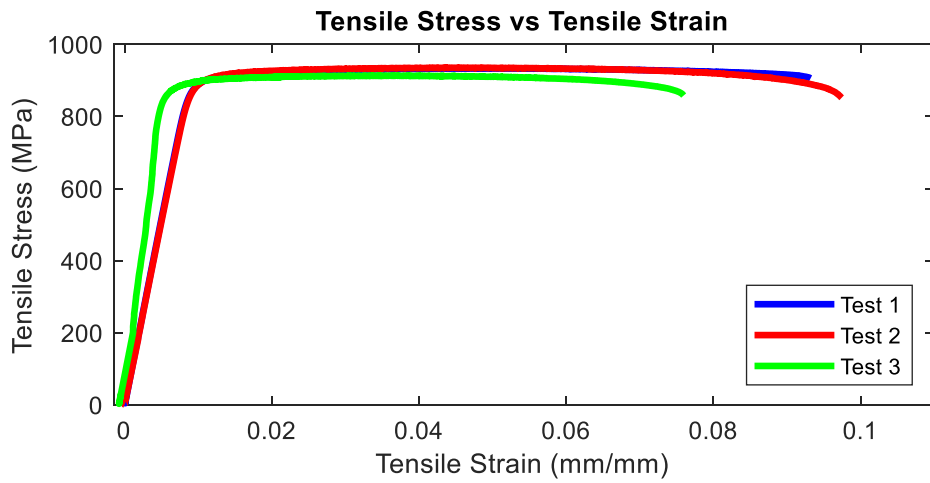


**Figure 59. 30 Micron/45 Degrees/Room Temperature**

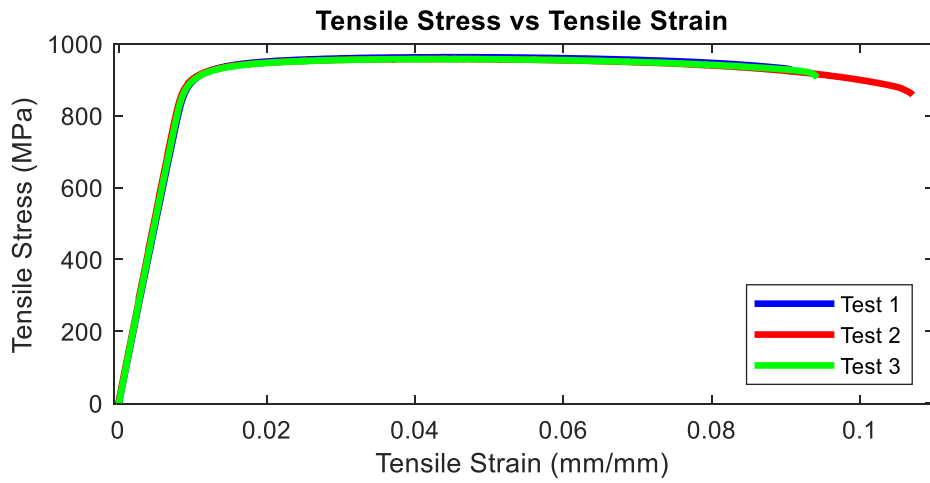


**Figure 60. 30 Micron/90 Degrees/Room Temperature**

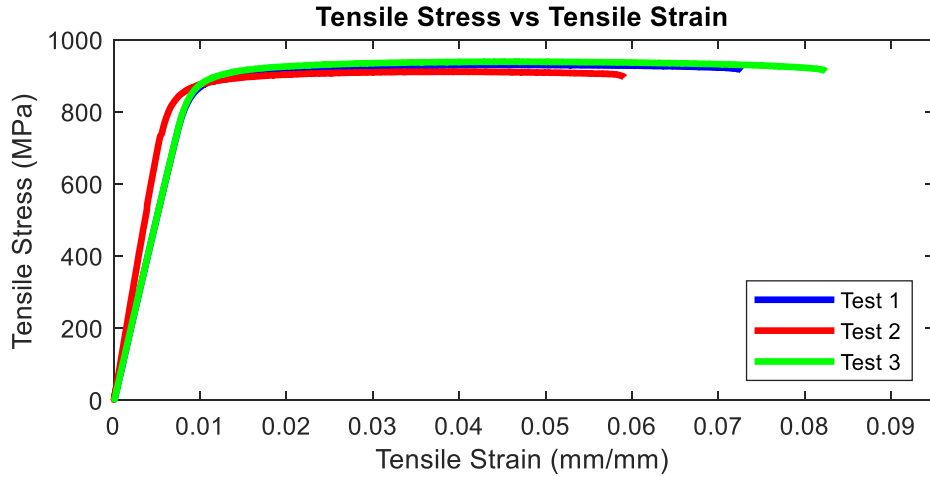


**Figure 61. 60 Micron/0 Degrees/Room Temperature**

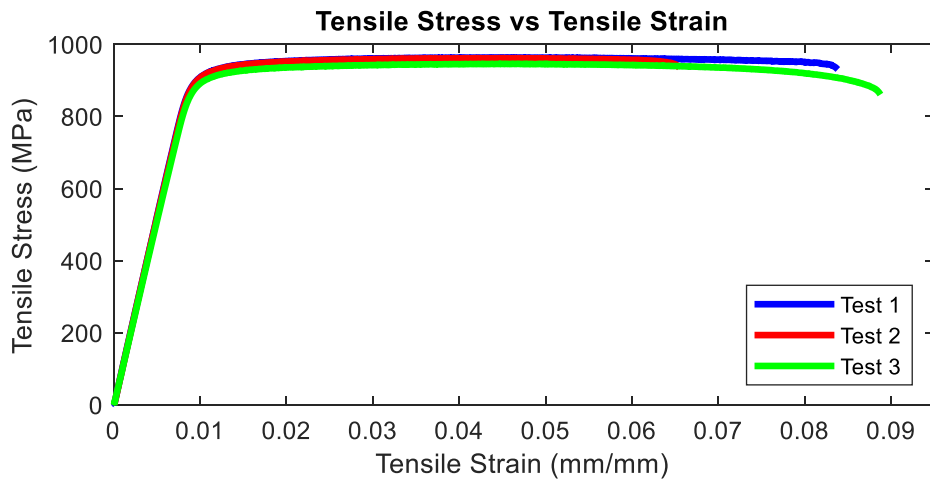


**Figure 62. 60 Micron/45 Degrees/Room Temperature**

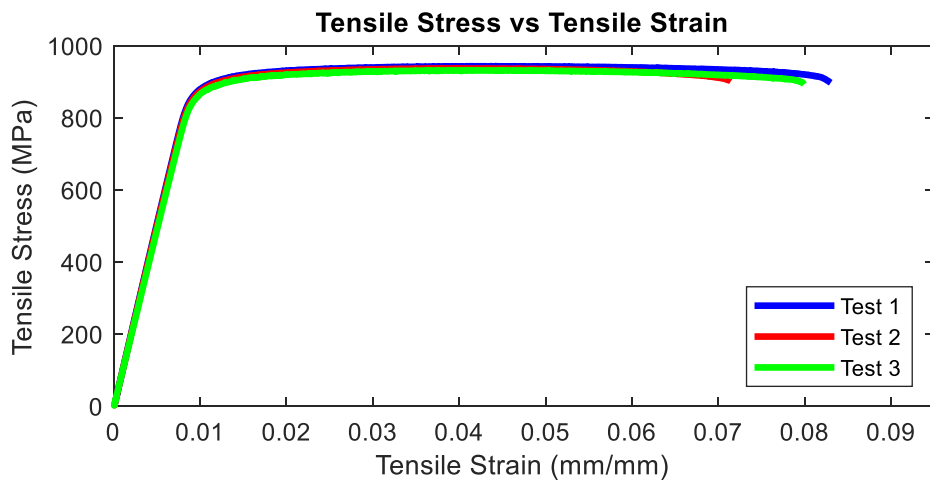


**Figure 63. 60 Micron/90 Degrees/Room Temperature**

**4.15 Comparison of Ground Room Temperature Tensile Tests and Traditionally  
Manufactured Ti 6-4**

To check if the additively manufactured tensile samples had a different mechanical response when compared to traditionally manufactured Ti 6-4, the results in Table 18 were compared to wrought Ti 6-4 data [31] using percentage differences. Table 19-Table 20 shown below displays the percent difference results.

**Table 19. Largest Percent Differences for Ground Room Temperature Tensile Tests**

	<b>Largest Percent Difference (%)</b>	<b>Sample Compared</b>
<b>Modulus of Elasticity</b>	13.1	30 Micron/0 Degrees
<b>Yield Stress</b>	5.0	30 Micron/0 Degrees
<b>Ultimate Stress</b>	6.6	30 Micron/0 Degrees
<b>Fracture Stress</b>	56.1	60 Micron/0 Degrees

**Table 20. Smallest Percent Differences for Ground Room Temperature Tensile Tests**

	<b>Smallest Percent Difference (%)</b>	<b>Sample Compared</b>
<b>Modulus of Elasticity</b>	0.88	60 Micron/0 Degrees
<b>Yield Stress</b>	0.68	60 Micron/0 Degrees
<b>Ultimate Stress</b>	0.73	60 Micron/45 Degrees
<b>Fracture Stress</b>	50.0	30 Micron/0 Degrees

As seen from Table 19-Table 20, the ground room temperature tensile samples lined up very well with the wrought Ti 6-4 data outside of the fracture stress. This is seen since the largest percent difference is still very low outside of the fracture stress. The smallest percent differences were all under one percent except fracture stress. This shows how close the additively manufactured Ti 6-4 samples lined up with the wrought Ti 6-4 data.

As seen above in Figure 58-Figure 63, the graphs show very similar results for all the different sample build heights and print directions. All the tests have a very linear elastic region and a long and flat plastic region that is commonly seen in Ti 6-4. The biggest difference between the graphs is the strain at which fracture occurs. Otherwise the graphs lined up very well with each other when comparing print direction and sample build height and the graphs predict the usual tensile Ti 6-4 mechanical response seen in traditionally manufactured Ti 6-4 samples.

#### **4.16 Comparison of Yield and Ultimate Stress Results for Tensile Samples**

To compare all the print orientations and sample build heights from the tensile tests, a plot was created to compare all the tensile test yield stress values. Figure 64 shown below displays the room temperature yield stress results for the tensile samples. On the graph, filled shapes represent ground samples while open shapes represent unground samples. Triangles represent a build height of 30 micron while circles represent a build height of 60 micron.

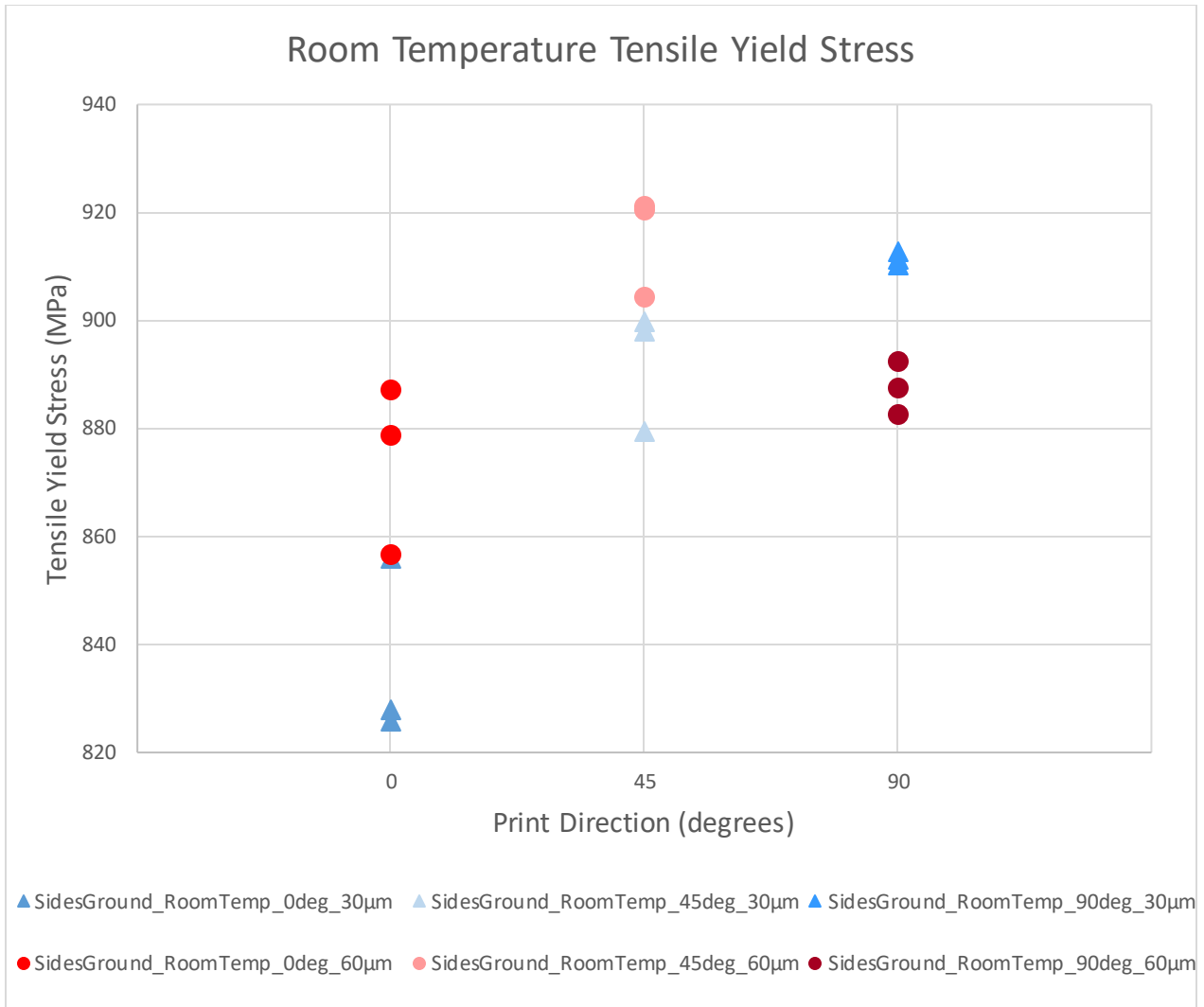


**Figure 64. Yield Stress Comparison for Room Temperature Tensile Samples**

To compare all the print orientations and sample build heights from the tensile tests, a plot was created to compare all the tensile test ultimate stress values. Figure 65 shown below displays the room temperature ultimate stress results for the tensile samples. On the graph, filled shapes represent ground samples while open shapes represent unground samples. Triangles represent a build height of 30 micron while circles represent a build height of 60 micron.

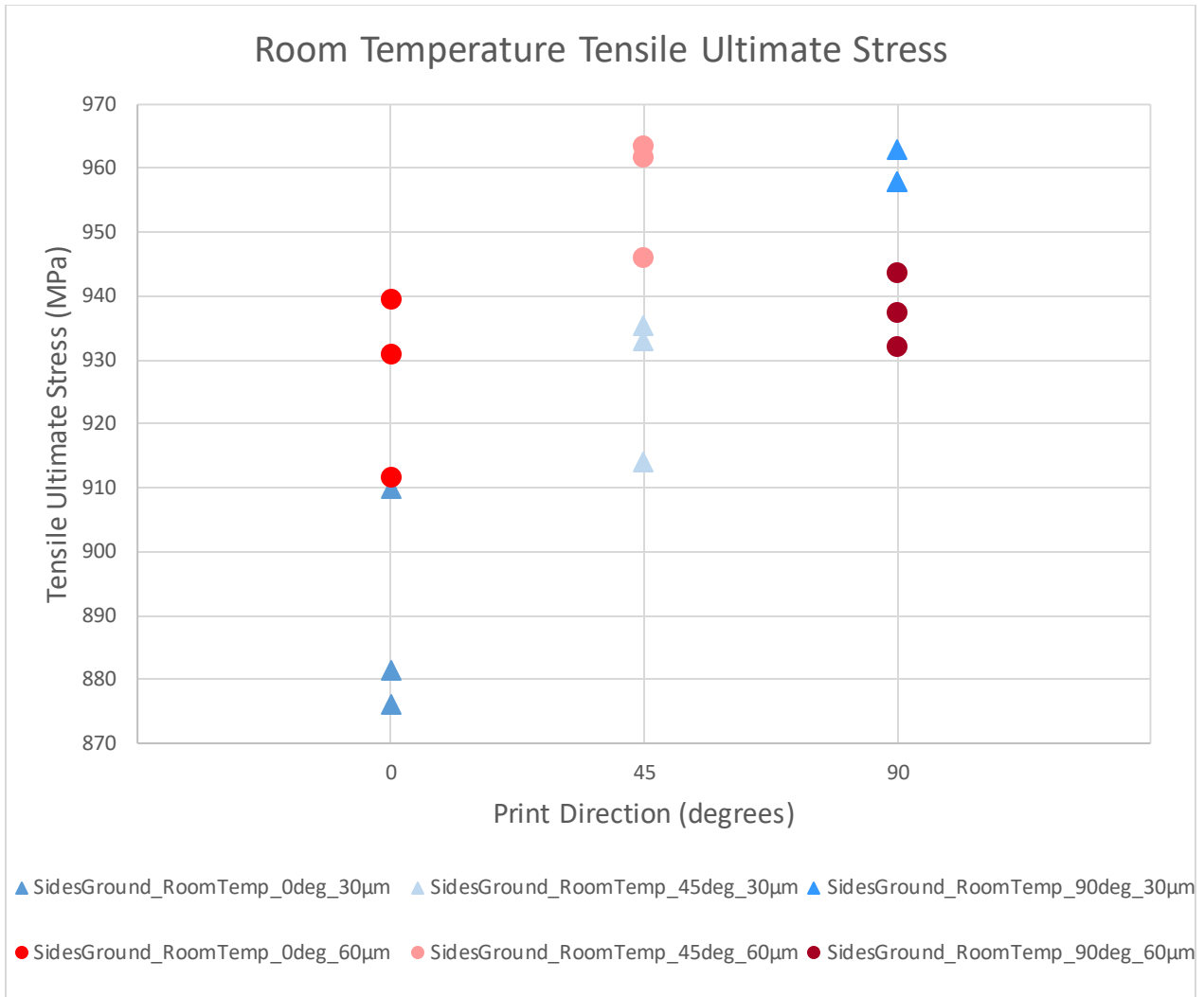


**Figure 65. Ultimate Stress Comparison for Room Temperature Tensile Samples**

As seen in Figure 64-Figure 65, the different sample build heights exhibited similar results for the yield stress values seen in the different tests. This was also the case for the different sample build heights when looking at the ultimate stress values in the different print directions. The print directions also exhibited similar results for the 0, 45, and 90 degree print orientations for the yield and ultimate stress values. There was no comparison of ground versus unground tensile samples since no unground tensile samples were tested.

#### **4.17 Microscopy**

In addition to experimentation and data analysis, microscopy was also performed on the samples. Fracture surfaces of the compression and tensile samples were considered using the Scanning Electron Microscope (SEM). The three point bend samples were ground and etched to investigate grain growth during manufacturing and testing. The powder used to manufacture the samples was looked at using Energy-Dispersive X-ray Spectroscopy (EDS) to look at the elemental composition of the powder. The sample powder was also investigated using the SEM to investigate powder size and distribution. Both the 30 and 60 micron samples were looked at using EDS to investigate the elemental composition of the individual sample build heights.

First, the tensile sample fracture surfaces were investigated using the SEM. Figure 66-Figure 68 below shows the SEM pictures captured for the 30 micron build height tensile samples.

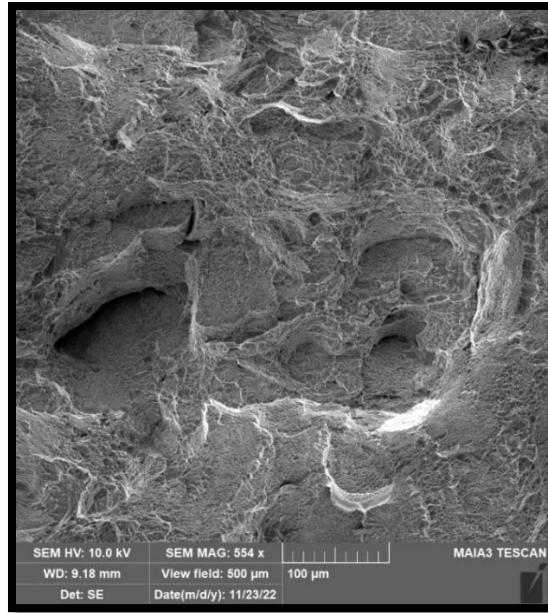
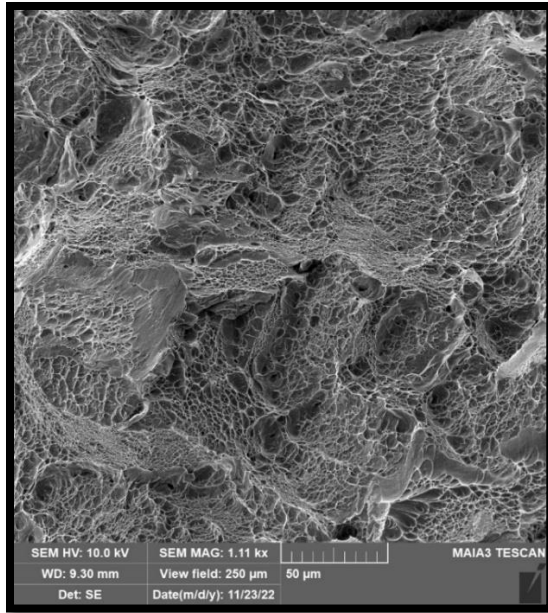


**Figure 66. 30 Micron/0 Degrees/RT/Tensile    Figure 67. 30 Micron/45 Degrees/RT/Tensile**

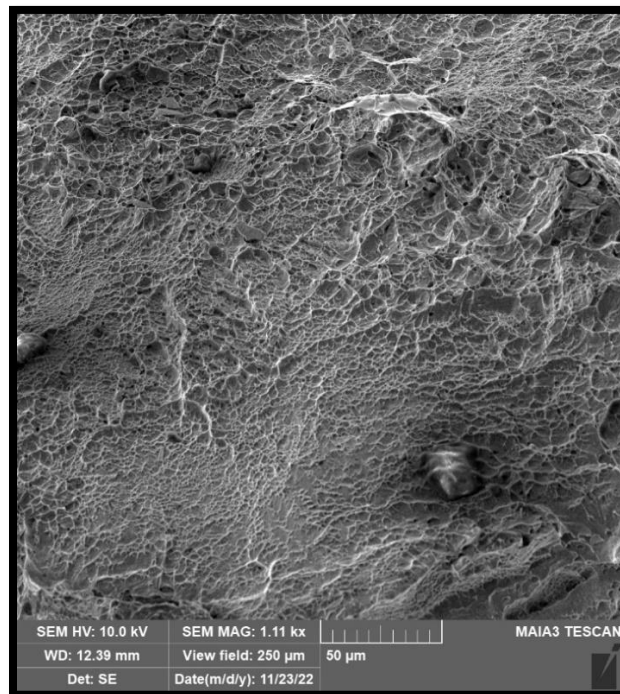


**Figure 68. 30 Micron/90 Degrees/Room Temperature/Tensile**

As seen in Figure 66-Figure 68, all the 30 micron tensile fracture surfaces exhibited microvoid coalescence. This is expected since Ti 6-4 is a metallic alloy and this fracture mechanism is common in many metallic alloys. The 60 micron build height tensile fracture surfaces also show all the print orientations exhibiting microvoid coalescence as seen above.

The tensile specimens showed differing macro-scale fracture surfaces. The 0 degree samples fractured with a rough surface since the grains were in the direction of the force applied and had to be broken to cause failure leaving the surface with a rough finish. The 45 degree samples fractured with a 45 degree angle on the ends of the sample since all the samples failed due to shear along the 45 degree grain boundaries. The 90 degree samples fractured with a flat surface since the specimen was printed with the grains perpendicular to the applied force and this allowed for failure along grain boundaries. Figure 69-Figure 71 below demonstrates this for the 60 micron build height tensile samples. This was also seen in the 30 micron build height tensile samples.

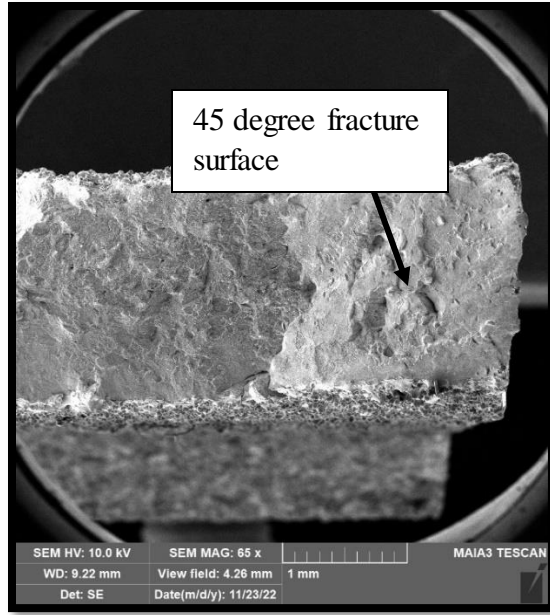
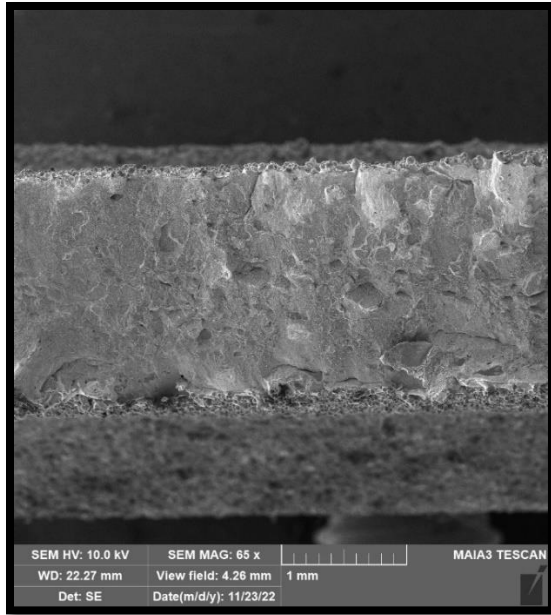


**Figure 69. 60 Micron/0 Degrees/ RT/Tensile    Figure 70. 60 Micron/45 Degrees/ RT/Tensile**

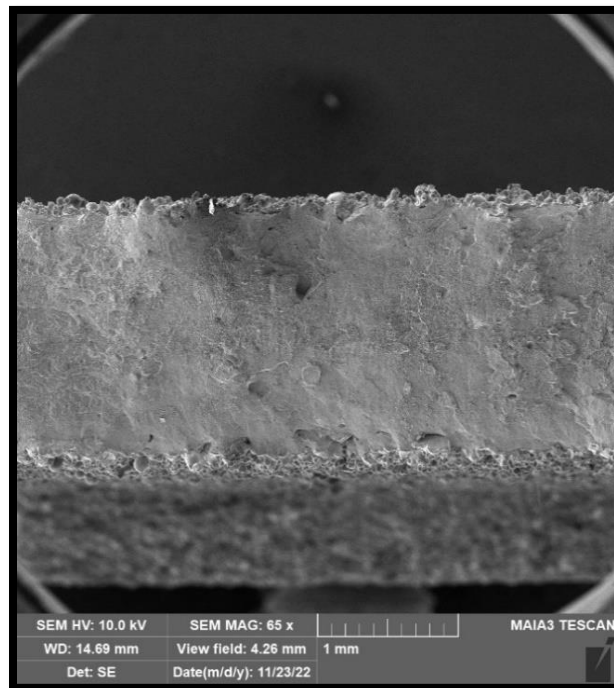


**Figure 71. 60 Micron/90 Degrees/Room Temperature/Tensile**

The compression samples were also considered using the SEM. Figure 72-Figure 75 below shows the images captured for the 30 micron build height compression samples with all the sides ground.

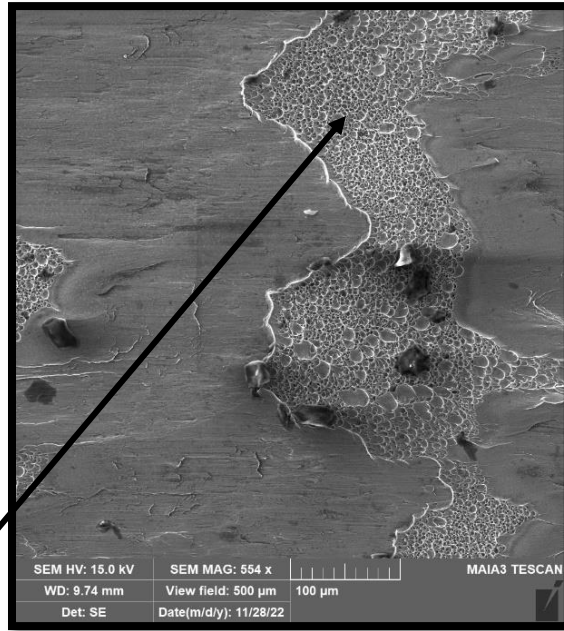


**Figure 72. 30 Micron/0 Degrees/RT/Compressive**

Microvoid Coalescence

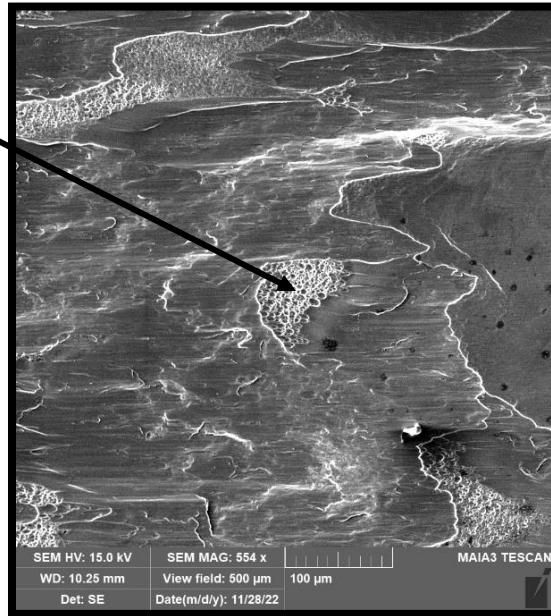
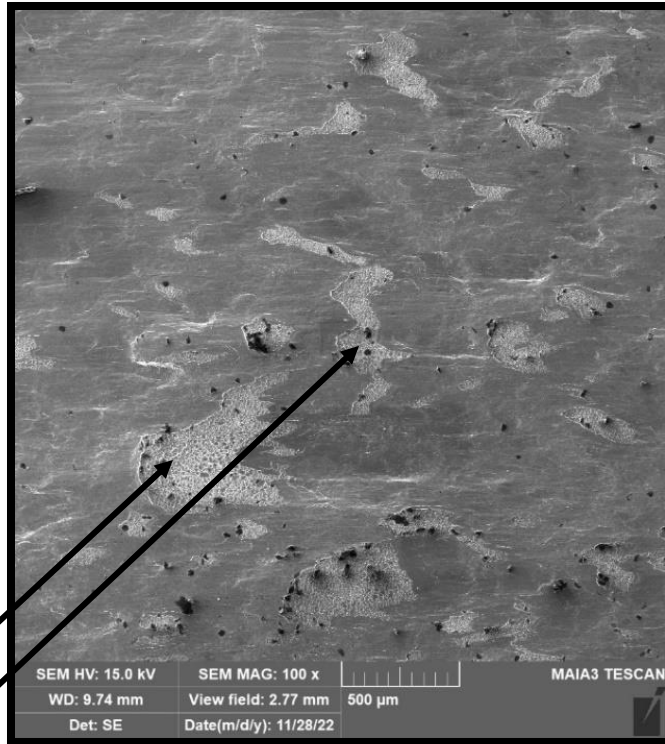


**Figure 73. 30 Micron/90 Degrees/RT/Compressive**



Microvoid Coalescence

**Figure 74. 30 Micron/0 Degrees/RT/Compressive**

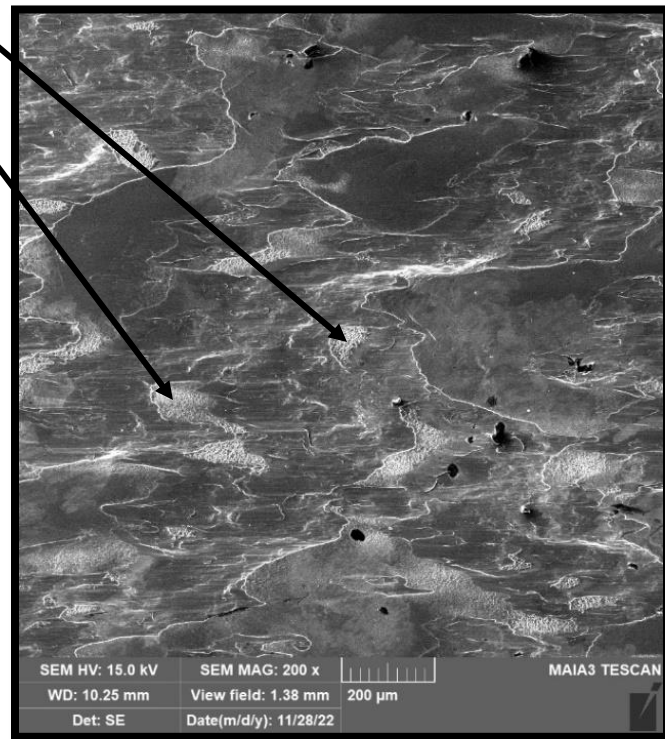


**Figure 75. 30 Micron/90 Degrees/RT/Compressive**

As seen from Figure 72-Figure 75, the compression samples experienced both microvoid coalescence and transgranular fracture mechanisms. All the samples also failed at a 45 degree angle along the diagonal (Figure 76 below) which was caused by the samples failing in shear like the tensile samples. All these failure behaviors were seen for every 30 and 60 micron build height ground and unground compression sample. The build height, print direction, and surface finish did not contribute to the fracture mechanisms or type of failure seen in the compression samples.

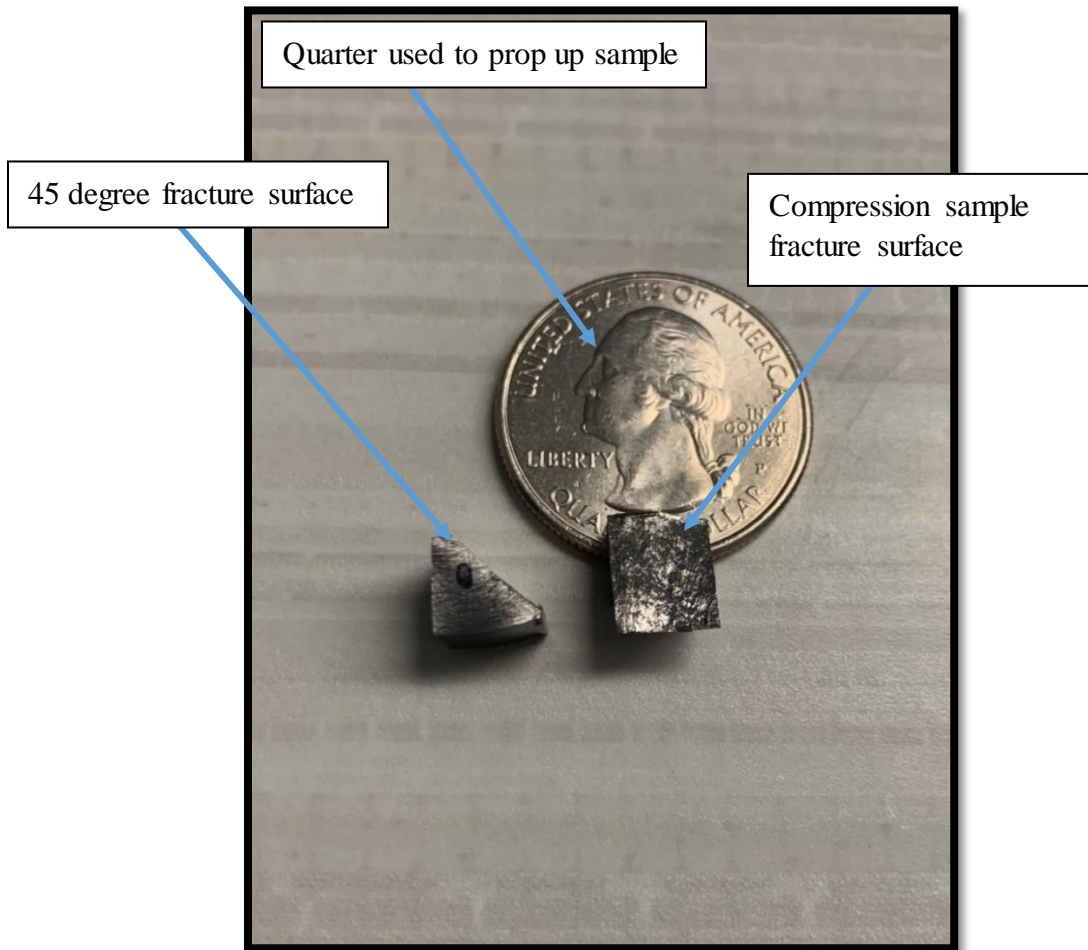


**Figure 76. Failed Compression Sample**

Next, EDS was performed on a 30 and 60 micron build height tensile sample to examine the elemental makeup of the different samples. 15 kV and a capture time of 30 seconds was used during data collection. Table 21-Table 22 below show the results for both the 30 and 60 micron build height samples.

**Table 21. 30 Micron Build Height Sample Elemental Makeup**

<b>Element</b>	<b>Weight %</b>	<b>Atomic %</b>	<b>Error %</b>
<b>Al</b>	5.55	9.47	5.68
<b>Ti</b>	89.86	86.38	1.96
<b>V</b>	4.59	4.15	5.51

**Table 22. 60 Micron Build Height Sample Elemental Makeup**

<b>Element</b>	<b>Weight %</b>	<b>Atomic %</b>	<b>Error %</b>
<b>Al</b>	6.43	10.9	6.01
<b>Ti</b>	88.89	84.9	1.97
<b>V</b>	4.68	4.2	5.5

As seen in Table 21-Table 22, the elemental makeup in both the 30 and 60 micron build height samples reflects very closely to the correct elemental makeup of Ti 6-4 (90 percent titanium, 6 percent aluminum, and 4 percent vanadium) with only a small weight percentage deviation. After the samples were looked at, the powder used to manufacture the samples was also investigated in the SEM to determine the powder distribution. The powder was checked to make sure the different powder sizes were evenly distributed throughout the powder batch. Figure 77 below shows the powder distribution.

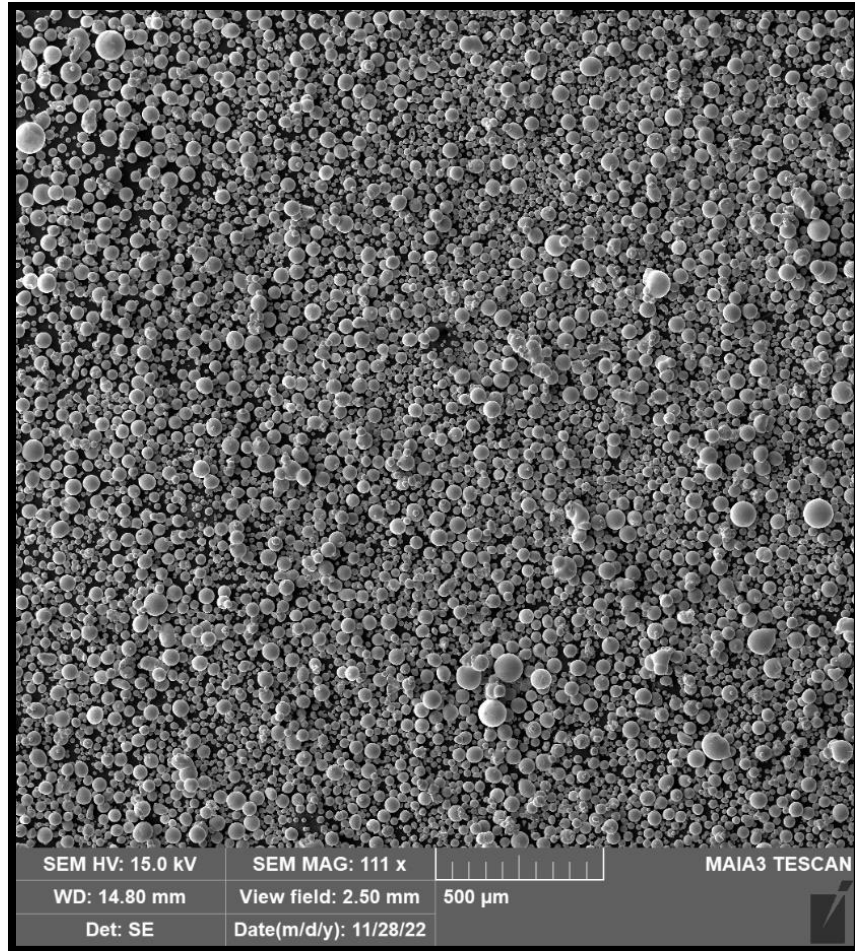


**Figure 77. Sample Powder Distribution**

As seen in Figure 77, there is a good distribution of powder sizes with the different sized balls evenly distributed throughout the entire image. After this was completed, the sample powder was investigated in the SEM with a larger magnification to determine the different powder sizes present in the sample batch. Figure 78 below shows the magnified powder image.

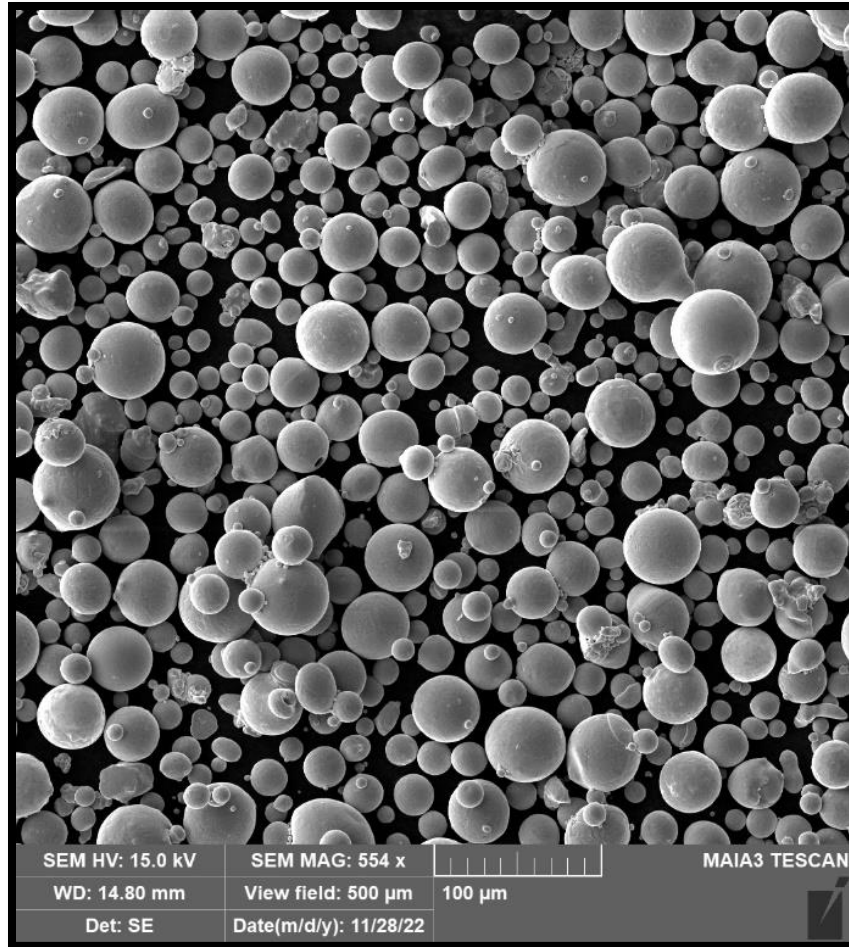


**Figure 78. Sample Powder**

As seen in Figure 78, there are two general sizes to the powder. There is a larger size and a smaller size powder present. To determine the elemental makeup of the different powder sizes, EDS was performed on the different sample powder sizes to investigate the powder further. 15 kV and a capture time of 30 seconds was used during data collection. Table 23-Table 24 below show the powder EDS results.

**Table 23. Large Sample Powder Elemental Makeup**

<b>Element</b>	<b>Weight %</b>	<b>Atomic %</b>	<b>Error %</b>
<b>Al</b>	7.23	12.18	5.73
<b>Ti</b>	88.56	84.06	2.05
<b>V</b>	4.21	3.76	7.54

**Table 24. Small Sample Powder Elemental Makeup**

<b>Element</b>	<b>Weight %</b>	<b>Atomic %</b>	<b>Error %</b>
<b>C</b>	84.71	91.12	3
<b>V</b>	5.23	1.33	35.23
<b>O</b>	8.94	7.22	14.98
<b>Al</b>	0.16	0.07	15.87
<b>Ti</b>	0.96	0.26	11.76

As seen from Table 23-Table 24, the larger powder spheres are Ti 6-4 powder. These powder spheres were pre-formed into Ti 6-4 even before the samples were manufactured. The small powder spheres are mostly carbon with oxygen and some trace elements that make up Ti 6-4. The carbon and oxygen seen in the small spheres does not appear in the manufactured samples as seen in the tensile bar EDS results.

Lastly, the three point bend tests were pucked, ground, and etched to observe the grain growth in the samples. When looking at the samples under the microscope, all the room temperature samples had the same surface finish resulting from the etching regardless of print direction, sample build height, or surface finish. In addition, no grains could be discerned in any of the images. Figure 79-Figure 81 below shows the results of the ground and unground room temperature three point bend etched samples.

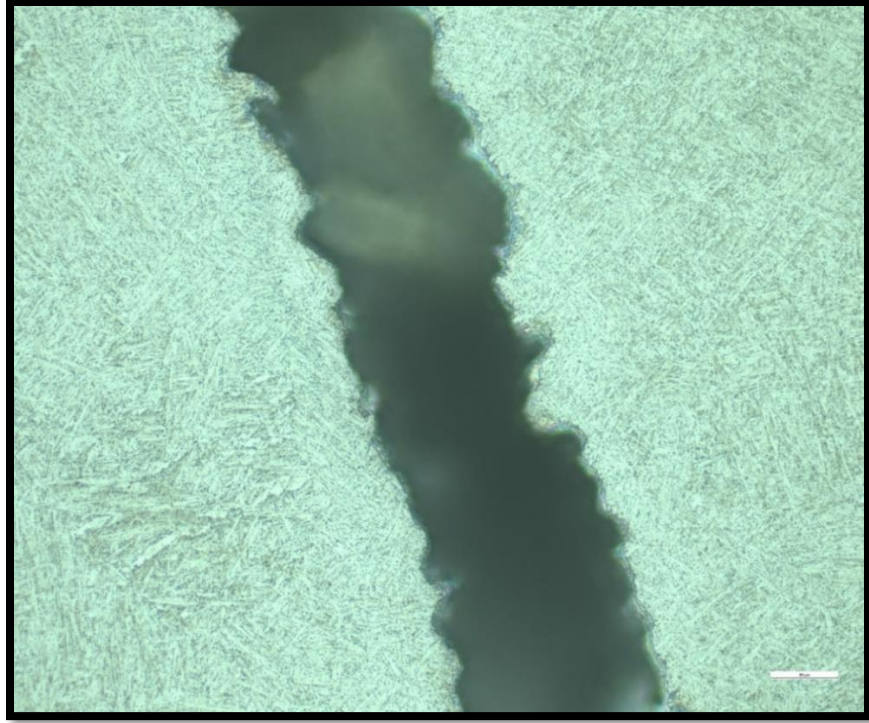


**Figure 79. Unground Room Temperature Three Point Bend Sample**

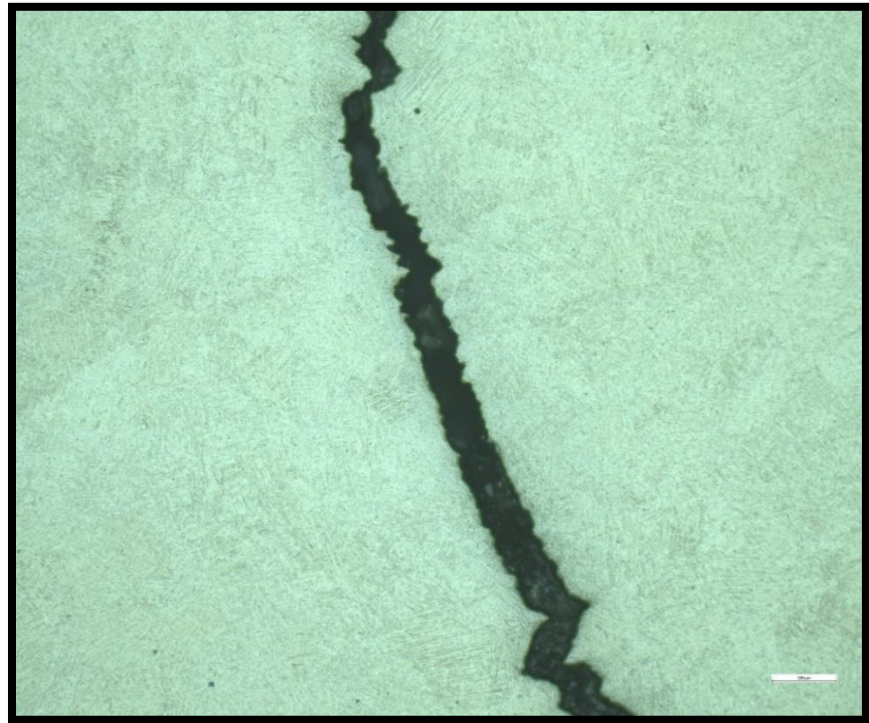


**Figure 80. Fracture Surface for an Unground Room Temperature Three Point Bend Sample**



**Figure 81. Ground Room Temperature Three Point Bend Sample**

When looking at the etched high temperature three point bend samples, the etched surfaces had a slightly different finish. This surface finish, seen below in Figure 82, was observed in all the high temperature three point bend samples regardless of print direction or sample build height.

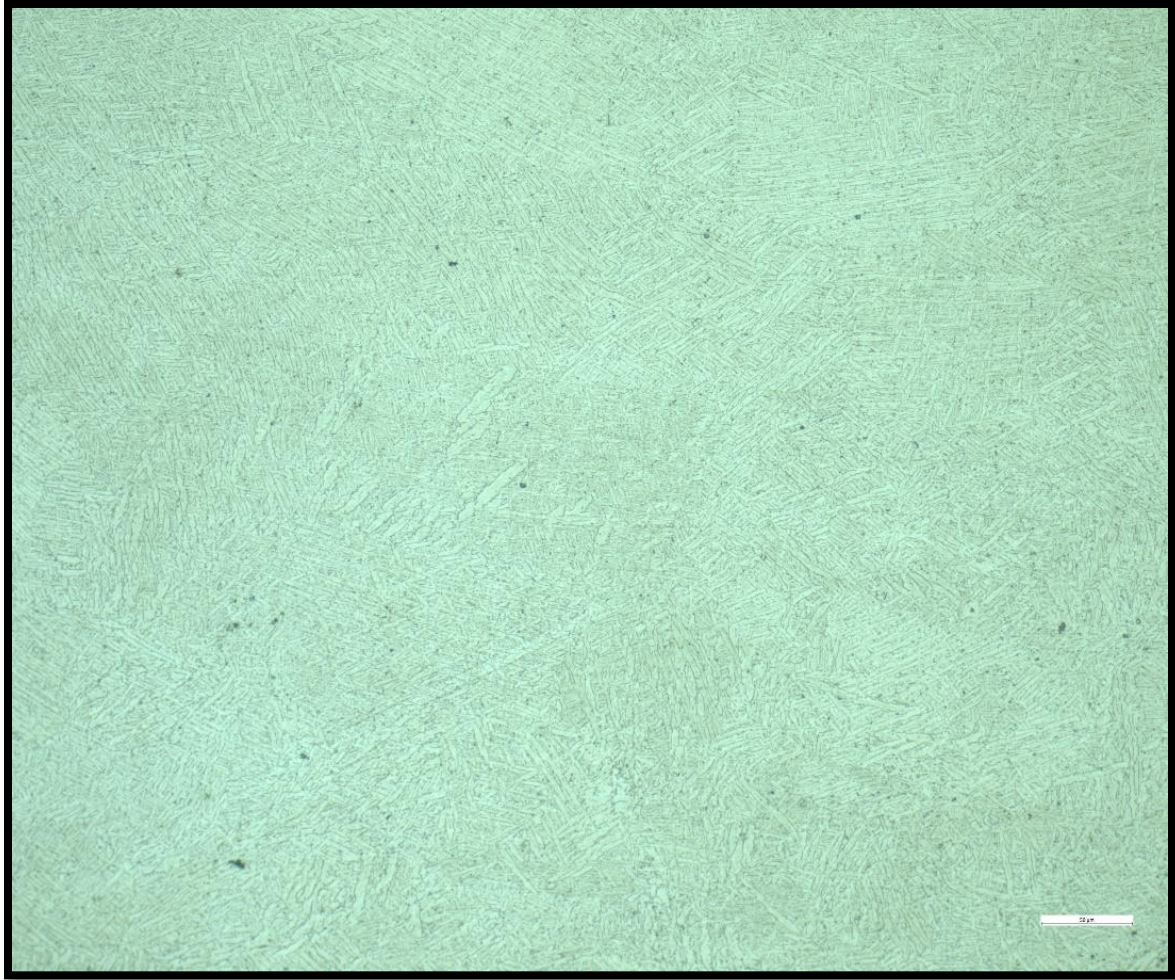


**Figure 82. Ground High Temperature Three Point Bend Sample**

As seen in Figure 82, the sample exhibits a needle like design throughout the entire etched surface. This pattern is “due to the extreme temperature changes as the laser traces across the powder bed (during manufacturing) [33].” The needle design seen is martensitic Ti 6-4. The room temperature three point bend samples have some martensitic Ti 6-4 seen in them but more is seen in the high temperature three point bend samples.

#### **4.18 Summary**

This chapter looked at the data produced from the three point bend tests, compression tests, and tensile tests. Stress-strain curves, important points, and characteristics from the stress-strain plots were analyzed and compared. Statistical analysis was also conducted on the results. Reasoning behind the results was explained to gain an understanding of how print direction, surface finish, size of build height, and temperature affected the mechanical response of the additively manufactured Ti 6-4 samples under compressive, tensile, and bending loads. Lastly, the microstructures of the parts were analyzed using different microscopy techniques.

## **V. Conclusions and Recommendations**

### **5.1 Chapter Overview**

This thesis has looked into the material characterization of additively manufactured Ti 6-4. The goal was to compare how build height, print direction, surface roughness, and temperature affected the material under tensile, compressive, and three point bend loading scenarios. This chapter will discuss conclusion drawn from the different tests, the importance of this research and subsequent research, future research recommendations, and a summary.

### **5.2 Research Conclusions**

The goal of this research effort was to characterize Ti 6-4 using tensile, compression, and three point bend testing. Samples were tested and compared to each other based on test type, surface finish, print direction, testing temperature, and sample build height. From these experiments and comparisons, some conclusions can be drawn.

1. Grinding the three point bend test samples had a large impact on the mechanical response, especially the stress and modulus of elasticity response, when compared to the mechanical response of the unground three point bend samples.
2. Temperature had a big impact on the response of the three point bend samples, especially the stress and modulus of elasticity response, as a significant difference was

found to exist between the room temperature three point bend sample test results and the high temperature three point bend sample test results.

3. Grinding the compression samples did not have a large impact on the mechanical response of the material during compression testing due to crack initiation points closing due to the compressive force and the samples being sufficiently thick where the rough surface finish from the manufacturing process not being able to support load did not affect the overall sample response. The minimal difference seen in the mechanical responses were seen when comparing the ground and unground compression samples.

4. The tensile samples had a very similar mechanical response when compared to wrought Ti 6-4 data showing additively manufactured Ti 6-4 was just as strong in uniaxial tension when compared to traditionally manufactured Ti 6-4.

5. In general, no large differences in the mechanical response of the material was seen between the different print directions for a given test with common sample characteristics. The exception was some differences were seen in the high temperature three point bend tests.

6. In general, no large differences in the mechanical response of the material was seen between the different sample build heights for a given test with common sample characteristics. The exception was some differences were seen in the high temperature three point bend tests.

7. On the micro scale, the samples fractured the same when compared to the same sample test type regardless of the sample build height. The tensile samples fractured differently

based on print direction. All the other samples fractured the same when compared to the same sample test type regardless of print direction.

8. The sample powder used to make all the samples used throughout testing had the correct elemental makeup of Ti 6-4.

9. More research is needed to examine grain growth in additively manufactured Ti 6-4 samples.

### **5.3 Significance of Research**

Ti 6-4 is a very common material used in the defense and aerospace industry, and understanding how the material performs under different loading scenarios is very important. With the ability to additively manufacture Ti 6-4, there opens a new opportunity for novel ways to manufacture the material into forms and shapes not possible with traditional manufacturing methods. The catch is that the printed materials still must handle different loading scenarios similarly to the traditionally manufactured materials. This will warrant continued research under different loading scenarios and conditions to find the most advantageous material properties that best match or exceed the material properties of traditionally manufactured Ti 6-4.

## 5.4 Recommendations for Future Research

There still exists many areas where research is needed to fully characterize the properties of additively manufactured Ti 6-4 under different load scenarios with varying build heights, print directions, surface roughness, and temperatures. The first recommendation is to look more into the high temperature response of additively manufactured Ti 6-4. Expanding on the three point bend test conducted at 800 degrees Celsius by conducting testing at 200, 400, and 600 degrees Celsius is important to see how varying temperatures affect the materials response. Conducting testing at 200, 400, 600, and 800 degrees Celsius in tension and compression is also important to see how the material responds during these testing scenarios. In addition, only tensile samples with the sides ground to delay crack initiation because of the rough surface finish were tested. Future research looking into the mechanical response of fully ground samples to see how the response differs from the samples tested in this experiment is also needed. This will determine if grinding the samples is needed or if the rough surface brought about by the manufacturing process does not need to be removed.

The material will need to be subjected to fatigue testing to generate S-N curves for comparison to traditionally manufactured Ti 6-4. Since fatigue is a common cause of cracks and eventually failure, studying it is important. This will be very important when comparing the ground and unground samples since the unground samples have a rough surface which allows cracks to start and propagate easier than a ground surface. This will make fatigue a great cause for concern.

Axial torsion testing will need to be conducted to analyze the material under complex loading scenarios. The surface finish, print orientation, and build height will need to be analyzed and compared to find favorable print parameters for Ti 6-4 when subjected to complex loading scenarios. From the results of these tests, yield surfaces can be generated. This will allow for additively manufactured Ti 6-4 failure to be better predicted under complex loading scenarios. Finite element analysis simulations should be conducted to build models of the failure behavior for additively manufactured Ti 6-4 and compared to the experimental results to check the validity of the models.

All these recommended tests will need to be compared to each other and previous testing done in this thesis to see what print direction and build height is most advantageous at each temperature for a given test. The different tests will also need to be compared to traditionally manufactured Ti 6-4 under the above recommended temperatures to see how much the results differ and by how much. This will shed insight into what manufacturing process leads to a better material based on strength, ductility, toughness, and manufacturability. Examining grain growth in additively manufactured Ti 6-4 samples will need more work to get clear images of grain boundaries in these samples for imaging and comparison purposes.

## **5.5 Summary**

Additive manufacturing presents an opportunity to manufacture aircraft parts traditional manufacturing has not had the capability to produce. Due to Ti 6-4s prevalence in the aerospace field because of its high strength, high ductility, high

temperature resistance, and light weight, studying and understanding the response of additively manufactured Ti 6-4 is very important to ensure aircraft parts do not fail before their service life is met and aircraft do not fail while in flight. With continued research into this material, additively manufactured Ti 6-4 can eventually become an important part of aircraft structures and design. This will open the door for common aerospace materials, like Ti 6-4, to be manufactured in new and unique ways to meet the demands of the aerospace and defense fields of the future.

## Appendix A

30 Micron, Three Point Bend Tests, All Surfaces Ground, High Temperature Dimensions

sample	width (mm)	thickness (mm)	mass (g)
90_1	4.377	1.760	0.563
90_2	4.393	1.763	0.571
90_3	4.043	1.683	0.506
45_1	3.767	1.723	0.486
45_2	3.780	1.773	0.520
45_3	3.780	1.787	0.486
0_1	3.770	1.760	0.501
0_2	3.747	1.750	0.507
0_3	3.747	1.783	0.510

Span = 14 mm

30 Micron, Three Point Bend Tests, All Surfaces Ground, Room Temperature

Dimensions

sample	width (mm)	thickness (mm)	mass (g)
90_1	4.390	1.760	0.591
90_2	4.427	1.783	0.584
90_3	4.463	1.760	0.595
45_1	3.767	1.667	0.467
45_2	3.780	1.747	0.473
45_3	3.730	1.770	0.497
0_1	3.760	1.803	0.517
0_2	3.720	1.787	0.501
0_3	3.760	1.747	0.469

Span = 14 mm

30 Micron, Three Point Bend Tests, Unground, Room Temperature Dimensions

sample	width (mm)	thickness (mm)	mass (g)
90_1	4.467	2.173	0.642
90_2	4.410	2.153	0.641
90_3	4.433	2.093	0.643
45_1	3.787	2.133	0.582
45_2	3.767	2.170	0.580
45_3	3.747	2.187	0.565
0_1	3.750	2.140	0.549
0_2	3.770	2.167	0.560
0_3	3.717	2.057	0.553

Span = 14 mm

30 Micron, Compression Tests, All Surfaces Ground, Room Temperature Dimensions

sample	height (mm)	width 1 (mm)	width 2 (mm)	mass (g)
90_1	8.80	6.96	6.32	1.67
90_2	8.77	6.27	6.93	1.67
90_3	8.75	6.25	6.94	1.67
0_1	9.45	6.27	6.27	1.62
0_2	8.90	6.28	6.27	1.53
0_3	9.46	6.25	6.28	1.61

30 Micron, Compression Tests, Unground, Room Temperature Dimensions

sample	height (mm)	width 1 (mm)	width 2 (mm)	mass (g)
90_1	8.75	6.62	7.22	1.75
90_2	8.80	7.26	6.65	1.75
90_3	8.78	6.65	7.26	1.76
0_1	9.44	6.64	6.65	1.69
0_2	9.21	6.61	6.65	1.64
0_3	9.38	6.64	6.64	1.68

30 Micron, Tensile Tests, Sides Ground, Room Temperature Dimensions

sample	width gauge section (mm)	thickness gauge section (mm)	area (mm <sup>2</sup> )	mass (g)
90_1	10.937	2.123	23.222	19.004
90_2	10.950	2.123	23.251	19.000
90_3	10.900	2.110	22.999	18.920
45_1	9.383	2.180	20.456	17.428
45_2	9.533	2.170	20.687	17.611
45_3	9.487	2.167	20.554	17.539
0_1	9.767	2.167	21.161	17.007
0_2	9.693	2.177	21.099	16.876
0_3	9.733	2.183	21.251	16.998

Original length (extensometer) = 25.465 mm

60 Micron, Three Point Bend Tests, All Surfaces Ground, High Temperature Dimensions

sample	width (mm)	thickness (mm)	mass (g)
90_1	4.403	1.757	0.614
90_2	4.357	1.773	0.604
90_3	3.520	1.610	0.436
45_1	3.740	1.243	0.283
45_2	3.660	1.737	0.375
45_3	3.813	1.687	0.412
0_1	3.733	1.750	0.408
0_2	3.720	1.650	0.416
0_3	3.793	1.787	0.491

Span = 14 mm

60 Micron, Three Point Bend Tests, All Surfaces Ground, Room Temperature

Dimensions

sample	width (mm)	thickness (mm)	mass (g)
90_1	4.347	1.810	0.611
90_2	4.383	1.800	0.602
90_3	4.277	1.707	0.550
45_1	3.637	1.743	0.388
45_2	3.463	1.713	0.394
45_3	3.767	1.553	0.391
0_1	3.810	1.820	0.529
0_2	3.823	1.850	0.541
0_3	3.827	1.843	0.538

Span = 14 mm

60 Micron, Three Point Bend Tests, Unground, Room Temperature Dimensions

sample	width (mm)	thickness (mm)	mass (g)
90_1	4.213	2.013	0.604
90_2	4.317	2.013	0.628
90_3	4.067	2.097	0.600
45_1	3.063	2.263	0.393
45_2	3.270	2.210	0.442
45_3	3.600	2.283	0.442
0_1	3.570	2.067	0.467
0_2	3.773	2.093	0.537
0_3	3.730	2.097	0.524

Span = 14 mm

60 Micron, Compression Tests, All Surfaces Ground, Room Temperature Dimensions

sample	height (mm)	width 1 (mm)	width 2 (mm)	mass (g)
90_1	8.7900	6.6433	6.3133	1.6161
90_2	8.7600	6.2833	6.6033	1.5800
90_3	8.7967	6.6033	6.3067	1.6108
0_1	9.1100	6.3067	6.3067	1.5882
0_2	9.1133	6.3167	6.2800	1.5852
0_3	9.1200	6.3000	6.2933	1.5758

60 Micron, Compression Tests, Uground, Room Temperature Dimensions

sample	height (mm)	width 1 (mm)	width 2 (mm)	mass (g)
90_1	8.753	6.677	6.913	1.672
90_2	8.803	6.910	6.697	1.670
90_3	8.710	6.937	6.690	1.656
0_1	9.100	6.677	6.680	1.639
0_2	9.107	6.710	6.703	1.656
0_3	9.103	6.663	6.660	1.645

60 Micron, Tensile Tests, Sides Ground, Room Temperature Dimensions

sample	width gauge section (mm)	thickness gauge section (mm)	area (mm <sup>2</sup> )	mass (g)
90_1	8.440	2.147	18.118	14.687
90_2	8.383	2.180	18.276	14.666
90_3	9.370	2.170	20.333	16.314
45_1	9.593	2.153	20.658	17.716
45_2	9.523	2.163	20.602	17.600
45_3	9.703	2.173	21.089	17.801
0_1	9.740	2.160	21.038	17.026
0_2	9.740	2.203	21.460	17.051
0_3	9.777	2.147	20.987	17.083

Original length (extensometer) = 25.465 mm

## Appendix B

### Matlab Code Used in Analysis

```
% User Inputs
% Code is non-dimensional, units will be what you input
% Excel file should be in load and displacemnt, stresses will be calculated
% Originally written for Bearing Stress so variable names may not match, but
% if as long as type of stress is specified it will be correct, it was
% modified after just didn't want to change all variable names
% Outputs will be 1 array and 1 stucture, Structure is statistical data
% Array is data for all samples inputed
% User inputs are specified by three % signs (%%)
input_types = ["Load","Strain"]; %% Input types ["Load" or "Stress",
"Displacement" or "Strain"]
prog_settings = ["Stress","Write Excel","No Downsample","No Smooth"]; %%
Various code settings, read below
% (1) "Bearing Stress" or "Stress" (Normal Stress) or "Flex Stress"
% (2) If want outputs in .xlsx "Write Excel", if not "No Excel"
% (3) "Downsample" to downsample data, "No Downsample" to turn off:
% Change "downsample_factor" below for downsampling rate
% (4) "Smooth" use matlab smooth command to average points together,
lookup
% smooth for how this works, this code only has yy = smooth(y), "No
Smooth" to turn off
test_name = ["Tension_0_Deg_processed.mat", "Tension_0_Deg_averages.mat"]; %%
Output Matlab file names
File = "Tension_0_Deg.xlsx"; %% Output Excel file name (include .xlsx at end
of file name)
omit_sample_yield = ["Include","Include","Include"]; %% If sample did not
yield, this will omit it from yield calc but inculde E, enter in "Omit" or
"Include"
lin_low = [5000,5000,5000]; %% low point for E calc, load is calced from this
lin_high = [15000,15000,15000]; %% High point for E calc
%% inputs for lin_low and lin_high should match input type in line 10,
%% "Stress" in line 10 = stess values in line 21&22
omit_sample_ult = ["Include","Include","Include"]; %% If sample was not taken
to ult load, this will omit, enter in "Omit" or "Include"
omit_sample_frac = ["Include","Include","Include"]; %% If sample was not
taken to frac load, this will omit, enter in "Omit" or "Include"
target_disp = 20; %% This is for average curves, point where your test ends,
code won't include points after this number
target_strain = 2; %% This is for average curves, point where your test
ends, code won't include points after this number
downsample_factor = 10; %% Downsample every x points
smooth_factor = 10; %% Smooth x points together
label_x_stress = "Tensile Strain (mm/mm)"; %% Label x axis for "Yield
Calculation Data" graphs that auto generate
label_y_stress = "Tensile Stress (MPa)"; %% Label y axis for "Yield
Calculation Data" graphs that auto generate
```

```

label_x_load = "Displacement (mm)"; %% Label x axis for "Yield Calculation
Data" graphs that auto generate
label_y_load = "Load (N)"; %% Label y axis for "Yield Calculation Data"
graphs that auto generate
distribution_type = "tLocationScale"; %% Distribution type for confidence
interval see fitdist command in matlab for options
CI_alpha = 0.05; %% alpha for CI calc
deg_of_freedom = length(omit_sample_yield)-1;

% Hybrid 18-Ply Dbl Shear 2 struct (Read in Excel file edit unless noted)
sample_names = ["Tension_0_1";"Tension_0_2";"Tension_0_3"]; %% Output sample
names in Excel file
number_fields = length(sample_names); % Do Not edit
sample_description = ["Full";"Full";"Full"]; %% Sample descriptions
Length = [25.465,25.465,25.465]; %% This is the original length for "normal"
stress/strain or span for flexural stress/strain
Area = [21.038,21.460,20.987]; %% This is thickness for flexural
stress/strain or area for "normal" stress/strain
if prog_settings(1) == "Flex Stress"
    width = [1,1,1]; %% Only for flexural stress/strain
end
excel_file = ["Gunderson_0_1.xlsx";"Gunderson_0_2.xlsx";"Gunderson_0_3.xlsx"];
%% Excel file input names
sheet_name = ["Sheet1";"Sheet1";"Sheet1"]; %% Sheet names for input Excel
file
load_cells = ["E3:E1538";"E3:E1441";"E3:E1692"]; %% Cells w/ data for input
Excel file
disp_cells = ["C3:C1538";"C3:C1441";"C3:C1692"]; %% Cells w/ data for input
Excel file
averages.name = 'Averages'; % This structure will store Standard Deviations
(std) and Means, means are just the field title and stds have std after them
averages.description = 'statistical values of test';

%% General note: All vectors above must match in length
%%

if prog_settings(1) == "Flex Stress"
    D = 'span';
    t = 'thickness';
end
if prog_settings(1) == "Bearing Stress"
    D = 'diameter';
    t = 'thickness';
end
if prog_settings(1) == "Stress"
    D = 'length';
    t = 'area';
end
load = 'load';
stress = 'stress';
disp = 'disp';
strain = 'strain';

```

```

for n = 1:number_fields
    test(n).name = sample_names(n);
    test(n).description = sample_description(n);
    test(n).(D) = Length(n); %%% This is the original length for "normal"
stress/strain or span for flexural stress/strain, also update "length" or
"span" variable throughout whole code
    test(n).(t) = Area(n); %%% This is thickness for flexural stress/strain or
area for "normal" stress/strain, also update "area" or "thickness" variable
throughout whole code
    if prog_settings(1) == "Flex Stress"
        test(n).w = width(n);
    end
    test(n).(load) = xlsread(excel_file(n),sheet_name(n),load_cells(n));
    test(n).(disp) = xlsread(excel_file(n),sheet_name(n),disp_cells(n));
end
lin_high_load = nan(length(lin_high),1);
lin_low_load = nan(length(lin_low),1);

if prog_settings(3) == "Downsample"
    for n = 1:length(test)
        figure()
        plot(test(n).disp,test(n).(load))
        xlm = [0 1.25*max([test(n).(disp)])];
        ylm = [0 1.1*max([test(n).(load)])];
        ylim(ylm);
        xlim(xlm);
        xlabel('Displacement');
        ylabel('Load');
        title('Before Downsample',test(n).name)
    end
    for n = 1:length(test)
        if prog_settings(3) == "Downsample"
            test(n).load = downsample([test(n).(load)],downsample_factor);
            test(n).disp = downsample([test(n).(disp)],downsample_factor);
        end
    end
    for n = 1:length(test)
        figure()
        plot(test(n).disp,test(n).(load))
        xlm = [0 1.25*max([test(n).(disp)])];
        ylm = [0 1.1*max([test(n).(load)])];
        ylim(ylm);
        xlim(xlm);
        xlabel('Displacement');
        ylabel('Load');
        title('After Downsample',test(n).name)
    end
end
if prog_settings(4) == "Smooth"
    for n = 1:length(test)
        figure()
        plot(test(n).disp,test(n).(load))
        xlm = [0 1.25*max([test(n).(disp)])];

```

```

        ylim = [0 1.1*max([test(n).(loadd)]]);
        ylim(ylim);
        xlim(xlm);
        xlabel('Displacement');
        ylabel('Load');
        title('Before Smooth',test(n).name)
    end
    for n = 1:length(test)
        if prog_settings(4) == "Smooth"
            test(n).load = smooth([test(n).(loadd)],smooth_factor);
            test(n).disp = smooth([test(n).(disp)],smooth_factor);
        end
    end
    for n = 1:length(test)
        figure()
        plot(test(n).disp,test(n).(loadd))
        xlm = [0 1.25*max([test(n).(disp)]]);
        ylim = [0 1.1*max([test(n).(loadd)]]);
        ylim(ylim);
        xlim(xlm);
        xlabel('Displacement');
        ylabel('Load');
        title('After Smooth',test(n).name)
    end
end
% (1) Set Up Structure: Hybrid Double Shear
% Add Feilds to Structure 1 field added for averages
clc

% This starts with empty array to ensure numbers don't get messed up
for n = 1:(number_fields)
    test(n).E = [];
    test(n).stress = [];
    test(n).strain = [];
    test(n).yield_stress = [];
    test(n).yield_strain = [];
    test(n).ult_stress = [];
    test(n).yield_load = [];
    test(n).yield_disp = [];
    test(n).ult_load = [];
    test(n).corrected_strain = [];
    test(n).strain_energy = [];
end
averages.E_std = [];
averages.yield_stress_std = [];
averages.yield_strain_std = [];
averages.yield_load_std = [];
averages.yield_disp_std = [];
averages.ult_stress_std = [];
averages.ult_load_std = [];
% (2) Stress Strain Calcs
% Set up structure first (1)
for n = 1:length(test)

```

```

test(n).stress = [];
test(n).strain = [];
end
if input_types(1) == "Load" && input_types(2) == "Displacement"
    if prog_settings(1) == "Bearing Stress"
        for n = 1:(length(test))
            test(n).(stress) = test(n).(loadd)/(test(n).(t)*test(n).(D));
            test(n).(strain) = test(n).(disp)/(test(n).(D));
            lin_low_stress(n) = lin_low(n)*(1/(test(1).(t)*test(1).(D)));
            lin_high_stress(n) = lin_high(n)*(1/(test(1).(t)*test(1).(D)));
            lin_high_load = lin_high;
            lin_low_load = lin_low;
        end
    end
    if prog_settings(1) == "Stress"
        for n = 1:(length(test))
            test(n).(stress) = test(n).(loadd)/(test(n).(t));
            test(n).(strain) = test(n).(disp)/(test(n).(D));
            lin_low_stress(n) = lin_low(n)*(1/test(n).(t));
            lin_high_stress(n) = lin_high(n)*(1/test(n).(t));
            lin_high_load = lin_high;
            lin_low_load = lin_low;
        end
    end
    if prog_settings(1) == "Flex Stress"
        for n = 1:length(test)
            test(n).(stress) =
((3*test(n).(loadd)*test(n).(D))/(2*test(n).w*(test(n).(t)^2)));
            test(n).(strain) = (6*test(n).(disp)*test(n).(t))/(test(n).(D)^2);
            lin_low_stress(n) =
lin_low(n)*((3*test(n).(D))/(2*test(n).w*(test(n).(t)^2)));
            lin_high_stress(n) =
lin_high(n)*((3*test(n).(D))/(2*test(n).w*(test(n).(t)^2)));
            lin_high_load = lin_high;
            lin_low_load = lin_low;
        end
    end
end
if input_types(1) == "Load" && input_types(2) == "Strain"
    if prog_settings(1) == "Bearing Stress"
        for n = 1:(length(test))
            test(n).(stress) = test(n).(loadd)/(test(n).(t)*test(n).(D));
            test(n).(strain) = test(n).(disp);
            lin_low_stress(n) = lin_low(n)*(1/(test(1).(t)*test(1).(D)));
            lin_high_stress(n) = lin_high(n)*(1/(test(1).(t)*test(1).(D)));
            lin_high_load = lin_high;
            lin_low_load = lin_low;
            test(n).(disp) = test(n).(strain)*test(n).(D);
        end
    end
    if prog_settings(1) == "Stress"
        for n = 1:(length(test))
            test(n).(stress) = test(n).(loadd)/(test(n).(t));

```

```

        test(n).(strain) = test(n).(disp);
        lin_low_stress(n) = lin_low(n)*(1/test(n).(t));
        lin_high_stress(n) = lin_high(n)*(1/test(n).(t));
        lin_high_load = lin_high;
        lin_low_load = lin_low;
        test(n).(disp) = test(n).(strain)*test(n).(D);
    end
end
if prog_settings(1) == "Flex Stress"
    for n = 1:length(test)
        test(n).(stress) =
            ((3*test(n).(loadd)*test(n).(D))/(2*test(n).w*(test(n).(t)^2)));
        test(n).(strain) = test(n).(disp);
        lin_low_stress(n) =
            lin_low(n)*((3*test(n).(D))/(2*test(n).w*(test(n).(t)^2)));
        lin_high_stress(n) =
            lin_high(n)*((3*test(n).(D))/(2*test(n).w*(test(n).(t)^2)));
        lin_high_load = lin_high;
        lin_low_load = lin_low;
        test(n).(disp) =
            test(n).(strain)*(1/((6*test(n).(t))/(test(n).(D)^2)));
    end
end
end
if input_types(1) == "Stress" && input_types(2) == "Strain"
    if prog_settings(1) == "Bearing Stress"
        for n = 1:(length(test))
            test(n).(stress) = test(n).(loadd);
            test(n).(strain) = test(n).(disp);
            lin_low_stress(n) = lin_low(n);
            lin_high_stress(n) = lin_high(n);
            lin_high_load(n) = lin_high*(test(1).(t)*test(1).(D));
            lin_low_load(n) = lin_low*(test(1).(t)*test(1).(D));
            test(n).(loadd) = test(n).(stress)*test(n).(t)*test(n).(D);
            test(n).(disp) = test(n).(strain)*test(n).(D);
        end
    end
    if prog_settings(1) == "Stress"
        for n = 1:(length(test))
            test(n).(stress) = test(n).(loadd);
            test(n).(strain) = test(n).(disp);
            lin_low_stress(n) = lin_low(n);
            lin_high_stress(n) = lin_high(n);
            lin_high_load = lin_high*(test(n).(t));
            lin_low_load = lin_low*(test(n).(t));
            test(n).(loadd) = test(n).(stress)*(test(n).(t));
            test(n).(disp) = test(n).(strain)*(test(n).(D));
        end
    end
    if prog_settings(1) == "Flex Stress"
        for n = 1:length(test)
            test(n).(stress) = test(n).(loadd);
            test(n).(strain) = test(n).(disp);
        end
    end
end

```

```

        lin_low_stress(n) = lin_low(n);
        lin_high_stress(n) = lin_high(n);
        lin_high_load =
lin_high*(1/(3*test(n).(D)/(2*test(n).w*(test(n).(t)^2))));
        lin_low_load =
lin_low*(1/(3*test(n).(D)/(2*test(n).w*(test(n).(t)^2))));
        test(n).(loadd) =
test(n).(stress)*(1/(3*test(n).(D)/(2*test(n).w*(test(n).(t)^2))));
        test(n).(disp) =
test(n).(strain)*(1/((6*test(n).(t))/(test(n).(D)^2)));
    end
end
end
if input_types(1) == "Stress" && input_types(2) == "Displacement"
    if prog_settings(1) == "Bearing Stress"
        for n = 1:(length(test))
            test(n).(stress) = test(n).(loadd);
            test(n).(strain) = test(n).(disp)*(1/test(n).(D));
            lin_low_stress(n) = lin_low(n);
            lin_high_stress(n) = lin_high(n);
            lin_high_load(n) = lin_high*(test(1).(t)*test(1).(D));
            lin_low_load(n) = lin_low*(test(1).(t)*test(1).(D));
            test(n).(loadd) = test(n).(stress)*(test(n).(t)*test(n).(D));
        end
    end
end
if prog_settings(1) == "Stress"
    for n = 1:(length(test))
        test(n).(stress) = test(n).(loadd);
        test(n).(strain) = test(n).(disp)/(test(n).(D));
        lin_low_stress(n) = lin_low(n);
        lin_high_stress(n) = lin_high(n);
        lin_high_load = lin_high*(test(n).(t));
        lin_low_load = lin_low*(test(n).(t));
        test(n).(loadd) = test(n).(stress)*(test(n).(t));
    end
end
if prog_settings(1) == "Flex Stress"
    for n = 1:length(test)
        test(n).(stress) = test(n).(loadd);
        test(n).(strain) =
(test(n).(disp)*(6*test(n).(t))/(test(n).(D)^2));
        lin_low_stress(n) = lin_low(n);
        lin_high_stress(n) = lin_high(n);
        lin_high_load =
lin_high*(1/(3*test(n).(D)/(2*test(n).w*(test(n).(t)^2))));
        lin_low_load =
lin_low*(1/(3*test(n).(D)/(2*test(n).w*(test(n).(t)^2))));
        test(n).(loadd) =
test(n).(stress)*(1/(3*test(n).(D)/(2*test(n).w*(test(n).(t)^2))));
    end
end
end
% (3) Stress Strain Yield Calc

```

```

for n = 1:length(test)
    % clears fields canceled in this section to ensure no overlap
    test(n).yield_stress = [];
    test(n).yield_strain = [];
    test(n).corrected_strain = [];
    test(n).E = [];
    test(n).ult_stress = [];
    test(n).ult_load = [];
end
averages.yield_stress_std = [];
averages.yield_strain_std = [];
averages.E_std = [];
averages.ult_stress_std = [];
averages.ult_load_std = [];

for n = 1:(length(test))
    if omit_sample_yield(n) == "Include"

[ test(n).yield_strain, test(n).yield_stress, test(n).corrected_strain, test(n).E ]
=
Yield_Calc(test(n).stress, test(n).strain, lin_low_stress(n), lin_high_stress(n),
1, test(n).name, label_x_stress, label_y_stress);
        end
        if omit_sample_yield(n) == "Omit"
            % omits samples not taken to yield

[ test(n).yield_strain, test(n).yield_stress, test(n).corrected_strain, test(n).E ]
=
Yield_Calc(test(n).stress, test(n).strain, lin_low_stress(n), lin_high_stress(n),
1, test(n).name, label_x_stress, label_y_stress);
            test(n).yield_strain = nan;
            test(n).yield_stress = nan;
        end
    end

averages.E = mean([test.E], "omitnan");
averages.E_std = std([test.E], "omitnan");
% hybrid_dbl(length(hybrid_dbl)).E_N = length([hybrid_dbl.E]) -1;
yield_stress = [test.yield_stress];
averages.yield_stress = mean(yield_stress, "omitnan");
averages.yield_stress_std = std(yield_stress, "omitnan");
yield_strain = [test.yield_strain];
averages.yield_strain = mean(yield_strain, "omitnan");
averages.yield_strain_std = std(yield_strain, "omitnan");

% (4) Load Disp Yield Calc
for n = length(test)
    test(n).yield_disp = [];
    test(n).yield_load = [];
    test(n).corrected_disp = [];
    %     test(n).yield_disp_std = [];
    %     test(n).yield_load_std = [];
    %     hybrid_dbl(n).strain_energy = [];
end

```

```

end
for n = 1:(length(test))
    if prog_settings(1) == "Felx Stress"
        if omit_sample_yield(n) == "Include"
            [test(n).yield_disp, test(n).yield_load, test(n).corrected_disp] =
            Yield_Calc(test(n).load, test(n).disp, lin_low_load(n), lin_high_load(n), 1/(6*tes
            t(n).disp*test(n).(t))/(test(n).(D)^2), test(n).name, label_x_load, label_y_load)
            ;
            end
            if omit_sample_yield(n) == "Omit"
                % omits smaple not taken to yield
                [test(n).yield_disp, test(n).yield_load, test(n).corrected_disp] =
                Yield_Calc(test(n).load, test(n).disp, lin_low_load(n), lin_high_load(n), 1/(6*tes
                t(n).disp*test(n).(t))/(test(n).(D)^2), test(n).name, label_x_load, label_y_load)
                ;
                test(n).yield_disp = nan;
                test(n).yield_load = nan;
            end
        else
            if omit_sample_yield(n) == "Include"
                [test(n).yield_disp, test(n).yield_load, test(n).corrected_disp] =
                Yield_Calc(test(n).load, test(n).disp, lin_low_load(n), lin_high_load(n), test(n).
                (D), test(n).name, label_x_load, label_y_load);
            end
            if omit_sample_yield(n) == "Omit"
                % omits smaple not taken to yield
                [test(n).yield_disp, test(n).yield_load, test(n).corrected_disp] =
                Yield_Calc(test(n).load, test(n).disp, lin_low_load(n), lin_high_load(n), test(n).
                (D), test(n).name, label_x_load, label_y_load);
                test(n).yield_disp = nan;
                test(n).yield_load = nan;
            end
        end
        if omit_sample_ult(n) == "Include"
            % omits progressive failure samples
            test(n).ult_stress = max(test(n).stress);
            test(n).ult_load = max(test(n).load);
            % x = linspace(0.1, 0.12, length(test(n).stress));
            % test(n).strain_energy = trapz(x, test(n).stress); % Am I doing this
            right?
        end
        if omit_sample_frac(n) == "Include"
            test(n).frac_stress = test(n).stress(end);
            test(n).frac_strain = test(n).corrected_strain(end);
            test(n).frac_load = test(n).load(end);
            test(n).frac_disp = test(n).corrected_disp(end);
        end
    end
end
for n = 1:length(omit_sample_frac)
    if omit_sample_frac(n) == "Include"
        averages.frac_stress = mean([test.frac_stress]);
        averages.frac_stress_std = std([test.frac_stress]);
        averages.frac_strain = mean([test.frac_strain]);
    end
end

```

```

        averages.frac_strain_std = std([test.frac_strain]);
        averages.frac_load = mean([test.frac_load]);
        averages.frac_load_std = std([test.frac_load]);
        averages.frac_disp = mean([test.frac_disp]);
        averages.frac_disp_std = std([test.frac_disp]);
        break
    end
end
ult_load = [test.ult_load];
averages.ult_load = mean(ult_load);
averages.ult_load_std = std(ult_load);
ult_stress = [test.ult_stress];
averages.ult_stress = mean(ult_stress);
averages.ult_stress_std = std(ult_stress);
sa_all = nan(6000,number_fields);
ea_all = nan(6000,number_fields);
% average stress strain Curves
for n = 1:(length(test))
    s = [test(n).stress];
    e = [test(n).corrected_strain];
    for idx3 = 1:length(e)
        if s(idx3) == test(n).ult_stress
            test(n).ult_strain = e(idx3);
        end
        if e(idx3) >= target_strain
            e((idx3+1):end) = NaN;
            s((idx3+1):end) = NaN;
        end
    end
    z = max(e);
    for idx = 1:length(e)
        if e(idx) == z
            sa = s(1:idx);
            ea = e(1:idx);
        end
    end
    for idx2 = 1:length(sa)
        sa_all(idx2,n) = sa(idx2);
        ea_all(idx2,n) = ea(idx2);
    end
end
la_all = nan(6000,number_fields);
da_all = nan(6000,number_fields);
for n = 1:(length(test))
    l = [test(n).load];
    d = [test(n).corrected_disp];
    for idx3 = 1:length(d)
        if d(idx3) >= target_disp
            d((idx3+1):end) = NaN;
            l((idx3+1):end) = NaN;
        end
    end
    v = max(d);
end

```

```

    for idx = 1:length(d)
        if d(idx) == v
            la = l(1:idx);
            da = d(1:idx);
        end
    end
    for idx2 = 1:length(la)
        la_all(idx2,n) = la(idx2);
        da_all(idx2,n) = da(idx2);
    end
end
averages.ult_strain = mean([test.ult_strain]);
averages.ult_strain_std = std([test.ult_strain]);
averages.stress = mean(sa_all,2,"omitnan");
averages.stress_std = std(sa_all,0,2,"omitnan"); % normalized by n-1
averages.corrected_strain = mean(ea_all,2,"omitnan");
averages.load = mean(la_all,2,"omitnan");
averages.load_std = std(la_all,0,2,"omitnan"); % normalized by n-1
averages.corrected_disp = mean(da_all,2,"omitnan");
yield_load = [test.yield_load];
averages.yield_load = mean(yield_load, "omitnan");
averages.yield_load_std = std(yield_load,"omitnan");
yield_disp = [test.yield_disp];
averages.yield_disp = mean(yield_disp,"omitnan");
averages.yield_disp_std = std(yield_disp,"omitnan");
%test(length(test)).strain_energy = mean([test.strain_energy]);
if prog_settings(1) == "Bearing Stress"
    averages.area = mean([test.area]);
    averages.area_std = std([test.area]);
    averages.length = mean([test.length]);
    averages.length_std = std([test.length]);
end
if prog_settings(1) == "Stress"
    averages.area = mean([test.area]);
    averages.area_std = std([test.area]);
    averages.length = mean([test.length]);
    averages.length_std = std([test.length]);
end
if prog_settings(1) == "Flex Stress"
    averages.w = mean([test.w]);
    averages.w_std = std([test.w]);
    averages.length = mean([test.length]);
    averages.length_std = std([test.length]);
    averages.area = mean([test.area]);
    averages.area_std = std([test.area]);
end

pd = fitdist([test.E]',distribution_type);
averages.E_CI = paramci(pd,'alpha',CI_alpha);

for n = 1:length(omit_sample_yield)
    if omit_sample_yield(n) == "Include"
        pd = fitdist([test.yield_stress]',distribution_type);
    end
end

```

```

    averages.yield_stress_CI = paramci(pd, 'alpha', CI_alpha);
    pd = fitdist([test.yield_strain]', distribution_type);
    averages.yield_strain_CI = paramci(pd, 'alpha', CI_alpha);
    pd = fitdist([test.yield_load]', distribution_type);
    averages.yield_load_CI = paramci(pd, 'alpha', CI_alpha);
    pd = fitdist([test.yield_disp]', distribution_type);
    averages.yield_disp_CI = paramci(pd, 'alpha', CI_alpha);
end
end

for n = 1:length(omit_sample_ult)
    if omit_sample_ult(n) == "Omit"
        test(n).ult_stress = nan;
        test(n).ult_strain = nan;
        test(n).ult_load = nan;
    end
end

for n = 1:length(omit_sample_frac)
    if omit_sample_frac(n) == "Omit"
        test(n).frac_stress = nan;
        test(n).frac_strain = nan;
        test(n).frac_load = nan;
        test(n).frac_disp = nan;
    end
end

for n = 1:length(omit_sample_ult)
    if omit_sample_ult(n) == "Include"
        pd = fitdist([test.ult_stress]', distribution_type);
        averages.ult_stress_CI = paramci(pd, 'alpha', CI_alpha);
        pd = fitdist([test.ult_strain]', distribution_type);
        averages.ult_strain_CI = paramci(pd, 'alpha', CI_alpha);
        pd = fitdist([test.ult_load]', distribution_type);
        averages.ult_load_CI = paramci(pd, 'alpha', CI_alpha);
    end
end

for n = 1:length(omit_sample_frac)
    if omit_sample_frac(n) == "Include"
        pd = fitdist([test.frac_stress]', distribution_type);
        averages.frac_stress_CI = paramci(pd, 'alpha', CI_alpha);
        pd = fitdist([test.frac_strain]', distribution_type);
        averages.frac_strain_CI = paramci(pd, 'alpha', CI_alpha);
        pd = fitdist([test.frac_load]', distribution_type);
        averages.frac_load_CI = paramci(pd, 'alpha', CI_alpha);
        pd = fitdist([test.frac_disp]', distribution_type);
        averages.frac_disp_CI = paramci(pd, 'alpha', CI_alpha);
    end
end

if prog_settings(1) == "Bearing Stress"
    pd = makedist('normal', 'mu', averages.area, 'sigma', averages.area_std);
end

```

```

averages.area_CI = paramci(pd, 'alpha', CI_alpha);
pd = makedist('normal', 'mu', averages.length, 'sigma', averages.length_std);
averages.length_CI = paramci(pd, 'alpha', CI_alpha);
end
if prog_settings(1) == "Stress"
    pd = makedist('normal', 'mu', averages.area, 'sigma', averages.area_std);
    averages.area_CI = paramci(pd, 'alpha', CI_alpha);
    pd = makedist('normal', 'mu', averages.length, 'sigma', averages.length_std);
    averages.length_CI = paramci(pd, 'alpha', CI_alpha);
end
if prog_settings(1) == "Flex Stress"
    pd = makedist('normal', 'mu', averages.w, 'sigma', averages.w_std);
    averages.w_CI = paramci(pd, 'alpha', CI_alpha);
    pd = makedist('normal', 'mu', averages.area, 'sigma', averages.area_std);
    averages.area_CI = paramci(pd, 'alpha', CI_alpha);
    pd = makedist('normal', 'mu', averages.length, 'sigma', averages.length_std);
    averages.length_CI = paramci(pd, 'alpha', CI_alpha);
end
save(test_name(1), 'test')
save(test_name(2), 'averages')

figure()
plot(averages.corrected_strain, averages.stress, "LineWidth", 2.5, "Color", 'b');
xlabel('Tensile Strain (mm/mm)'); %% Change label for averages graph
ylabel('Tensile Stress (MPa)'); %% Change label for averages graph
title('Tensile Stress vs Tensile Strain'); %% Change title for averages graph

figure()
plot(test(1).corrected_strain, test(1).stress, "LineWidth", 2.5, "Color", 'b');
hold on
plot(test(2).corrected_strain, test(2).stress, "LineWidth", 2.5, "Color", 'r');
plot(test(3).corrected_strain, test(3).stress, "LineWidth", 2.5, "Color", 'g');
xlabel('Tensile Strain (mm/mm)'); %% Change label for graph
ylabel('Tensile Stress (MPa)'); %% Change label for graph
title('Tensile Stress vs Tensile Strain'); %% Change title for graph
legend('Test 1', 'Test 2', 'Test 3', 'Location', 'southeast'); %% Change legend
for graph
hold off

% (5) Export to Excel
if prog_settings(2) == "Write Excel"
    for n = 1:length(test)
        writematrix([test(n).(t)], File, 'Sheet', test(n).name, 'Range', 'B2')
        writematrix([test(n).(D)], File, 'Sheet', test(n).name, 'Range', 'B3')
        writematrix([test(n).E], File, 'Sheet', test(n).name, 'Range', 'B4')

        for idx=1:length(omit_sample_yield)
            if omit_sample_yield(idx) == "Include"

writematrix([test(n).yield_stress], File, 'Sheet', test(n).name, 'Range', 'B5')

writematrix([test(n).yield_strain], File, 'Sheet', test(n).name, 'Range', 'B6')

```

```

writematrix([test(n).yield_load],File,'Sheet',test(n).name,'Range','B7')
writematrix([test(n).yield_disp],File,'Sheet',test(n).name,'Range','B8')
    end
end

    for idx=1:length(omit_sample_ult)
        if omit_sample_ult(idx) == "Include"

writematrix([test(n).ult_stress],File,'Sheet',test(n).name,'Range','B9')
writematrix([test(n).ult_load],File,'Sheet',test(n).name,'Range','B10')
writematrix([test(n).ult_strain],File,'Sheet',test(n).name,'Range','B11')
            end
        end

        for idx=1:length(omit_sample_frac)
            if omit_sample_frac(idx) == "Include"

writematrix([test(n).frac_stress],File,'Sheet',test(n).name,'Range','B12')
writematrix([test(n).frac_strain],File,'Sheet',test(n).name,'Range','B13')
writematrix([test(n).frac_load],File,'Sheet',test(n).name,'Range','B14')
writematrix([test(n).frac_disp],File,'Sheet',test(n).name,'Range','B15')
                end
            end

            % Titles for Calced Data
            writematrix("Area (mm^2)",File,'Sheet',test(n).name,'Range','A2') %%
Change to area for "normal" stress/strain, thickness for flexural
stress/strain
            writematrix("Length (mm)",File,'Sheet',test(n).name,'Range','A3') %%
Change to length for "normal" stress/strain, span for flexural stress/strain
            writematrix("Young's Modulus
(MPa)",File,'Sheet',test(n).name,'Range','A4')
            writematrix("Yield Stress (MPa)",File,'Sheet',test(n).name,'Range','A5')
            writematrix("Yield Strain (MPa)",File,'Sheet',test(n).name,'Range','A6')
            writematrix("Yield Load (MPa)",File,'Sheet',test(n).name,'Range','A7')
            writematrix("Yield Disp (mm)",File,'Sheet',test(n).name,'Range','A8')
            writematrix("Ult Stress (MPa)",File,'Sheet',test(n).name,'Range','A9')
            writematrix("Ult Load (MPa)",File,'Sheet',test(n).name,'Range','A10')
            writematrix("Ult Strain (mm/mm)",File,'Sheet',test(n).name,'Range','A11')
            writematrix("Fracture Stress
(MPa)",File,'Sheet',test(n).name,'Range','A12')
            writematrix("Fracture Strain
(mm/mm)",File,'Sheet',test(n).name,'Range','A13')
            writematrix("Fracture Load (N)",File,'Sheet',test(n).name,'Range','A14')
            writematrix("Fracture Disp (mm)",File,'Sheet',test(n).name,'Range','A15')
            % Load/Stress Data

```

```

writematrix([test(n).load],File,'sheet',test(n).name,'Range','C2:C2500')
writematrix([test(n).disp],File,'sheet',test(n).name,'Range','D2:D2500')
writematrix([test(n).strain],File,'sheet',test(n).name,'Range','G2:G2500')
writematrix([test(n).stress],File,'sheet',test(n).name,'Range','F2:F2500')

writematrix([test(n).corrected_disp],File,'sheet',test(n).name,'Range','E2:E2500')

writematrix([test(n).corrected_strain],File,'sheet',test(n).name,'Range','H2:H2500')
% Titles for load/disp curves
writematrix("Load (N)",File,'sheet',test(n).name,'Range','C1')
writematrix("Disp (mm)",File,'sheet',test(n).name,'Range','D1')
writematrix("Strain (mm/mm)",File,'sheet',test(n).name,'Range','G1')
writematrix("Stress (MPa)",File,'sheet',test(n).name,'Range','F1')
writematrix("Corrected Disp (mm)",File,'sheet',test(n).name,'Range','E1')
writematrix("Corrected Strain (mm/mm)",File,'sheet',test(n).name,'Range','H1')
end
writematrix([averages.E_std],File,'sheet',averages.name,'Range','B11');

%writematrix([hybrid_dbl(n).E_N],File,'sheet',hybrid_dbl(n).name,'Range','B12');

for idx=1:length(omit_sample_yield)
    if omit_sample_yield(idx) == "Include"

writematrix([averages.yield_stress_std],File,'sheet',averages.name,'Range','B13');

%writematrix([averages.yield_stress_LT],File,'sheet',averages.name,'Range','B14');

writematrix([averages.yield_load_std],File,'sheet',averages.name,'Range','B15');

%writematrix([averages.yield_load_LT],File,'sheet',averages.name,'Range','B16');

writematrix([averages.yield_strain_std],File,'sheet',averages.name,'Range','B17');

%writematrix([averages.yield_strain_LT],File,'sheet',averages.name,'Range','B18');

writematrix([averages.yield_disp_std],File,'sheet',averages.name,'Range','B19');

%writematrix([averages.yield_disp_LT],File,'sheet',averages.name,'Range','B20');

    end
end

```

```

        for idx=1:length(omit_sample_ult)
            if omit_sample_ult(idx) == "Include"

writematrix([averages.ult_stress_std],File,'sheet',averages.name,'Range','B21'
);

%writematrix([averages.ult_stress_LT],File,'sheet',averages.name,'Range','B22'
);

writematrix([averages.ult_load_std],File,'sheet',averages.name,'Range','B23');

%writematrix([averages.ult_load_LT],File,'sheet',averages.name,'Range','B24');
            end
        end

writematrix([averages.area_std],File,'sheet',averages.name,'Range','B25');
writematrix([averages.length_std],File,'sheet',averages.name,'Range','B26');
writematrix([averages.load],File,'sheet',averages.name,'Range','C2:C2500')
writematrix([averages.stress],File,'sheet',averages.name,'Range','D2:F2500')
writematrix([averages.corrected_disp],File,'sheet',averages.name,'Range','E2:E
2500')
writematrix([averages.corrected_strain],File,'sheet',averages.name,'Range','F2
:H2500')

        for idx=1:length(omit_sample_ult)
            if omit_sample_ult(idx) == "Include"

writematrix([averages.ult_strain_std],File,'Sheet',averages.name,'Range','B27'
)
            end
        end

        for idx=1:length(omit_sample_frac)
            if omit_sample_frac(idx) == "Include"

writematrix([averages.frac_stress_std],File,'Sheet',averages.name,'Range','B28
')
writematrix([averages.frac_strain_std],File,'Sheet',averages.name,'Range','B29
')
writematrix([averages.frac_load_std],File,'Sheet',averages.name,'Range','B30')
writematrix([averages.frac_disp_std],File,'Sheet',averages.name,'Range','B31')
            end
        end
end

```

```

% Title Blocks
writematrix("Young's Modulus St
Dev",File,'sheet',averages.name,'Range','A11');
%writematrix("Young's Modulus
N",File,'sheet',hybrid_dbl(n).name,'Range','A12');
writematrix("Yield Stress St
Dev",File,'sheet',averages.name,'Range','A13');
writematrix("Yield Stress St Dev
LT",File,'sheet',averages.name,'Range','A14');
writematrix("Yield Load St
Dev",File,'sheet',averages.name,'Range','A15');
writematrix("Yield Load LT",File,'sheet',averages.name,'Range','A16');
writematrix("Yield Strain St
Dev",File,'sheet',averages.name,'Range','A17');
writematrix("Yield Strain
LT",File,'sheet',averages.name,'Range','A18');
writematrix("Yield Disp St
Dev",File,'sheet',averages.name,'Range','A19');
writematrix("Yield Disp LT",File,'sheet',averages.name,'Range','A20');
writematrix("Ult Stress St
Dev",File,'sheet',averages.name,'Range','A21');
writematrix("Ult Stress LT",File,'sheet',averages.name,'Range','A22');
writematrix("Ult Load St
Dev",File,'sheet',averages.name,'Range','A23');
writematrix("Ult Load LT",File,'sheet',averages.name,'Range','A24');
writematrix("Area St Dev",File,'sheet',averages.name,'Range','A25');
%% Change to area for "normal" stress/strain, thickness for flexural
stress/strain
writematrix("Length St Dev",File,'sheet',averages.name,'Range','A26');
%% Change to length for "normal" stress/strain, span for flexural
stress/strain
writematrix("Load (N)",File,'sheet',averages.name,'Range','C1')
writematrix("Stress (MPa)",File,'sheet',averages.name,'Range','D1')
writematrix("Corrected Disp
(mm)",File,'sheet',averages.name,'Range','E1')
writematrix("Corrected Strain
(mm/mm)",File,'sheet',averages.name,'Range','F1')
writematrix("Ult Strain St Dev
(mm/mm)",File,'sheet',averages.name,'Range','A27')
writematrix("Fracture Stress St Dev
(MPa)",File,'sheet',averages.name,'Range','A28')
writematrix("Fracture Strain St Dev
(mm/mm)",File,'sheet',averages.name,'Range','A29')
writematrix("Fracture Load St Dev
(N)",File,'sheet',averages.name,'Range','A30')
writematrix("Fracture Disp St Dev
(mm)",File,'sheet',averages.name,'Range','A31')
end
msgbox("Check your answer against you engineering intuition","You Win!")
% %% (1) Hybrid Double Shear: Plot Stress Strain
% figure()
% % for n = 1:(length(hybrid_dbl)-1)
% %     hold on

```

```

%%      if (1<=n) && (n<=3)
%%          % Full Failure Samples
%%
plot(hybrid_dbl(n).corrected_strain,hybrid_dbl(n).stress,"LineWidth",1.5,"Color", 'b')
%%      end
%% %      if (4<=n) && (n<=6)
%% %          % Progressive Failure Samples
%% %
plot(hybrid_dbl(n).corrected_strain,hybrid_dbl(n).stress,"LineWidth",1.5,"LineStyle", "-.", "Color", 'r')
%% %      end
%%      if(7<=n) && (n<=9)
%%          % Low Torque Samples
%%
plot(hybrid_dbl(n).corrected_strain,hybrid_dbl(n).stress,"LineWidth",1.5,"LineStyle", "--", "Color", 'k')
%%      end
%% end
% plot(test(1).corrected_strain,test(1).stress,"LineWidth",1.5,"Color", 'b')
% xlim([0 0.325])
% title('18-Ply Double Shear Reults')
% xlabel('Bearing Strain (in/in)')
% ylabel('Bearing Stress (ksi)')
% legend('H-21-1', 'Location', 'southeast')
% hold off
%% (2) Plot Load Disp
% figure()
% for n = 1:(length(test)-1)
%     hold on
%     if (1<=n) && (n<=3)
%         % Full Failure Samples
%
plot(test(n).corrected_disp,test(n).load,"LineWidth",1.5,"Color", 'b')
%     end
%     if (4<=n) && (n<=6)
%         % Progressive Failure Samples
%
plot(test(n).corrected_disp,test(n).load,"LineWidth",1.5,"LineStyle", "-.", "Color", 'r')
%     end
%     if(7<=n) && (n<=9)
%         % Low Torque Samples
%
plot(test(n).corrected_disp,test(n).load,"LineWidth",1.5,"LineStyle", "--", "Color", 'k')
%     end
% end
% xlm = [0 0.1];
% ylm = [0 1.1*max([test.ult_load])];
% ylim(ylm);
% xlim(xlm);
% [ax] = plot2axes(NaN, NaN, 'ro', 'yscale',4.448,'xscale',25.4);

```

```

% xlabel(ax(1),'Displacemt (in)'); xlabel(ax(2),{'\fontsize{14}\bf18-Ply
Double Shear Results','\fontsize{11}\rmDisplacement (mm)'});
% ylabel(ax(1),'Load (kips)'); ylabel(ax(2),'Load (kN)')
% legend('Full Failure','','','Progressive Failure','','','Low
Torque','location','southeast')
% hold off
% % 3 Hybrid Double Shear Control/Adhesive/Non-Adhesive
% figure()
% hold on
% for n = 1:(length(test)-1)
%     plot(test(n).corrected_disp,test(n).load,"LineWidth",1.5,"Color","b")
% end
% for n = 1:(length(control_dbl)-1)
%
% plot(control_dbl(n).corrected_disp,control_dbl(n).load,"LineWidth",1.5,"Color"
% ,"r")
% end
% for n = 1:(length(control_dbl)-1)
%
% plot(adhesive_dbl(n).corrected_disp,adhesive_dbl(n).load,"LineWidth",1.5,"Colo
% r","k")
% end
% xlm = [0 0.1];
% ylm = [0 1.1*max([test.ult_load])];
% ylim(ylm);
% xlim(xlm);
% [ax] = plot2axes(NaN, NaN, 'ro', 'yscale',4.448,'xscale',25.4);
% xlabel(ax(1),'Displacemt (in)'); xlabel(ax(2),{'\fontsize{12}\bf18-Ply
Hybrid/Adhesive/Control Results','\fontsize{11}\rmDisplacement (mm)'});
% ylabel(ax(1),'Load (kips)'); ylabel(ax(2),'Load (kN)');
%
% legend('Hybrid','','','','','','','','','Control','','','','','Adhesive','loca
% tion','southeast')
% hold off
% % 3 Hybrid Double Shear Control/Adhesive/Non-Adhesive
% figure()
% hold on
%
% plot(test(length(test)).corrected_disp,test(length(test)).load,"LineWidth",1.5
% ,"Color","b")
%
% plot(control_dbl(length(control_dbl)).corrected_disp,control_dbl(length(contro
% l_dbl)).load,"LineWidth",1.5,"Color","r")
%
% plot(adhesive_dbl(length(adhesive_dbl)).corrected_disp,adhesive_dbl(length(adh
% esive_dbl)).load,"LineWidth",1.5,"Color","k")
%
% plot(test(length(test)).corrected_disp_LT,test(length(test)).load_LT,"LineWidt
% h",1.5,"Color","m")
% xlm = [0 0.1];
% ylm = [0 1.1*max([test.ult_load])];
% ylim(ylm);
% xlim(xlm);

```

```

% [ax] = plot2axes(NaN, NaN, 'ro', 'yscale',4.448,'xscale',25.4);
% xlabel(ax(1),'Displacemt (in)'); xlabel(ax(2),{'\fontsize{12}\bf18-Ply
Hybrid/Adhesive/Control Mean Results','\fontsize{11}\rmDisplacement (mm)'});
% ylabel(ax(1),'Load (kips)'); ylabel(ax(2),'Load (kN)');
% legend('Hybrid','Control','Adhesive','Low Torque','location','southeast')
% hold off
%% (3) Hybrid Double Shear load disp vs Control Load Disp
% figure()
% for n = 1:(length(test)-1)
%     hold on
%     plot(test(n).corrected_disp,test(n).load,"LineWidth",1.5,"Color","b")
% end
% for n = 1:(length(control_dbl)-1)
%
plot(control_dbl(n).corrected_disp,control_dbl(n).load,"LineWidth",1.5,"Color"
,"r")
% end
% xlm = [0 0.1];
% ylm = [0 1.1*max([test.ult_load])];
% ylim(ylm);
% xlim(xlm);
% [ax] = plot2axes(NaN, NaN, 'ro', 'yscale',4.448,'xscale',25.4);
% xlabel(ax(1),'Displacemt (in)'); xlabel(ax(2),{'\fontsize{14}\bf18-Ply
Hybrid Double Shear vs Control Results','\fontsize{11}\rmDisplacement (mm)'});
% ylabel(ax(1),'Load (kips)'); ylabel(ax(2),'Load (kN)');
% legend('Hybrid','','','','','','','','','Control','location','southeast')
% hold off
%% (4) Hybrid Double Shear stress strain vs Control stress strain
% figure()
% for n = 1:6
%     hold on
%     if n >=1 && n <=3
%
plot(test(n).corrected_strain,test(n).stress,"LineWidth",1.5,"Color","b")
%     end
%     if n >=4 && n <= 6
%
plot(test(n).corrected_strain,test(n).stress,"LineWidth",1.5,"Color","b","Line
Style","--")
%     end
% end
% for n = 1:(length(control_dbl)-1)
%     if n>=1 && n<=3
%
plot(control_dbl(n).corrected_strain,control_dbl(n).stress,"LineWidth",1.5,"Co
lor","k")
%     end
%     if n >= 4
%
plot(control_dbl(n).corrected_strain,control_dbl(n).stress,"LineWidth",1.5,"Co
lor","k","LineStyle","--")
%     end
% end

```

```

% a = linspace(0,1.1*max([test.ult_stress]),9);
% b = mean([control_dbl(1:3).ult_strain])+zeros(9,1);
% plot(b,a,"LineWidth",1.5,"Color","m")
% xlm = [0 0.325];
% ylm = [0 1.1*max([test.ult_stress])];
% xlim(xlm)
% ylim(ylm)
% ax = plot2axes(NaN, NaN, 'ro', 'yscale',6.89475728,'xscale',1);
% xlabel(ax(1),'Bearing Strain (in/in)'); xlabel(ax(2),{'\fontsize{14}\bf18-
Ply Hybrid Double Shear vs Control Results','\fontsize{11}\rmBearing Strain
(mm/mm)'});
% ylabel(ax(1),'Bearing Stress (ksi)'); ylabel(ax(2),'Bearing Stress (MPa)');
% legend('Hybrid','','','Hybrid Progressive
Failure','','','Control','','','Control Progressive Failure','','Mean Ult
Strain','location','southeast')
% hold off
% %% (4) Hybrid Double Shear stress strain vs Control Load Displacemnt
% figure()
% for n = 1:6
%     hold on
%     if n >=1 && n <=3
%         plot(test(n).corrected_disp,test(n).load,"LineWidth",1.5,"Color","b")
%     end
%     if n >=4 && n <= 6
%
% plot(test(n).corrected_disp,test(n).load,"LineWidth",1.5,"Color","b","LineStyl
e","--")
%     end
% end
% for n = 1:(length(control_dbl)-1)
%     if n>=1 && n<=3
%
% plot(control_dbl(n).corrected_disp,control_dbl(n).load,"LineWidth",1.5,"Color"
,"k")
%     end
%     if n >= 4
%
% plot(control_dbl(n).corrected_disp,control_dbl(n).load,"LineWidth",1.5,"Color"
,"k","LineStyle","--")
%     end
% end
% xlm = [0 0.1];
% ylm = [0 1.1*max([test.ult_load])];
% ylim(ylm);
% xlim(xlm);
% [ax] = plot2axes(NaN, NaN, 'ro', 'yscale',4.448,'xscale',25.4);
% xlabel(ax(1),'Displacemt (in)'); xlabel(ax(2),{'\fontsize{14}\bf18-Ply
Hybrid Double Shear vs Control Results','\fontsize{11}\rmDisplacement (mm)'});
% ylabel(ax(1),'Load (kips)'); ylabel(ax(2),'Load (kN)');
% legend('Hybrid','','','','','','','','','Control','location','southeast')
% hold off
% %% Hybrid double Shear Control/Adhesive/Non-Adhesive Stress-Strain
% figure()

```

```

% for n = 1:(length(test)-1)
%     hold on
%
plot(test(n).corrected_strain,test(n).stress,"LineWidth",1.5,"Color","b")
% end
% for n = 1:(length(control_dbl)-1)
%
plot(control_dbl(n).corrected_strain,control_dbl(n).stress,"LineWidth",1.5,"Color","r")
% end
% for n = 1:(length(adhesive_dbl)-1)
%
plot(adhesive_dbl(n).corrected_strain,adhesive_dbl(n).stress,"LineWidth",1.5,"Color","k")
% end
% xlm = [0 0.325];
% ylm = [0 1.1*max([test.ult_stress])];
% ylim(ylm);
% xlim(xlm);
% [ax] = plot2axes(NaN, NaN, 'ro', 'yscale',6.89475728,'xscale',1);
% xlabel(ax(1),'Bearing Strain (in/in)'); xlabel(ax(2),{'\fontsize{14}\bf18-
Ply Hybrid/Adhesive/Control Single Shear Results','\fontsize{11}\rmBearing
Strain (mm/mm)'});
% ylabel(ax(1),'Stress (ksi)'); ylabel(ax(2),'Stress (MPa)');
%
legend('Hybrid','','','','','','','Control','','','Adhesive','location','southeast')
% hold off
% %% Average Curves Hybrid Single Shear Control/Adhesive/Non-Adhesive/LT
Stress-Strain
% figure()
% hold on
% plot(averages.corrected_strain,averages.stress,"LineWidth",1.5,"Color","b")
% %
plot(control_dbl(length(control_dbl)).corrected_strain,control_dbl(length(control_dbl)).stress,"LineWidth",1.5,"Color","k")
% %
plot(adhesive_dbl(length(adhesive_dbl)).corrected_strain,adhesive_dbl(length(adhesive_dbl)).stress,"LineWidth",1.5,"Color","r")
% %
plot(hybrid_dbl(length(hybrid_dbl)).corrected_strain_LT,hybrid_dbl(length(hybrid_dbl)).stress_LT,"LineWidth",1.5,"Color","r")
% xlm = [0 0.325]; % this xlim was chosen since this was the max disp
converted to bearing strain
% ylm = [0 1.1*max([test.ult_stress])];
% ylim(ylm);
% xlim(xlm);
% [ax] = plot2axes(NaN, NaN, 'ro', 'yscale',6.89475728,'xscale',1);
% xlabel(ax(1),'Bearing Strain (in/in)'); xlabel(ax(2),{'\fontsize{14}\bf18-
Ply Hybrid/Adhesive/Control Mean Results','\fontsize{11}\rmBearing Strain
(mm/mm)'});
% ylabel(ax(1),'Bearing Stress (ksi)'); ylabel(ax(2),'Bearing Stress (MPa)');
% legend('Hybrid','Control','With Adhesive','location','southeast')

```





## Bibliography

- [1] J. Flagel, "Matmatch," 1 December 2020. [Online]. Available: <https://matmatch.com/resources/blog/most-useful-metals-for-high-temperature-applications/>. [Accessed 4 November 2022].
- [2] J. McMullen, "Dorsetware Limited," 20 September 2017. [Online]. Available: <https://www.dorsetware.com/steel-vs-titanium/#:~:text=When%20compared%20to%20steel%20in,radio%20of%20all%20known%20metals..> [Accessed 4 November 2022].
- [3] "Titanium Processing Center," Titanium Processing Center, [Online]. Available: <https://www.titaniumprocessingcenter.com/titanium-history-developments-and-applications/>. [Accessed 28 1 2023].
- [4] "Lenntech," Lenntech, [Online]. Available: <https://www.lenntech.com/periodic/periodic-chart.htm>. [Accessed 24 1 2023].
- [5] "MatWeb," MatWeb, [Online]. Available: <https://www.matweb.com/Search/MaterialGroupSearch.aspx?GroupID=9>. [Accessed 25 1 2023].
- [6] R. Castells, "Element," Element, 24 1 2023. [Online]. Available: <https://www.element.com/nucleus/2016/dmls-vs-slm-3d-printing-for-metal-manufacturing>. [Accessed 26 1 2023].
- [7] "i3DMFG," i3DMFG, [Online]. Available: [https://www.i3dmfg.com/dmls-direct-metal-laser-sintering/#:~:text=Direct%20Metal%20Laser%20Solidification%20\(DMLS%C2%AE\)%2C%20is%20the%20process,geometries%20from%203D%20design%20files.](https://www.i3dmfg.com/dmls-direct-metal-laser-sintering/#:~:text=Direct%20Metal%20Laser%20Solidification%20(DMLS%C2%AE)%2C%20is%20the%20process,geometries%20from%203D%20design%20files.) [Accessed 27 1 2023].
- [8] "3D Printing Service," Lava, [Online]. Available: <https://www.3dprintingservice.cc/3d-printing-technologies/dmls-3d-printing/>. [Accessed 20 1 2023].
- [9] P. G. Martinho, "Rapid Manufacturing and Tooling," *Design and Manufacturing of Plastics Products*, pp. 381-456, 2021.
- [10] "What is Sintering? (a Definitive Guide)," TWI, [Online]. Available: <https://www.twi-global.com/technical-knowledge/faqs/what-is-sintering>. [Accessed 8 2 2023].

- [11] G. Jones, "All3DP," All3DP, 15 4 2021. [Online]. Available: <https://all3dp.com/2/direct-metal-laser-sintering-dmls-simply-explained/>. [Accessed 20 1 2023].
- [12] A. Choudhry, "Aurum3D," Aurum3D, [Online]. Available: <https://www.aurum3d.com/blog/dmls-advantages-disadvantages/>. [Accessed 26 1 2023].
- [13] S. S. J. E. Q. L. M. B. M. Q. W. Xu, "Ti-6Al-4V Additively Manufactured by Selective Laser Melting with Superior Mechanical Properties," *The Journal of The Minerals, Metals & Materials Society*, vol. 67, p. 668–673, 2015.
- [14] S. I. S. C. D. U. Giovanna Rotella, "Surface integrity of machined additively manufactured Ti alloys," *Journal of Materials Processing Technology*, vol. 259, pp. 180-185, 2018.
- [15] S. S. S. B. A. G. A. Bordin, "Experimental investigation on the feasibility of dry and cryogenic machining as sustainable strategies when turning Ti6Al4V produced by Additive Manufacturing," *Journal of Cleaner Production*, vol. 142, no. 4, pp. 4142-4151, 2017.
- [16] A. Y. L. B. S. M. T. Nima Shamsaei, "An overview of Direct Laser Deposition for additive manufacturing; Part II: Mechanical behavior, process parameter optimization and control," *Additive Manufacturing*, vol. 8, pp. 12-35, 2015.
- [17] J. W. H. M. S. Bagehorn, "Application of mechanical surface finishing processes for roughness reduction and fatigue improvement of additively manufactured Ti-6Al-4V parts," *International Journal of Fatigue*, vol. 102, pp. 135-142, 2017.
- [18] M. R. P. Edwards, "Fatigue performance evaluation of selective laser melted Ti-6Al-4V," *Materials Science and Engineering*, vol. 598, pp. 327-337, 2014.
- [19] A. S. S. S. D. H. F. W. C. E. Eric Wycisk, "Effects of Defects in Laser Additive Manufactured Ti-6Al-4V on Fatigue Properties," *Physics Procedia*, vol. 56, pp. 371-378, 2014.
- [20] G. F. S. L. A. J. A. A. Z. J. Z. Xiang-Yu Zhang, "Effect of subtransus heat treatment on the microstructure and mechanical properties of additively manufactured Ti-6Al-4V alloy," *Journal of Alloys and Compounds*, vol. 735, pp. 1562-1575, 2018.
- [21] "i3DMFG," i3DMFG, [Online]. Available: <https://www.i3dmfg.com/about-i3dmfg/>. [Accessed 20 1 2023].
- [22] "3D Natives," 3D Natives, [Online]. Available: <https://www.3dnatives.com/3D-compare/en/3d-printers/eos-m-400/>. [Accessed 22 1 2023].

- [23] "eos," eos, [Online]. Available: <https://www.eos.info/en/additive-manufacturing/3d-printing-metal/eos-metal-systems/eos-m-400-4>. [Accessed 27 1 2023].
- [24] "i3DMFG," [Online]. Available: <https://www.i3dmfg.com/>. [Accessed 8 2 2023].
- [25] "Test Resources," 10 September 2013. [Online]. Available: <https://www.testresources.net/blog/can-i-trust-strain-data-from-crosshead-position-or-must-i-use-an-extensometer/>. [Accessed 17 November 2022].
- [26] ASTM, *ASTM D790-17*, 2017.
- [27] D. Collins, "Linear Motion Tips," 8 March 2019. [Online]. Available: <https://www.linearmotiontips.com/mechanical-properties-of-materials-stress-and-strain/>. [Accessed 17 November 2022].
- [28] "The Main Characteristics of Titanium and Titanium Alloys," Struers, [Online]. Available: <https://www.struers.com/en/Knowledge/Materials/Titanium#>. [Accessed 7 December 2022].
- [29] "MedCalc," MedCalc, [Online]. Available: [https://www.medcalc.org/calc/comparison\\_of\\_means.php](https://www.medcalc.org/calc/comparison_of_means.php). [Accessed 13 1 2023].
- [30] A. C. S. P. M. M. P. J. L. Dominic A. Stewardson, "The flexural properties of endodontic post materials," *Dental Materials*, vol. 26, pp. 730-736, 2010.
- [31] "Titanium Ti-6Al-4V (Grade 5), Annealed," ASM Aerospace Specification Metals Inc., [Online]. Available: <https://asm.matweb.com/search/SpecificMaterial.asp?bassnum=mtp641>. [Accessed 12 1 2023].
- [32] "Titanium Alloys - Ti6Al4V Grade 5," AZO Materials, [Online]. Available: <https://www.azom.com/properties.aspx?ArticleID=1547>. [Accessed 25 2 2023].
- [33] C. Knowles, T. Becker and R. Tait, "Residual stress measurements and structural integrity implications for selective laser melted TI-6AL-4V," *South African Journal of Industrial Engineering*, vol. 23, no. 3, pp. 119-129, 2012.

## **Vita**

First Lieutenant James M. Gunderson graduated from Thomas Jefferson High School in Bloomington, Minnesota in June 2015. He attended The United States Merchant Marine Academy in Kings Point, New York where he graduated with a Bachelor of Science Degree Magna Cum Laude in Marine Engineering and Shipyard Management and a commission in the United States Air Force in June 2019.

His first assignment was at Wright Patterson Air Force Base where he worked as a Systems Analysis Engineer starting in November 2019. He then was accepted into the Air Force Institute of Technology and began his studies in the Graduate School of Engineering & Management in August 2021. Upon graduation, he will be assigned to Fort Sam Houston.

<b>REPORT DOCUMENTATION PAGE</b>				<i>Form Approved</i> OMB No. 074-0188	
The public reporting burden for this collection of information is estimated to average 1 hour per response, including the time for reviewing instructions, searching existing data sources, gathering and maintaining the data needed, and completing and reviewing the collection of information. Send comments regarding this burden estimate or any other aspect of the collection of information, including suggestions for reducing this burden to Department of Defense, Washington Headquarters Services, Directorate for Information Operations and Reports (0704-0188), 1215 Jefferson Davis Highway, Suite 1204, Arlington, VA 22202-4302. Respondents should be aware that notwithstanding any other provision of law, no person shall be subject to a penalty for failing to comply with a collection of information if it does not display a currently valid OMB control number.					
<b>PLEASE DO NOT RETURN YOUR FORM TO THE ABOVE ADDRESS.</b>					
<b>1. REPORT DATE</b> (DD-MM-YYYY) 06-03-2023		<b>2. REPORT TYPE</b> Master's Thesis		<b>3. DATES COVERED</b> (From - To) March 2022 - March 2023	
<b>TITLE AND SUBTITLE</b> ANISOTROPIC CHARACTERIZATION OF ADDITIVELY MANUFACTURED Ti 6-4 VIA TENSION, COMPRESSION, AND THREE POINT BEND EXPERIMENTATION				<b>5a. CONTRACT NUMBER</b>	
				<b>5b. GRANT NUMBER</b>	
				<b>5c. PROGRAM ELEMENT NUMBER</b>	
<b>6. AUTHOR(S)</b> Gunderson, James M., First Lieutenant, USAF				<b>5d. PROJECT NUMBER</b>	
				<b>5e. TASK NUMBER</b>	
				<b>5f. WORK UNIT NUMBER</b>	
<b>7. PERFORMING ORGANIZATION NAMES(S) AND ADDRESS(S)</b> Air Force Institute of Technology Graduate School of Engineering and Management (AFIT/EN) 2950 Hobson Way, Building 640 WPAFB OH 45433-7765				<b>8. PERFORMING ORGANIZATION REPORT NUMBER</b>  AFIT-ENY-MS-23-M-270	
<b>9. SPONSORING/MONITORING AGENCY NAME(S) AND ADDRESS(ES)</b>  Air Force Research Laboratory				<b>10. SPONSOR/MONITOR'S ACRONYM(S)</b>  AFRL/RW	
				<b>11. SPONSOR/MONITOR'S REPORT NUMBER(S)</b>	
<b>12. DISTRIBUTION/AVAILABILITY STATEMENT</b> DISTRIBUTION STATEMENT A. APPROVED FOR PUBLIC RELEASE; DISTRIBUTION UNLIMITED.					
<b>13. SUPPLEMENTARY NOTES</b> This material is declared a work of the U.S. Government and is not subject to copyright protection in the United States.					
<b>14. ABSTRACT</b>  Titanium's ability to fill existing material gaps because of its higher strength and higher melting temperature compared to other common materials used in aircraft structures requires a need to understand the behavior of the material. Titanium's properties and the development of additive manufacturing also open an opportunity for it to be used in aerospace systems of the future in applications where traditionally manufactured titanium cannot meet the desired system requirements. Compressive, tensile, and three point bend experimental data collected from this research under varying temperatures, print orientations, print layer build heights, and surface finishes were analyzed to determine favorable material parameters for the Titanium alloy Ti-6Al-4V.					
<b>15. SUBJECT TERMS</b> Additive Manufacturing, Direct Metal Laser Sintering, Titanium, Ti 6-4, Material Characterization, Tensile Testing, Compression Testing, Three Point Bend Testing, Print Orientation, Build Height, Surface Finish, Temperature					
<b>16. SECURITY CLASSIFICATION OF:</b>			<b>17. LIMITATION OF ABSTRACT</b>  UU	<b>18. NUMBER OF PAGES</b>  148	<b>19a. NAME OF RESPONSIBLE PERSON</b> John Brewer, AFIT/ENY
<b>a. REPORT</b>  U	<b>b. ABSTRACT</b>  U	<b>c. THIS PAGE</b>  U			<b>19b. TELEPHONE NUMBER (Include area code)</b> (937) 255-3636, ext 4282 John.Brewer@afit.edu

Standard Form 298 (Rev. 8-98)  
Prescribed by ANSI Std. Z39-18